THE UNIVERSITY OF CHICAGO

MOLECULAR NEUROENDOCRINOLOGY OF MATERNAL BEHAVIORS AND DEATH IN THE CALIFORNIA TWO-SPOT OCTOPUS, *OCTOPUS BIMACULOIDES*

A DISSERTATION SUBMITTED TO

THE FACULTY OF THE DIVISION OF THE BIOLOGICAL SCIENCES

AND THE PRITZKER SCHOOL OF MEDICINE

IN CANDIDACY FOR THE DEGREE OF

DOCTOR OF PHILOSOPHY

COMMITTEE ON NEUROBIOLOGY

BY

ZHENGYAN WANG

CHICAGO, ILLINOIS

DECEMBER 2018

COPYRIGHT

To my mother, 曾慧玲

To my father, 王存孝

TABLE OF CONTENTS

ACKNOWLEDGEMENTS

I acknowledge that this research was conducted on the occupied lands of the Potawatomi, Miami, Sauk and Fox, and more.

I am grateful to those who have made this project both possible and pleasurable. Carrie Albertin, Steve Briscoe, Stav Assimocopolous, Isabella Penido, William Jones: thank you for sharing your wisdom and friendship with me each day. Sofia Collins, Magda Glotzer, Emily Garcia, and Olivia Harden: thank you for trusting me. Stephanie Cologna, thank you for embodying the spirit of scientific collaboration. Melissa Pergande, Ralph Tobias, Mi Nguyen, Chathurika Rathnayake, Chandimal Pathmasiri: thank you for becoming my second lab family. Peggy Mason, Melina Hale, Brian Prendergast, and Vinny Lynch: thank you for pushing and reassuring me. Cliff Ragsdale, I am happy and proud to be a member of your lab. Thank you for giving me space to be me. Thank you for your boldness and kindness. I cherish our many meandering conversations, and I will very much miss working in your lab.

To my mother, Huiling Zeng, my father, Cunxiao Wang, and my brother, Z Ming Wang: thank you for growing this little heart. Thank you to family in this hemisphere and the other, ancestors in this world and the next. Thank you to family beyond family, my survival depended on you: Natalia Piland for reading in thegrassesthegrassesthegrasses with me; Tom Gijssels for showing me when and how to climb higher; Katie Henderson for your infectious joy and boundless integrity; Fowzia Khan for pushing the limits of care; Cris Alvaro for your ghost stories and love stories alike; Kendra Saldana for your inspiring tenderness always; Kelly Fitzpatrick for blessing me with your manifestations; David Durstewitz for building homes that enabled me to stay the many times I wanted to go. Thank you to all the animals. To Sama Ahmed, willful Argonaut, I humbly offer you my gratitude and love.

LIST OF FIGURES

LIST OF TABLES

ABSTRACT

Post-reproductive life in the female octopus is characterized by an extreme pattern of maternal care: the mother cares for her clutch of eggs without feeding until her death. These maternal behaviors are completely eradicated if the optic glands, the octopus analog of the vertebrate pituitary gland, are removed from brooding females. Despite the optic gland's importance in regulating maternal behavior, the possible mechanisms underlying optic gland function are unknown. In this thesis, I investigate the optic glands from molecular, anatomical, and neurochemical perspectives to uncover its mechanisms of function in octopus maternal behaviors.

To identify signaling systems implicated in end-of-life behaviors, I observed behavior in non-mated and brooding female octopuses and performed transcriptomic analyses on their optic glands. I categorized adult life of *Octopus bimaculoides* females into four distinct phases: non-mated, feeding, fasting, and senescent decline. I found that the optic gland undergoes remarkable molecular changes coincident with transitions between these behavioral stages. These include the dramatic up- and down-regulation of catecholamine, steroid, insulin, and feeding peptide pathways. Transcriptome analyses in other tissues demonstrate that these molecular changes are not generalized markers of senescence, but instead, specific features of optic gland maturation. My findings indicate that, rather than a single "self-destruct" hormone, the optic glands employ multiple pathways as systemic hormonal signals of behavioral control.

How these different signals are produced in the optic glands is unclear: they are functionally analogous to the vertebrate pituitary gland, but the optic glands have classically been described as having no internal organization. By contrast, separate populations of pituitary cells produce different hormones that act on the gonads and other downstream targets. To

explore the cellular architecture of the optic glands, I used parallel bioinformatic approaches to identify putative markers of the optic gland. I queried the optic gland transcriptomes for transcripts with sequence homology to known invertebrate neuropeptides, and performed a bioinformatic survey on the most enriched transcripts to identify novel prepropeptides. With traditional histochemistry and *in situ* hybridization, I revealed that the optic gland has regional organization along the oral/aboral axis. At least two major signaling territories divide the optic glands of non-mated females: a steroidogenic region at the most aboral end of the optic gland and a multi-ligand zone that extends to the oral end of the optic gland. The non-steroidogenic, multi-ligand zone includes both neuropeptidergic and catecholaminergic cells.

These data draw a functional connection between the optic glands and the pituitary gland: both neuroendocrine organs utilize neuropeptides for signaling. However, unlike the pituitary gland, the optic gland also employs steroid signaling, as evidenced in both the *in situ* and transcriptomic data. To identify the possible steroid secretions of the optic gland, I performed tandem liquid chromatography-mass spectrometry on extracts from the optic glands of non-mated and mated feeding female octopuses. We identified steroid hormones and found ~200 compounds that showed at least a 4-fold change between non-mated and mated females. The presence of 7-dehydrocholesterol in the optic glands indicates conserved enzymatic activity of the putative cholesterol desaturase we identified bioinformatically. Our study shows, for the first time, that the optic gland produces steroid hormones and demonstrates a link between steroid biosynthesis in the optic glands and octopus behavior.

Findings from this thesis represent the first major contribution to the understanding of octopus neuroendocrinology and reproductive behaviors in almost half a century. The methods

and results detailed here are applicable beyond octopus biology and offer new approaches to the study of mechanisms underlying natural behaviors in large, invertebrate animals.

CHAPTER 1

Introduction

Cephalopod molluscs are highly mobile predators with complex nervous systems and a wide array of charismatic behaviors. The last common ancestors of all cephalopods arose around 530 million years ago and diversified into the 700+ species of coleoid (squid, cuttlefish and octopus) and nautilus cephalopods that survive today [1]. The octopus is exceptional among the cephalopods: its striking camouflage displays and keen problem-solving abilities have long captured human fascination [1,2]. Octopuses have the most complex central nervous systems of all invertebrates, with almost 40 different lobes dedicated to a wide range of functions and massive axial nerve cords in each of its arms (Figure 1.1). Due to its large size and highly encephalized nature, the central brain of the octopus facilitated many foundational studies in behavioral neurobiology [3].

All cephalopods share a basic central nervous system organization (Figure 1.1) consisting of central supra- and subesophageal brain masses surrounding the esophagus, paired optic lobes, and axial nerve cords in each of the appendages. In *Octopus vulgaris*, these neural tissues comprise almost half a billion neurons [2]. Mature brain lobes are organized in invertebrate fashion with cell bodies lining the perimeter and neuropil filling the center. As is true for nearly all other invertebrates, cephalopods lack myelin: short, regional neural connections dominate over long-range ones [2]. Foundational lesion and histological studies have extensively characterized the function and anatomy of major neural regions, including the optic lobes and frontal-vertical lobes [2,4].

While neurobiological processes such as visual processing and learning and memory have been extensively studied, the hormonal signaling underlying natural behaviors in the

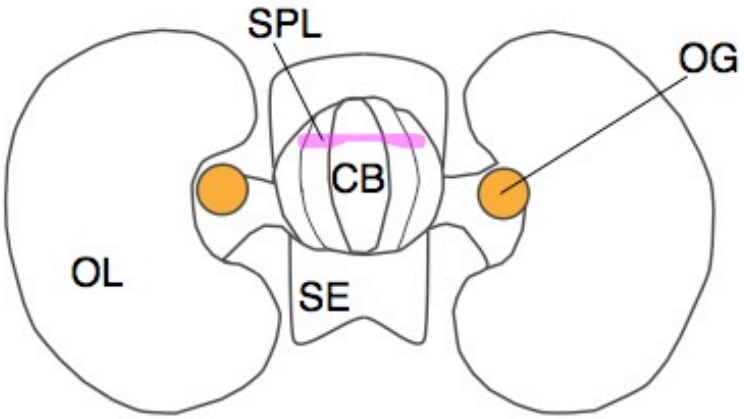

Fig 1.1 Anatomy of the octopus nervous system, dorsal view. The central nervous system of the octopus is comprised of a circumesophageal brain mass (CB), paired optic lobes (OLs), and an axial nerve cord in each arm (not shown). The subpedunculate lobe (SPL, pink) lies deep to the surface of the circumesophageal mass and innervates the optic glands (OG, orange). The subesophageal brain (SE) also contains neurosecretory cells.

octopus have remained largely unexplored with modern techniques. For example, almost nothing is known about the octopus's complex neuroendocrine center, the optic glands, which controls some of life's most important events, including mating and death.

Octopus life history

The California two-spot octopus, *Octopus bimaculoides*, the species studied in this thesis, is a solitary, short-lived coleoid species that is found in the benthic zones of the Pacific Ocean, from southern California to Mexico [5]. Embryos of this large-egged species undergo direct development, resulting in a hatchling that closely resembles its adult form in morphology and behavior [6]. After hatching, young juveniles disperse and actively hunt for small prey. Octopuses sustain a rapid pace of growth during this initial growth period before sexual maturation, growing by 4-7% of their body mass daily [7]. This exponential period of growth is particularly susceptible to influence by environmental factors, such as water temperature and availability of light [8,9]. Warmer water temperatures speed up maturation and growth, while colder temperatures slow development [7,8,10]. In the lab, *O. bimaculoides* can tolerate temperatures from 18°C-23°C. Animals raised in warmer temperatures experience a dramatic increase in growth rate during the exponential phase, which slows around 5-6 months of age [7].

In the lab, first signs of reproductive maturity typically appear around 5-6 months of age [7]. In males of some octopus species, the hectocotylus, a modification of the third right arm used to transport spermatophores, becomes visually distinct from the other arms [11,12]. In *O. bimaculoides*, the hectocotylus is not always easily distinguishable, and surgical dissection is used to positively determine sex (see Chapter 2). Females do not exhibit external physiological

signs of sexual maturation, but begin to mate at around this same time period. Interestingly, octopuses can maintain a logarithmic growth rate even after sexual maturation [8,13,14].

O. bimaculoides individuals come together as adults only to reproduce [15]. Although courtship displays precede mating in some octopus species, they are not typical in *O. bimaculoides* [16,17]. Males initiate contact with females and transfer spermatophores to the female's mantle either by mounting her dorsally or probing her from a distance with the hectocotylus [16,18]. Spermatophores are stored in the female's oviducal gland until egg-laying [11,19]), and multiple paternity is not uncommon [20].

Most coleoid species, including *O. bimaculoides*, spawn only once in their lives and die following a single reproductive event [5,15]. Following egg-laying, females undergo dramatic behavioral changes. While tending and protecting her clutch of eggs, the female abstains from actively hunting prey and stops eating. As the brood period continues, the female experiences a marked decline in body condition, including a loss of body mass and paling in color [4,21]. Field and laboratory studies show that *O. bimaculoides* individuals complete their life cycles in about one year [5,22].

Neurosecretory control of reproduction

Sexual maturation and reproductive behaviors of both vertebrates and octopuses are under neuroendocrine regulation [13,23]. In vertebrates, the hypothalamic-pituitary-gonadal axis (also known as the HPG or reproductive axis) controls normal development of the gonads through a dynamic network of feed forward excitation from the brain and feedback inhibition from downstream glandular and tissue targets. The production and release of gonadotropin releasing hormone (GNRH) from the hypothalamus stimulates the anterior pituitary gland to

release luteinizing hormone and follicle-stimulating hormone, which act directly on the gonadal tissues to cause maturation of the gametes and production of sex steroids[24]. The estrogens and androgens produced by the gonads form a negative feedback loop by inhibiting production of peptide hormones by the hypothalamus and pituitary gland [25].

Far less is known about the hormonal secretions, anatomy, and feedback mechanisms of the octopus reproductive axis. GNRH-like peptides have been identified in octopuses as well as other molluscs [26-29]. Functional studies have shown that this octopus GNRH-like peptide is able to promote LH release in quail anterior pituitary cells, strongly suggesting a conservation in signaling competency between the vertebrate and octopus peptides [30]. GNRH-immunoreactive cell bodies and fibers have been localized in several neural regions in the octopus brain, including the posterior dorsal basal lobe, the vertical lobes, and the subpedunculate lobe [27,31]. The wide distribution of GNRH throughout the supraesophageal brain raises the possibility that it functions as a general neuromodulator, in addition to possible neuroendocrine capacities.

The presence of GNRH in the subpedunculate lobe is of particular interest to the study of octopus neuroendocrinology. These paired lobes are located at the aboral end of the supraesophageal brain, between the vertical lobes and the dorsal basal lobe [2]. In *O. bimaculoides*, each subpedunculate lobe contains at least 3 different interconnected lobules of neuropil [27]. The optic gland nerve brings efferent fibers of the lobules out of central brain mass by the optic tract [2,23,32]. Subpedunculate efferents terminate in the optic glands, a pair of neurosecretory organs located on the dorsal aboral optic stalk between the optic lobes and the circumesophageal brain (Figure 1.1) [2,23].

When the nerve supply from the subpedunculate lobe to the optic gland is experimentally lesioned, the glands undergo unchecked growth [4,23]. As it enlarges, the optic gland changes

from a pale cream color to a deep orange [2]. Glandular ripening is accompanied by secretion of an uncharacterized "optic gland hormone" [4,33]. Subsequently, the reproductive organs also become enlarged. In females, where the effect is most dramatic, the ovary can increase from $1/500^{th}$ to $1/5^{th}$ of total body mass within a month of experimental manipulation [23]. Glandular and gonadal growth is seen whether the subpedunculate lobe itself is lesioned, or the optic tract along with subpedunculate lobe efferents is severed [23]. In cases where the subpedunculate innervation is destroyed on one side of the body, only the optic gland ipsilateral to the operation increases in size [23]. Unilateral ablation of subpedunculate input also leads to downstream enlargement of the gonads.

Role of optic gland in maintenance of gametogenesis

The removal of subpedunculate input always triggers growth in its downstream targets, which strongly suggests that central input to the optic glands is in part inhibitory. Removal of the optic gland itself leads to a wider range of changes in the reproductive system. If glandectomy accompanies subpedunculate ablation, the gonad does not grow [23]. In the inverse experiment, removal of the optic gland from sexually mature males with intact subpedunculate efferents causes the testis to atrophy and eventually cease production of sperm and spermatophores [23,34]. These findings indicate that sexual maturation cannot occur without the optic glands and that maintenance of maturation and reproductive function requires ongoing interconnections among the subpedunculate lobe, optic glands, and gonads.

Transplant experiments in which a secreting optic gland from one adult octopus is implanted in a second results in growth of the host's gonad [35]. If the recipient had immature gonads at implantation, precocious sexual maturation would follow [35]. This effect does not

depend on the sex of either the donor or the recipient, suggesting that the secretions of the male and female optic gland do not differ in their gonadotropic capacities [35].

These findings led Wells and Wells to draw a functional analogy between the octopus optic gland and the vertebrate pituitary gland [34]: both endocrine centers are essential for the maturation of sexual organs and maintenance of gametogenesis. Key differences distinguish the two systems. First, secreted peptide hormones serve as the functional link between the hypothalamus and the anterior pituitary gland, whereas in the octopus, direct nerve connection connects the subpedunculate lobe with the optic gland [2,36]. Second, central input to the pituitary is excitatory, but subpedunculate innervation is inhibitory. As such, secretions from the optic gland occur in the absence of its central control, but the vertebrate pituitary gland cannot act without hypothalamic input [37]. These foundational optic gland studies did not address the biochemical identity of the optic gland secretions, so whether the pituitary-optic gland analogy can be extended to the secreted factors of the two neuroendocrine centers remains unknown.

Role of the optic gland in maintenance of reproductive behaviors

Under physiological conditions, the female octopus ceases to feed while brooding her clutch of eggs and experiences a pronounced decay in body condition before dying [15,23,33]. Death of the mother closely coincides with the hatching of her clutch.

Removal of the optic glands after sexual maturation and mating drastically alters the course of normal life history events in females. In 1977, Jerome Wodinsky experimentally removed the optic glands from fasting, brooding females [33]. Optic gland surgery led to dramatic behavioral and physiological changes in the mated female. Normally, brooding females rarely ever leave their eggs [17,23,33]. However, after recovering from surgery, glandectomized

females abandoned their clutch and refused to brood. Changes in brooding behavior were not observed after ablation of the subpedunculate lobe [23]. Eventually, these females began to feed again on live prey and showed an increase in body mass. Glandectomized females ultimately lived for 5.75 months longer than their intact counterparts. In some cases, iteroparity was achieved: females mated again and laid a second clutch [33].

Wodinsky called the optic gland and optic gland secretions a "self-destruct" system that ensures the death of the brooding female by the time the eggs are ready to hatch. His experiments demonstrated that, in addition to the optic glands' gonadotropic and gametogenic functions, their secretions contribute to feeding behaviors, maternal care, and post-reproductive death.

Together, these classical studies established the optic gland act as a critical connection between the central brain and the gonads: optic gland activity is essential for the ripening of sexual organs and maintenance of gametogenesis. Maternal behaviors and semelparity depends on the actions of the optic glands. A GNRH-like peptide or other secreted neural factors may serve as the inhibitory signal from the subpedunculate lobe to the optic gland. The gland's secretions promote gonadal growth, maternal care, and ultimately, death. The molecular features of and relationship between the subpedunculate lobe, the optic glands, and the gonads in the octopus are strikingly similar to that of the reproductive axis in vertebrates [38].

Internal anatomy of the optic gland anatomy

Although the optic gland is the center of the octopus neuroendocrine system, little is known about the molecular characteristics or mechanisms of brain regulation of the optic glands. The optic gland hormone(s) have never been identified, and few studies have focused on the

optic gland's internal anatomy. Likewise, mechanisms of hormone production and secretion in the optic gland are not understood.

Aside from the cells associated with vasculature, the optic glands are thought to have only two cell types: large stellate cells (10-15um in diameter) and smaller, glia-like support cells [39]. The stellate cells are thought to be responsible for producing optic gland secretions, while the support cells at the very least establish the connective tissue framework of the gland. Swelling of the optic gland during development is attributed to enlargement of the stellate cells [23]. The support cells do not appear to change morphology even as the secretory state of the gland changes, and neither the stellate cells nor the support cells are known to increase in number during the lifespan of the octopus. Early anatomists posited that the two cell types are homogenously distributed within the optic gland, with no apparent system of organization [4,39,40].

Aims and scope

In recent years, new advances have established *O. bimaculoides* as an attractive model organism for the laboratory study of invertebrate evolution and neurobiology [41]. *O. bimaculoides* is particularly amenable to aquaculture [22]. We are able to acquire wild-caught mated female octopuses with clutches at all stages of embryogenesis. This availability is highly advantageous for the study of post-reproductive behavior as we are able to observe wild-caught octopuses throughout the brooding period. This thesis combines the use of modern bioinformatics, molecular, and analytical chemical techniques with an evolutionary neuroscience perspective to gain a deeper understanding of the octopus neuroendocrine system.

Understanding the composition of the optic gland is the necessary first step in identifying the molecular and neural mechanisms underlying its actions. In Chapter 3, I measure maternal behaviors of wild-caught female octopuses in the laboratory and characterize adult life of *O. bimaculoides* into 4 stages: one period before mating (Non-mated), and three after mating: Feeding, Fasting, and Decline. I find that reproductive behaviors of brooding females are more nuanced than previously described. I perform RNA-sequencing on the optic lobes of female in each these categories to identify transcripts important to the signaling functions of the optic gland. My differential gene expression analysis reveal that the optic gland employs many different signaling systems: instead of a single "optic gland hormone", there likely exist numerous secreted factors to influence maternal physiology and behavior. I characterize steroidogenic, peptidergic, insulin, and catecholamine signaling molecules found in the optic gland transcriptomes.

The complexity of the optic gland signaling systems raised the question of how these factors are produced in an organ with no internal organization and only two types of cells. In Chapter 4, I revisit the matter of optic gland homogeneity by identifying neuropeptide markers and investigating representatives of the optic gland's signaling systems via *in situ* hybridization. These molecular experiments reveal a rich, internal anatomy, one that greatly expands previous anatomical characterization of the optic glands. I describe different regions that are specialized for the production of steroid, peptide, and catecholamine message.

These results reinforce and expand the pituitary-optic gland analogy. Most excitingly, my data demonstrate that the optic gland has signaling functions beyond those described in the pituitary gland. Whereas the pituitary gland produces only peptide signals, my work shows that multiple classes of signaling ligands are present in the optic gland. For example, although steroid

signaling is important for feedback control of the pituitary gland, only downstream targets of the pituitary, such as the gonads and the adrenal glands, produce steroids [37,42].

In collaboration with Dr. Stephanie Cologna at the University of Illinois Chicago, I pursued the putative steroidogenic pathways of the optic gland. Together, we developed a metabolomics discovery assay using liquid chromatography-mass spectrometry, detailed in Chapter 5. We find that the optic glands are abundant in cholesterol metabolites, and utilize a novel approach to identify previously uncharacterized chemical compounds. Through secondary bioinformatic, molecular, and gas chromatography mass spectrometry methods, I assign putative identities to cholesterol metabolites responsible for the behavioral changes seen in maternal octopuses. Most notable among these are 7-ketocholesterol, an oxysterol found to be significantly abundant in female octopus optic gland, and 7-dehydrocholesterol. These findings provide the basis for a working model of cholesterol metabolism in the reproductive axis octopus.

The work described in this thesis is a major step towards establishing *O. bimaculoides* as a neuroethological model for the study of natural reproductive behaviors. Several experiments described herein required the development and application of new analytical tools. In addition, my results make substantial contributions to the mechanistic understanding of the optic gland and octopus maternal behaviors, including death. In Chapter 6, I briefly review the major findings of my thesis and outline several directions of future research that take advantage of the new methodological tools and approaches described here.

CHAPTER 2

Materials and Methods

Octopus Behavioral Analyses and Tissue Collection

Animals and animal facilities

Wild-caught mated and non-mated female California two-spot octopuses (*O. bimaculoides*) were purchased from Aquatic Research Consultants (Catalina Island, CA) and shipped overnight to Chicago, IL.

All work was performed in compliance with the EU Directive 2010/63/EU guidelines on cephalopod use and the University of Chicago Animal Care and Use Committee [43-45]. Mated females were kept in their home dens with clutches as much as possible. Clutches were sparingly separated from females for other experiments. Animals were individually housed in artificial seawater (Tropic Marin) in 20- or 50-gallon aquaria, and offered a daily diet of live fiddler crabs (*Uca pugnax*, Northeast Brine Shrimp, Oak Hill, FL), cherrystone clam meat, and grass shrimp. Water temperature was maintained between 17-21°C and ambient room temperature at 21-23°C. Animal rooms were kept on a 12:12 hour light/dark cycle.

Behavioral Categorization

Upon arrival at our animal facilities, we examined octopuses for signs of senescence, such as pre-existing skin lesions and missing arm tips. We excluded these individuals, which included females with clutches, from further study. Clutches ranged in developmental stage from gastrulation to Stage 11 [46], suggesting there is great variation between egg incubation stage and maternal behavioral state.

Octopuses were kept undisturbed for 4 days so they could habituate to our aquarium setup and recover from the stress of flying. On the 4th day, we began offering live prey items. Each day, females had 4 live fiddler crabs available to them. Animals were observed twice daily (AM and PM) and recorded overnight with a Sony Handycam FDR-AX100 to characterize their behaviors. We observed 20 animals without clutches (non-mated) for at least 4 days before euthanizing and sexing them. 11/20 non-mated animals were males and were excluded from the study (Figure 2.1). In addition, we longitudinally observed 16 brooding females and categorized them into behavioral stages based on the traits detailed in Chapter 3 and summarized in Table 3.1.

Tissue Collection for LCMS

Octopuses were euthanized in 10% ethanol/sea water. Optic glands, optic lobes, and white bodies were harvested within 7 minutes of death, flash frozen on dry ice, and stored at -80°C until extraction. Prior to extraction, tissues were pooled by category and weighed. A volume of 1xPBS equal to the tissue mass was added to the samples. Samples were homogenized by sonication, alternating on and off ice every second for 1 minute.

Tissue Collection for RNA-sequencing

Octopuses were submerged in 5-10% ethanol/seawater for at least 20 minutes to achieve deep anesthesia, then decerebrated (mantle and arms removed from the head) [47,48]. The head was dissected on ice in diethyl pyrocarbonate-treated phosphate buffered solution (DEPC-PBS). Optic glands were accessed between the eyes, harvested, flash frozen in Trizol (Invitrogen), and

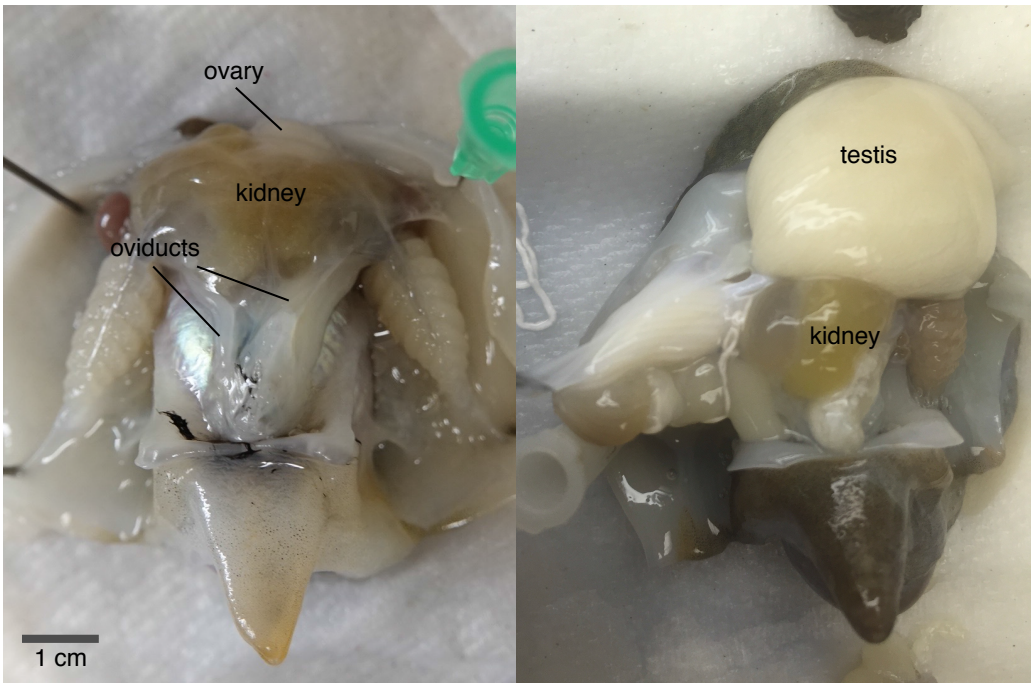

Fig 2.1. Internal anatomy of octopuses. a. Unmated females are positively identified by the ovary and oviducts. The oviducal glands lie deep to the kidney and are not visible in this dissection. b. Sexually mature males have one testis, which stores spermatophores.

stored at -76°C until RNA extraction. Because sexual dimorphism is difficult to observe in our species, animals were definitively sexed after tissue harvest. Only females with mature ovaries, ovarian follicles, and no evidence of fertilized eggs were considered non-mated females.

We also harvested arm tissue from the same cohort of animals. Transverse arm slices corresponding to the 10th row of suckers distal from the mouth on the second arms on the right and left sides were cut into quadrants to facilitate tissue homogenization. Each arm piece was separately flash frozen in Trizol and stored at -76°C until RNA extraction.

Tissue Collection for Histochemistry

Adult octopuses (n=17) were deeply anesthetized in 10% ethanol/ artificial sea water. The white body, a hematopoietic organ, was accessed by removing the top layers of skin on the head between the eyes. Animals were trans-orbitally perfused with freshly thawed 4% paraformaldehyde (PFA) in phosphate-buffered saline (PBS) delivered via a peristaltic pump (Cole Parmer Masterflex) through a 21½ gauge needle (Becton Dickinson). Left and right white bodies were targeted alternately and iteratively throughout the procedure. Following perfusion, the head was dissected from the arms and mantle, then post-fixed overnight at 4°C in 4% PFA. The next day, the central brain, together with the optic lobes, was dissected from the head mass. Brains were cryogenically protected in 30% sucrose/10% formalin in PBS at 4°C overnight, rinsed in 30% sucrose/PBS, and gel embedded in 30% sucrose/gelatin. Embedded brains were sucrose-sunk overnight in 30% sucrose/formalin in PBS at 4°C, hemisected along the oral/aboral axis, and stored at -80°C. The mantles of adult octopuses were further dissected after tissue harvest to confirm sex and reproductive status (Figure 2.1). Only females with mature ovaries, ovarian follicles, and no evidence of fertilized eggs were used for subsequent analyses.

Tissue was sectioned coronally on a freezing sledge microtome (Leica SM2000R) at a thickness of 24 um, collected in diethyl pyrocarbonate (DEPC)-treated PBS, mounted onto Superfrost Plus slides (Fisher), dried overnight at room temperature and frozen at -80°C until use.

In orienting the optic gland cross-sections, ventral refers to the direction of the subesophageal mass (see Figure 4.1b) and corresponds to the lower half of all panels in Figures 4.2-8.

Molecular Biology Methods

RNA extraction and sequencing

Whole optic glands were homogenized with pellet pestles (Fisherbrand) in microcentrifuge tubes. Arm sections were homogenized in a Potter-Elvehjem tissue grinder (Kimble, Rockwood, TN). RNA was extracted using Trizol and PhaseMaker Tubes (Life Technologies Corporation, Carlsbad, CA) following manufacturer's instructions. RNA integrity was checked with a Bioanalyzer 2100 (Agilent). Only samples with clean cephalopod rRNA peaks and little to no evidence of degradation were used. Tissue from the right arm was processed for RNA extraction and sequencing. The left arm was used in two samples of feeding females when RNA quality from the right arm was poor.

Total RNA was polyA-selected and directionally sequenced at the University of Chicago Genomics Facility on an Illumina HiSeq2500 machine, generating 100bp directional paired-end reads with an insert size of 300bp.

PCR isolation of genes

PCR primers (Table 4.1) for genes identified in the octopus genome or transcriptome were designed with MacVector software (version 12.6.0). PCR reactions were conducted using a RoboCycler Gradient 40 (Stratagene). Reaction solutions were incubated at 94°C for 5 minutes before undergoing 35-40 rounds of amplification cycles: 94°C for 1 min, 52-55°C for 1 min, and 72°C for 1.25 minutes. The final elongation step was at 72°C for 10 minutes followed by storage at 9°C. PCR reactions were studied by gel electrophoresis to confirm expected size of products.

Riboprobe preparation

PCR reactions were ligated to pGEM T-Easy plasmid (Promega). Closed inserts were Sanger sequenced by the UChicago Comprehensive Cancer Center DNA Sequencing Facility. Plasmids were linearized by SacII or SpeI (NEB) restriction enzyme digestion to generate an antisense template. Following phenol-chloroform extraction of the template, antisense digoxigenin (DIG)-labeled riboprobes (Roche) were transcribed with SP6 or T7 RNA polymerase (NEB). After transcription, residual template was digested with RNase-free DNase I (Roche) at 37°C for 45 minutes. Riboprobes were EtOH-precipitated twice and stored in 100ul of 100% formamide at -20°C until use.

***In situ* hybridization (n=17)**

Slides were equilibrated to room temperature and post-fixed for 15 minutes in PFA, then washed 3x for five minutes in DEPC-PBS and incubated at 37°C for 30 minutes in proteinase K solution (Roche Diagnostics; 1 μg proteinase K per milliliter of 100 mM Tris-HCl [pH 8.0], 50 mM EDTA [pH 8.0]). After proteinase K digestion, slides were post-fixed for 15 minutes in PFA, washed 3x for five minutes in DEPC-PBS, and stored in hybridization solution (50%

formamide, 5x SSC, 1% SDS, 200 μg/ml heparin, 125 mg/ml yeast RNA, 0.5mg/ml acetylated BSA) at -20°C.

Tissue was allowed to acclimate for at least one hour at 72°C in hybridization solution. Slides were transferred to mailers with 1-2 mg antisense riboprobe in 15mL hybridization solution and incubated overnight at 72°C. The next day, slides were rinsed once in preheated Solution X (50% formamide, 5x SSC, 1% SDS) and washed 3x in Solution X for 45 minutes at 72°C. Slides were washed 3x for fifteen minutes in room temperature TBST (Tris buffered saline with 1% Tween 20) and blocked at room temperature for two hours in 20% DIG buffer (Roche) in TBST.

Anti-DIG Fab fragments conjugated to alkaline phosphatase (AP, Roche) were preadsorbed with octopus embryo powder in 5% DIG buffer in TBST for at least one hour. Following blocking, slides were incubated on a rocker overnight at 4°C in preadsorbed antibody diluted to a final concentration of 1:5000 in 5% DIG buffer in TBST.

The next day, slides were washed 3x for 15 minutes then 2x for 1 hour in TBST. Slides were next washed 3x for 10 minutes in freshly prepared NTMT (100 mM Tris-HCl [pH 9.5], 100 mM NaCl, 50 mM MgCl2, 1% Tween 20). For the color reaction, slides were incubated in nitro blue tetrazolium (NBT, Denville Scientific) and 5-bromo-4-chloro-3-indolyl phosphate (BCIP, Denville Scientific) in NTMT. Color development proceeded at room temperature and was monitored for 1 to 5 days. Reactions were stopped in Stop TE (10 mM EDTA, 10mM Tris pH 7.5) and washed in TBST overnight. Slides were fixed overnight at 4°C, dehydrated through a series of ethanol washes into Histoclear (National Diagnostics) and cover-slipped with Eukitt (Sigma-Aldrich).

Antibody characterization

Characterization of the anti-DIG-AP antibody, including appropriate control experiments, was described previously (Rowell, Mallik, Dugas- Ford, & Ragsdale, 2010). Anti-DIG-AP binds to digoxigenin (Roche Diagnostics, sheep polyclonal, Fab fragments conjugated to alkaline phosphatase, catalog #11093274910, RRID: AB_514497; dilution used is 1:5,000), which is not endogenous to vertebrate tissue. In control experiments, digoxigenin-labeled RNA was omitted from the hybridization mixture. No signal was detected in the absence of digoxigenin-labeled riboprobes (not shown).

Histology

Tissue slides were equilibrated to room temperature and incubated overnight at 72°C in DEPB-PBS to remove gelatin. Following incubation, slides were rinsed twice in DEPC-PBS and once in DEPC-water. Hematoxylin and eosin (H&E) staining was performed with slight modifications to manufacturer's (ScyTek) instructions. Briefly, slides were submerged in hematoxylin for 3.5 minutes, transferred to bluing reagent for 30 seconds, and then to eosin solution for 1 minute.

Microscopy and image acquisition

Images were captured on an Axioskop 40 microscope (Zeiss) or a MZ FLIII fluorescence dissecting microscope (Leica) with attached Zeiss AxioCam HRc camera and Zeiss Axiovision 4.8 software.

Bioinformatic Methods

de novo transcriptome assembly and differential gene expression analyses

Following removal of adapters and low-quality sequences, reads were assembled with the Trinity software platform (v2.4.0) [49]. Both individual and pooled transcriptomes were created (Table 3.2). Gene and isoform expression levels were estimated with RSEM (v1.2.31) [50] and differential expression was analyzed with edgeR (v3.7) [51]. Heatmaps were created in R with the heatmaps.2 function and colored with palettes from the RColorBrewer package.

In the optic gland transcriptomes, 1,198 Trinity transcripts showed at least a 4-fold change between any two of the behavioral stages, at a p-value of 0.001. A branching diagram illustrating the relationship between differentially expressed genes was created based on Euclidean clustering (Figure 3.5). The tree was cut at a height of 0.3, which identified 25 subclusters. 20 genes from subclusters of interest (Figure 3.9) were confirmed by PCR amplification.

Identification of neuropeptide precursors

The unmated female optic gland transcriptome [52]1was screened for preproneuropeptide sequences using two parallel methods. 1) We performed a search for neuropeptides focusing only on the most highly expressed transcripts of the optic gland. We examined all transcripts with FPKM (fragments per kilobase of transcript per million mapped reads) value greater than 1000 with a custom Perl script designed by Dr. Felipe Aguilera [53]to detect specific protein sequence motifs in fastp files. We queried our data with the following common cleavage site: [KR]-[KR]-x(2,35)-[KR]-[KR]-x(2,35)-[KR]-[KR]-x(2,35)-[KR]-[KR]. Cleavage probabilities were determined by NeuroPred [54], with mollusc as the model predictor. Putative cleavage sites with a probability of cleavage below 0.9 were eliminated. We checked sequences for the presence of a

signal peptide with SignalP [55]and confirmed identity of putative neuropeptides using BLASTP against the *O. bimaculoides* genome and non-redundant sequences in NCBI [56]. 2. We directly queried the optic gland transcriptome using all known invertebrate neuropeptides deposited in Neuropred (current as of June 8th, 2018) as bait. The e-value cutoff for TBLASTN search was set at 1e-05. The positive transcriptome hits were manually curated and compared against octopus genome sequences [41]. Signal sequence and cleavage sites for candidate neuropeptides were determined as described above.

Analytical Chemistry Methods

Sterol standards

Synthetic heavy carbon standards (13C-progesterone and 13C-cholesterol), cyasterone, and cortisol standards were purchased from Sigma Aldrich (Germany). Synthetic cholesterol, progesterone, estradiol standards were acquired from Steraloids (Newport, RI). HPLC grade methanol, water, ammonium formate, isopropanol, hexane, and acetonitrile were purchased from Sigma Aldrich.

Standard Curves

Conventional flow standard curves were created for the heavy carbon internal standards and cyasterol standard using freshly-prepared stock solutions prepared in 100% MeOH. Data for the standard curve were generated by liquid chromatography tandem mass spectroscopy (LCMS) analysis using an Agilent 1290 Infinity II ultra high-performance liquid chromatograph coupled with an Agilent 6545 Q-TOF LC-MS/MS instrument. Ions were generated by electrospray ionization and monitored in positive ion mode. The ultra high-performance liquid chromatograph system used a reverse-phase chromatograph (Zorbax C18 4.1mm x 50mm column) beginning

with 85% mobile phase A (60/40 acetonitrile/isopropanol with 10mM ammonium formate) and 15% mobile phase B (90/10 isopropanol/water with 10mM ammonium formate) with a linear gradient to 50% mobile phase B over 2 minutes, followed by another linear gradient to 80% mobile phase B over 18 minutes. After 20 minutes, mobile phase B was increased to 99% and run isocratically for 3.5 min.

We used 4-7 concentration points (0.1-100pmol/ul on column) to construct calibration curves for each internal standard. All standard concentrations used were within the linear detection range of the LCMS instrument. Sample was delivered by flow injections (5ul) at a rate of 10ul/second. Each concentration was run in triplicate with a blank run in between. Neutral, dehydrated, and protonated exact masses (Table 2.1) were calculated manually using the Scientific Instrument Services, Inc tool (www.sisweb.com) and verified using the Lipid Maps database (www.lipidmaps.org). EICs were extracted using Agilent MassHunter Qualitative Analysis and linear regression analysis was performed using the area under the curve versus standard concentration.

Sterol	Neutral Mass	Dehydrated Ion $[M\text{-}H_2O+H^+]$, *m/z*	Protonated Ion $[M+H^+]$, *m/z*
Cortisol	362.46	345.2060	363.2166
Cholesterol	386.65	369.3516	387.3621
7-Dehydrocholesterol	384.64	367.3359	385.3465
Estradiol	272.38	355.1743	273.1849
27-hydrocholesterol	402.66	385.6447	403.6673
7-ketocholesterol	400.65	383.6347	401.6573
Pregnenolone	316.48	299.4647	317.4893
Progesterone	314.47	297.2213	315.2319
^{13}C-Cholesterol	389.36	389.3649	390.3728
^{13}C-Progesterone	317.23	300.2319	318.2425
Cyasterone	520.65	503.3009	521.3114

Table 2.1. Sterol mass spectrometric identification.

Sterol extractions

We tested 4 extraction methods on male optic lobe tissue. Prior to extraction, heavy carbon internal standards were added. At the end of each protocol, dried extracts were stored at -80°C until resuspension and injection onto the UHPLC column.

Methanol extraction: 50ul of cold MeOH was added to 20ul homogenized tissue and sample was incubated on wet ice for 15 min. Sample was centrifuged for 15 min at 14,000 rpm at 4°C. The supernatant was removed and evaporated in a CentriVac at 42°C. Pellet was saved for subsequent IPA extraction.

MeOH/IPA extraction. 50ul cold MeOH/IPA (1:1 v/v) was added to homogenized and MeOH-extracted pellet. Sample was incubated on wet ice for 15 min, then centrifuged for 15 min at 14,000 rpm at 4°C. Supernatant was removed and evaporated on a Speedvac at 42°C.

ACN/hexane extraction. Extraction of sterols was carried out using acetonitrile and hexane with some modifications of the Maeda protocol [57]. 100ul acetonitrile was added to sample, then centrifuged at 10,160 g for 10 min at 4°C. Supernatant was removed, and 30ml hexane was added, followed by 5 minutes of shaking. Supernatant was collected and evaporated on a Speedvac at 42°C.

MTBE extraction. Extraction of sterols was carried out using a biphasic solvent system of cold methanol, methyl *tert*-butyl ether (MTBE), and water with some modifications of the Feihn protocol [58]. In brief, 225ul of cold MeOH was added to 20ul homogenized tissue sample in a 1.5ml Eppendorf tube, then vortexed for 10s. Then, 750ul cold MTBE was added, followed by 10s vortexing, and 6 min shaking at room temperature. Phase separation was induced by adding 188ul MS-grade H2O and vortexing for 20s. The sample was centrifuged for 2 min at 14,000

rpm at 4°C, and the upper organic phase was collected in two 350ul aliquots and evaporated in a Speedvac at 42°C.

Sterol profiling by time-of-flight mass spectrometry

Mass spectrometry was performed on an Agilent Accurate Mass 6545 Quadrupole Time of Flight (Q-TOF) mass spectrometer equipped with dual-nebulizer electrospray ion source and robotic autosampler.

All samples were resuspended in 80ul of 100% MeOH and injected at a flow rate of 10ul/minute. Typical sample volumes of 20ul allowed 30 minutes of stable electrospray time. Fragments were detected within the *m/z* range of 100-1700. Each ms/ms spectrum was acquired by auto-segmentation with a cycle time of 3.1 sec. Three technical replicates were run for each sample. Sterol species were identified using a custom MS1 database created in MassHunter Personal Compound Database and Library Manager (Agilent, B.08.00), Global Natural Products Social Molecular Networking (GNPS, UC San Diego), and the LipidBlast *in silico* library [58].

Metabolomic discovery workflow

Molecular feature extraction

Molecular features of detected compounds were extracted with MassHunter Qualitative Analysis software (Agilent). To select for small molecules, target mass of compounds was set at between 250-1000 m/z with a mass defect of +/- 5ppm. Raw data files were imported into MassHunter Profinder (Agilent) for recursive feature extraction and the resulting compound families were manually curated based on height, abundance, peak shape, and mass. The final data set comprised centroided spectra from the final filter.

Fold-change analysis & spectral matching

Centroided data files were imported into MassHunter Profiler Professional for significance testing. Low abundance compounds (<5000 counts) and compounds appearing in <2 samples in each group were filtered out. Student's t-test was conducted on the control (unmated) and experimental (mated) group with a p-value cut-off of 0.01. The lower bound for fold-change cut-off was set at 4.

Individual entity lists were created for compounds found to be significantly abundant in either condition, then exported. Spectral peaks of differentially abundant compounds were submitted to Metlin (https://metlin.scripps.edu/) for MS/MS matching, with a precursor tolerance set at 20ppm.

Sterol measurements

Sterol metabolites were quantified by a clinical assay for cholesterol biosynthetic intermediates at the Biochemical Genetics Laboratory at Kennedy Krieger Institute. Gas chromatography/mass spectrometry was used to quantify levels of cholesterol, cholestenol, desmosterol, 7-dehydrocholesterol, 8-dehydrocholesterol, delta-7-lathosterol, dihydrolanosterol, and lanosterol in whole tissue samples of optic lobe, white body, and optic gland from one unmated female and one mated female.

CHAPTER 3

Signaling pathways implicated in octopus maternal behaviors

Abstract

Post-reproductive life in the female octopus is characterized by an extreme pattern of maternal care: the mother cares for her clutch of eggs without feeding until her death. These maternal behaviors are eradicated if the optic glands, the octopus analog of the vertebrate pituitary gland, are removed from brooding females. Despite the optic gland's importance in regulating maternal behavior, the molecular features underlying optic gland function are unknown. Here, we identify major signaling systems of the *Octopus bimaculoides* optic gland. Through behavioral analyses and transcriptome sequencing, we report that the optic gland undergoes remarkable molecular changes that coincide with transitions between behavioral stages. These include the dramatic up- and down-regulation of catecholamine, steroid, insulin, and feeding peptide pathways. Transcriptome analyses in other tissues demonstrate that these molecular changes are not generalized markers of senescence, but instead, specific features of the optic glands. Our study expands the classic optic gland-pituitary gland analogy and more specifically, it indicates that, rather than a single "self-destruct" hormone, the maternal optic glands employ multiple pathways as systemic hormonal signals of behavioral regulation.

Introduction

Octopuses and other soft-bodied (coleoid) cephalopods are short-lived, semelparous animals: adults die after a single reproductive period [15]. Typically, octopuses lead solitary lives and come together only to mate [4]. Females store sperm in specialized compartments in

their oviducal gland [4]. As eggs are laid, they pass through the oviducal gland and are fertilized. The female octopus anchors her eggs to substrate with mucal secretions and tends to her clutch as the embryos develop. During this brood period, she rarely leaves her clutch and abstains from food. By the time of hatching, the female dies [3,4,59].

In a key experiment from 1977, Jerome Wodinsky surgically resected optic glands from female Caribbean two-spot octopuses (*Octopus hummelincki*) that were brooding their clutches of eggs and had stopped feeding. Removal of the optic glands led to substantial behavioral changes: females abandoned their clutches, resumed feeding, gained weight, and some even mated again. Glandectomized individuals lived 5.75 months longer than their intact counterparts, leading Wodinsky to conclude that the optic gland and optic gland secretions constituted an octopus "self-destruct system" [33]. The molecular features underlying optic gland signaling have not been explored with modern investigative techniques and the putative "optic gland hormone" [4] remains unidentified to this day.

Classic work from Wells and Wells (1959) established that the optic glands are also necessary for the proper timing of sexual maturation. The optic glands are situated on the optic stalks, nestled between the large kidney-shaped optic lobes and the central brain. They are known to receive inhibitory signals from the subpedunculate lobe of the supraesophageal brain [13,23]. At sexual maturity, this inhibition is released; the optic gland swells in size and darkens in color [35]. This change causes the gonads and reproductive organs to mature [23]. Wells and Wells (1969) posited that the optic glands are the octopus analog to the vertebrate pituitary gland, acting as intermediaries between brain control centers and peripheral targets.

To gain insight on the molecular features underlying post-reproductive behavioral changes, we sequenced optic gland transcriptomes of the California two-spot octopus, *Octopus*

bimaculoides. *O. bimaculoides* lives off the coast of southern California and northern Mexico. We could observe normal maternal behaviors of this species in a laboratory setting. These behavioral findings guided our optic gland RNA sequencing and interpretation of bioinformatics results.

Results

Adult life in the female *O. bimaculoides* can be divided into 4 behavioral stages

Sexually mature female octopuses are known to be active predators [3]. We confirmed this behavior in non-mated females in the lab: these animals spent time outside of the den (Figure 3.1A and Table 3.1) and primarily hunted through a visually-directed jet-propelled "pounce" (Figure 3.1B) [4]. The female watched the prey out of one eye, then bobbed her head up and down, likely acquiring depth information. Even while moving her head, her pupil was kept perpendicular to gravity (Figure 3.1A). Following a swift pounce, prey was captured in the interbrachial web (Figure 3.1B and C). Non-mated females consumed 1.31±0.76 (mean ± standard deviation) crabs a day, sometimes skipping a day between meals.

Mated females in the first stage of brooding actively tended their clutch by guarding their den, stroking eggs with their suckers, and blowing water over the eggs with their funnel [3,4]. In the lab, feeding mated females consumed 1.17±0.70 crabs per day, with fewer than 3 days without a meal. Feeding females, however, rarely left their egg clutches. Instead of capturing prey by stalking and pouncing, feeding females peered out of their dens with one eye and grabbed prey as they moved passed the mouth of the den (Figure

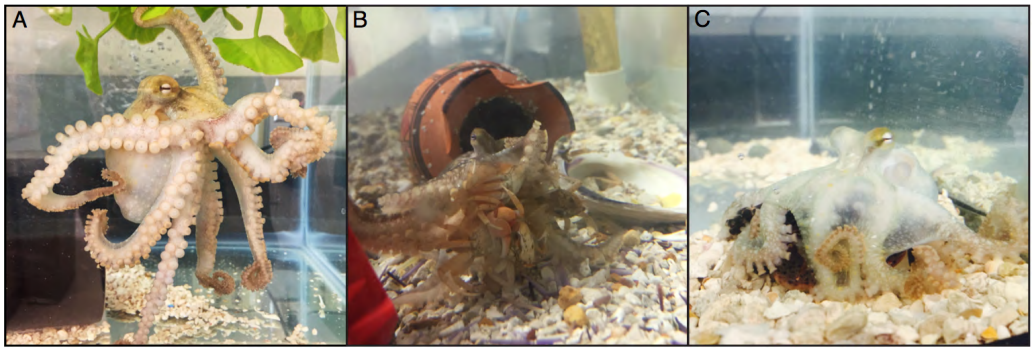

Fig 3.1 Non-mated, sexually mature females are active predators that hunt live prey. A) Females in this stage spend time outside of their home den. B) Non-mated females use visual direction to strike prey with a “pounce,” viewed here from the front. C) The webbing between the arms is spread wide to capture prey. Several fiddler crabs may be restrained under the interbrachial web at one time.

Stage	Traits
Non-mated	Actively hunts and consumes live prey: on average 1.31±0.76 crabs per day, sometimes skipping 1-2 days between meals Mature ovary and ovarian follicles No evidence of fertilized or developing eggs
Feeding	Consumes, but does not pursue, live prey: on average 1.17±0.70 crabs per day, sometimes skipping 1-2 days between meals Actively broods clutch of eggs by blowing water over them with funnel and cleaning them with suckers Extremely den-bound, exhibiting reluctance to leave the den, even for brief periods of time
Fasting	Abstains from capturing live prey or consuming any food for 4 consecutive days and never resumes feeding again Ongoing brooding Ongoing den-bound tendencies
Decline	Ongoing fasting Exhibits at least 2 of the following signs of physical deterioration: • skin lesions on the mantle, arm webbing, or head • missing arm tips or suckers • degradation of the vestibular-ocular reflex • retraction of skin around the eyes • extended bouts of self-grooming Spends considerable time roaming outside of the den Ends with death of female outside of the den

Table 3.1. Octopus female reproductive life is characterized by four stages of behavior.

3.1A and B). The presence of empty crab carapaces provided confirmation that feeding females consumed food, rather than merely capturing and killing prey, which has been reported in other species [8]. On average, mothers fed for 8±2.71 days before starting to fast.

Females in the second stage of brooding continued to care for eggs but abstained from feeding, even though live prey items were available at all times (Figure 3.2C). Females who stopped feeding for 4 consecutive days were never observed to feed again, and we grouped these animals into the fasting stage.

After 11±8.49 days, fasting mothers began a rapid decline. Behavioral signs of decline, some of which have not been described previously, were observed before physiological signs (Figure3A): females left their clutches and spent time outside of the den, languidly sitting on the bottom of the tank or persistently slamming into the corners of the tank. The latter action led to the rapid formation of deep avulsions on the mantle or arms that did not heal (Figure 3.3B and C). Females also engaged in excessive self-grooming behaviors. Normally, octopuses run their first pair of arms over their mantles and head to remove ectoparasites and debris [17]. Decline mothers moved all of their arms to groom, but often arms would only pass over other arms, creating a turbulent mass of entangled limbs (Figure 3.3A). In a few cases, this over-grooming behavior was directly followed by self-cannibalization of the arm tips or suckers (Figure 3.3B and C). Physiological features of females in decline included a retraction of the skin around the eyes, general paling of skin color, and loss of motor tone [59]. In addition, the pupils gradually lost their horizontal orientation with respect to gravity, raising the possibility that the central systems responsible for the vestibulo-ocular reflex deteriorate during this stage.

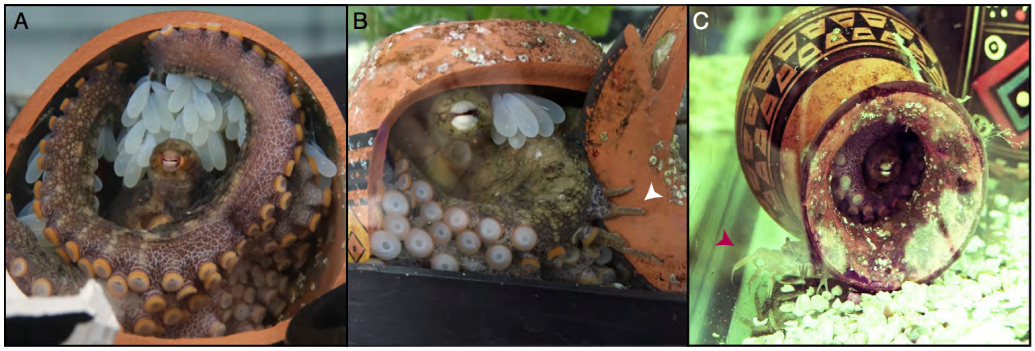

Fig 3.2 Brooding females feed and then fast. A) In the first stage of brooding, females actively tend to their eggs and feed. The pupils of feeding females remain perpendicular to gravity. B) Feeding females capture and kill live prey, but only without leaving the home den. White arrowhead indicates the legs of a captured fiddler crab extending from beneath the arms. C) Fasting females continue tending to their clutch but abstain from feeding even when live prey (red arrowhead) are within reach.

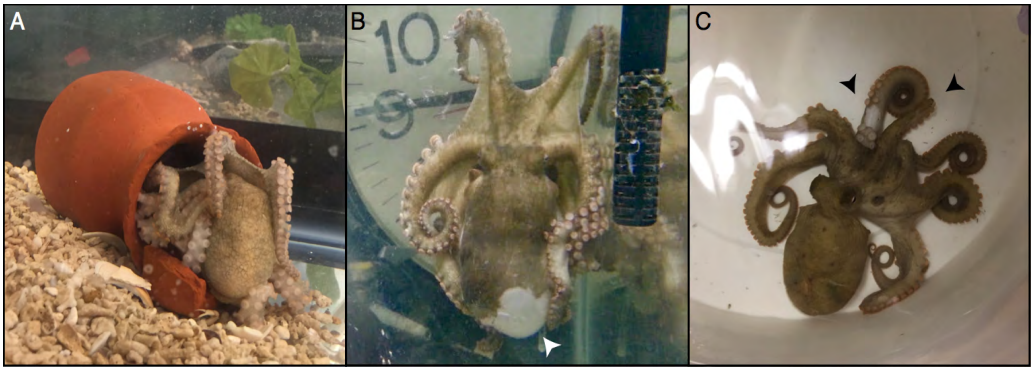

Fig 3.3 Females in decline continue fasting and undergo rapid senescence. A) Behavioral signs of decline include spending time outside of the home den and recruiting all the arms in bouts of aberrant, grooming-like behavior. Females also show physiological signs of decline, such as an apparent loss of muscle tone and unhealed wounds. B) Female with a patch of missing skin at the distal end of her mantle (white arrowhead). C) Female with several rows of missing suckers and a missing arm tip (black arrowheads), presumably from self-cannibalization.

These behavioral changes extend well beyond those seen in starving octopuses: in a laboratory setting, *Octopus vulgaris* females can survive over 38 days of fasting, and individuals who have lost substantial body mass remain alert and active (Wells and Wells 1975). In our study, all mated females progressed from feeding to fasting to decline before dying: that is, mated females did not transition from feeding directly to decline without fasting, and females did not die without showing indications of decline. This progression is reminiscent of what has been reported in male octopuses in captivity, though in males, the relation between these behavioral changes and reproductive state is less clear (Anderson 2002). Our observations suggest that after mating, female octopuses undergo a series of near-requisite behavioral transitions before death.

Transcriptomes of brooding females implicate many signaling systems in optic gland function.

We assembled transcriptomes of left and right optic glands harvested from multiple individuals in each of the 4 stages (Table 3.2). Our assembled transcriptomes showed that the optic glands from non-mated animals were the most different from the other optic gland samples (Figure 3.4). After estimating transcript abundance with RSEM, we identified 1,198 differentially expressed transcripts with edgeR and grouped them into 25 subclusters (Figure 3.5). Wodinsky's work suggested that optic gland signaling changes steadily over time until reaching a threshold that triggers fasting and later death [33]. In selecting subclusters for further study, we were guided by two criteria. We excluded 12 subclusters that showed a departure from monotonicity: for example, when expression peaked in only the feeding or fasting stages (Figure 3.6). Another 5 subclusters demonstrated the most marked transcript enrichment or impoverishment at the decline stage, the last stage of brooding before death

Transcriptome	# of libraries prepared	Total Trinity 'Genes'	Total Trinity Transcripts	N10 (bp)	N50 (bp)	Average Contig Length (bp)	Total Assembled Bases (bp)
Unmated Female Optic Gland	3	267380	314115	4012	882	604.80	189975279
Feeding Mom Optic Gland	3	290774	344673	4078	909	616.68	212552829
Fasting Mom Optic Gland	3	254893	301599	4011	938	627.42	189228407
Decline Mom Optic Gland	2	217478	261725	4554	1165	688.47	180189329
Combined Optic Gland	--	598083	706186	3897	767	574.65	405807628
Unmated Female Arm	3	120017	189097	5771	1781	904.15	170971875
Feeding Mom Arm	3	296853	406986	5196	1165	676.91	275491458
Fasting Mom Arm	3	183259	278194	5683	1621	823.35	229050350
Decline Mom Arm	2	153752	233040	5514	1650	841.44	196090319
Combined Arm	--	493537	686453	4485	959	639.22	438793048

Table 3.2. *O. bimaculoides* optic gland transcriptome assembly summary. Whole optic glands and transverse arm sections were harvested (see Methods). Separate libraries were prepared for each sample, and reads were later concatenated for transcriptome assembly. Statistics are based on transcript contigs. Total Trinity 'genes' refers to the number of transcript clusters generated by the assembly (isogroups), while Total Trinity Transcripts indicates the number of isoforms (isotigs). The Nx length statistic indicates that at least x% of the assembled transcript bases are found on contigs that are of at least Nx length; for example, at least 10% of the assembled bases in the unmated female optic gland transcriptome are found on transcript contigs that are at least 4012 bp long.

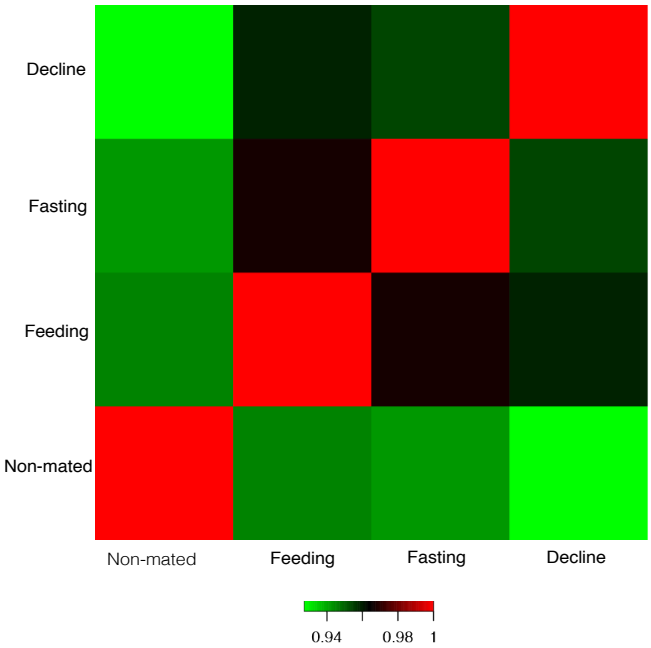

Fig 3.4 Behavioral stage correlation matrix heatmap.

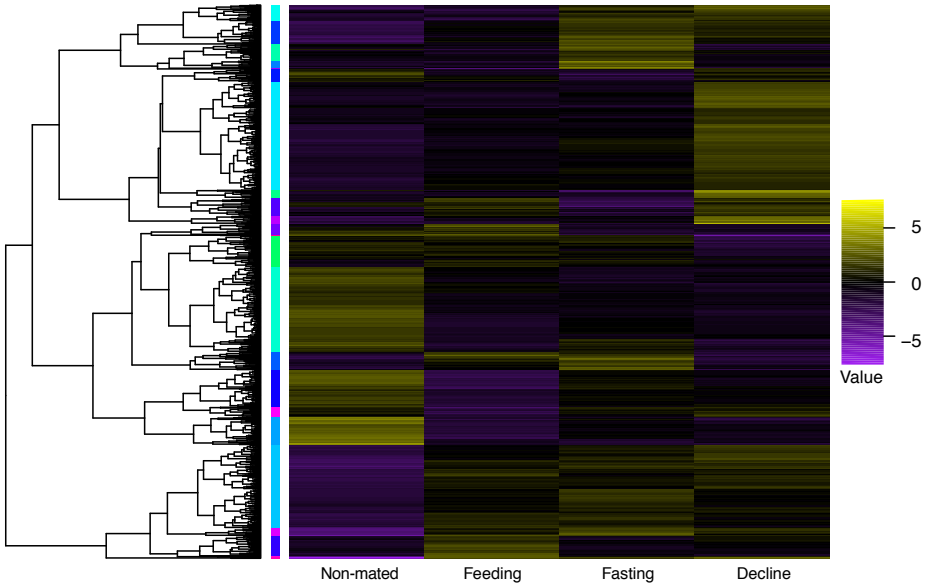

Fig 3.5 Transcripts show significant fold-change between different stages of adult life. Heatmap is based on FPKM values. Transcript similarity, clustered by Euclidean distance, is shown on the left. The 25 subclusters created by “cutting” the tree at 30% are highlighted by vertical bars.

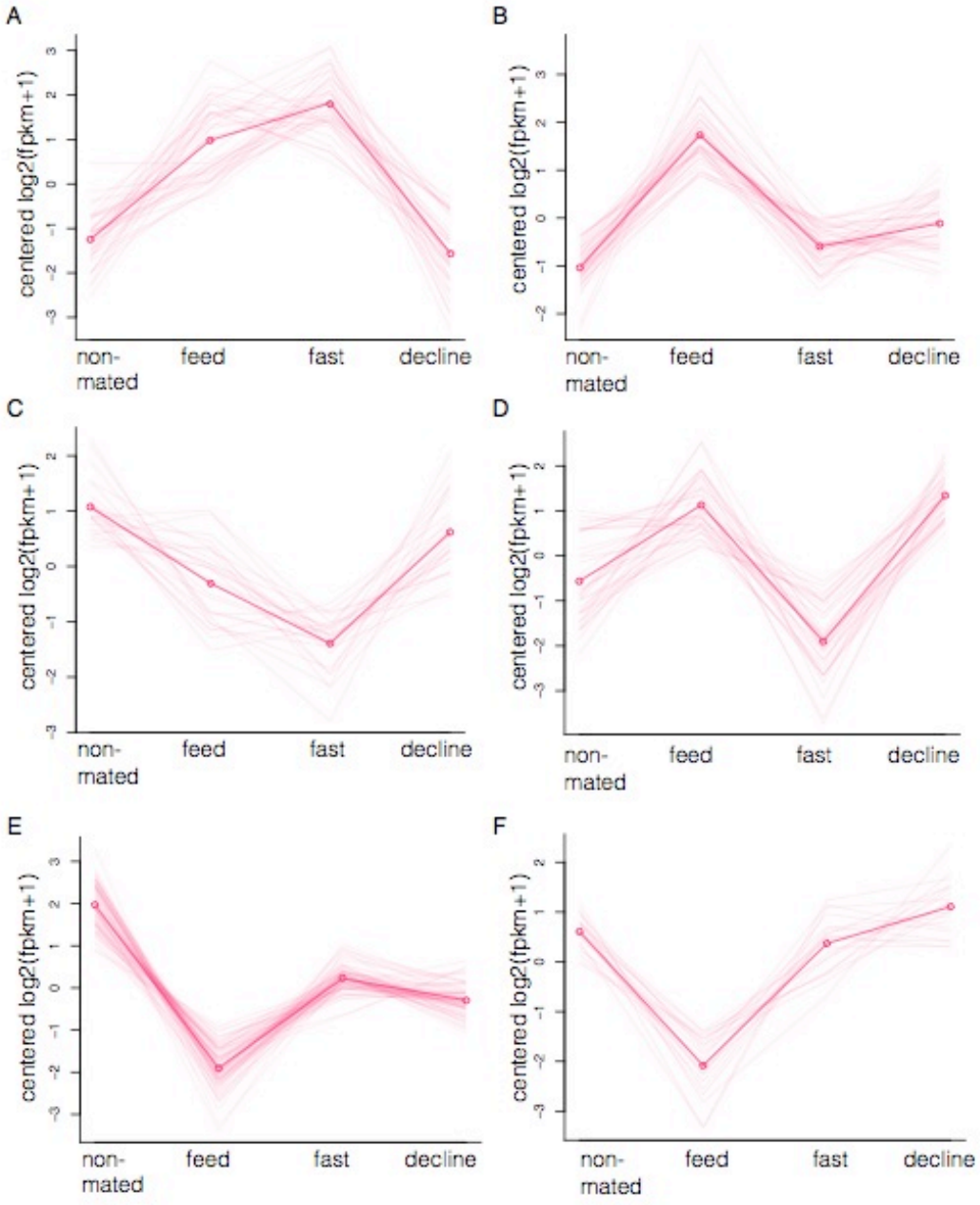

Fig 3.6 Subclusters eliminated due to departure from monotonicity.

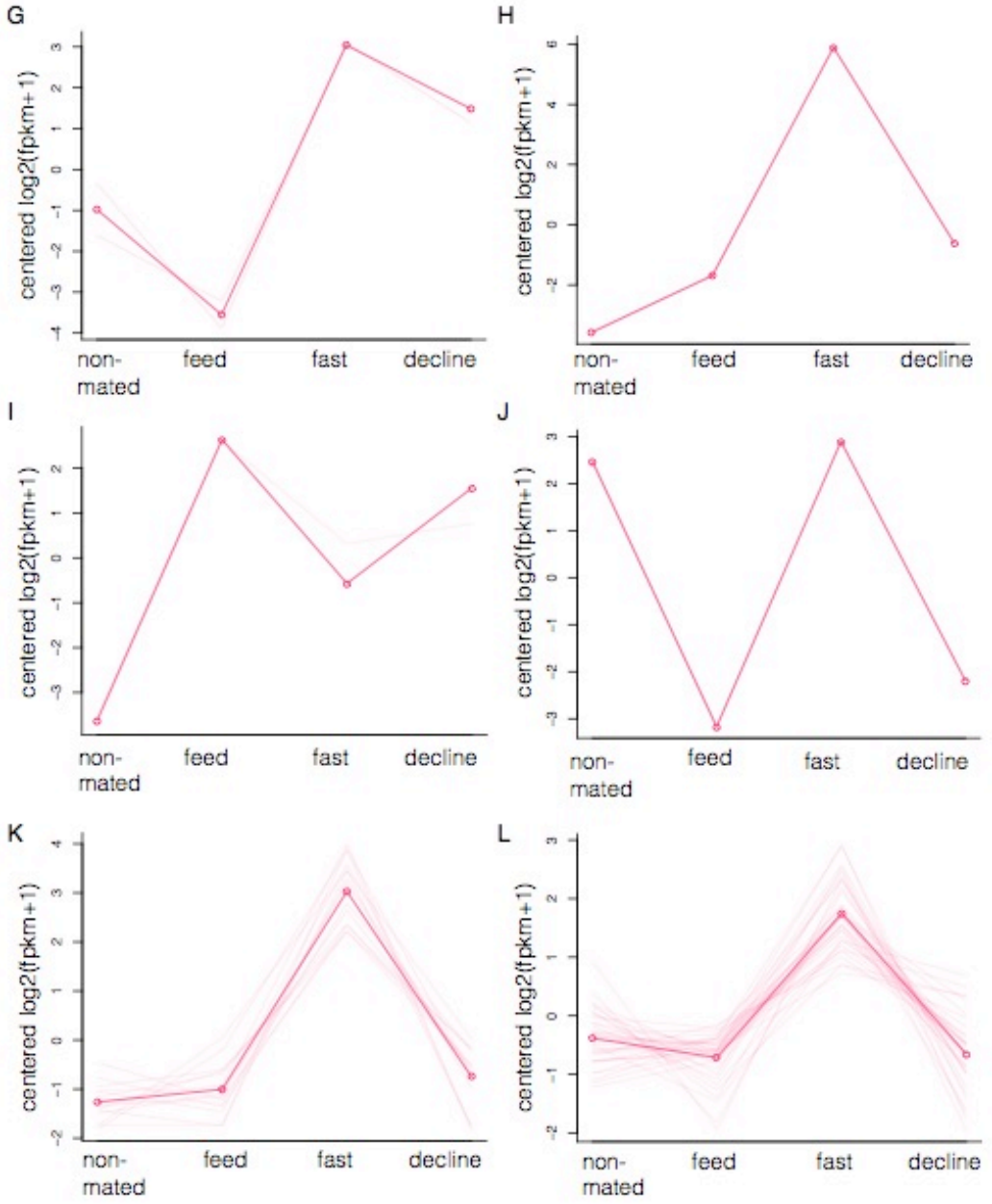

Fig 3.6 continued

(Figure 3.7). Because of sample scarcity (only 2 RNA-sequencing samples in decline stage and a limited ability to pursue follow-up studies), we did not explore these subclusters further. Five additional clusters showed monotonic changes and were studied with BLASTP as described below (Figure 3.8). No candidate signaling molecules were identified in these five clusters. In total, we excluded 855 genes in 22 subclusters from further analyses.

We focused on the 343 remaining genes in 3 subclusters. Among these subclusters (Figure 3.9), we saw dramatic transitions in differential gene abundance across behavioral stages. Two subclusters showed increases in expression over time (Figure 3.9A and B), while the third showed a drop in expression at the non-mated female to feeding mated female transition (Figure 3.9C).

We used BLASTN, BLASTP, and PFAM [56,60] to identify transcripts (Figure 3.10). In all clusters examined, there were many housekeeping genes, such as actin and collagen. We also found predicted proteins with no homology to genes of other species in available databases (downloaded October 28, 2015). These uncharacterized genes may represent octopus- or cephalopod-specific proteins. All three clusters did, however, contain a number of transcripts of particular relevance to optic gland biology.

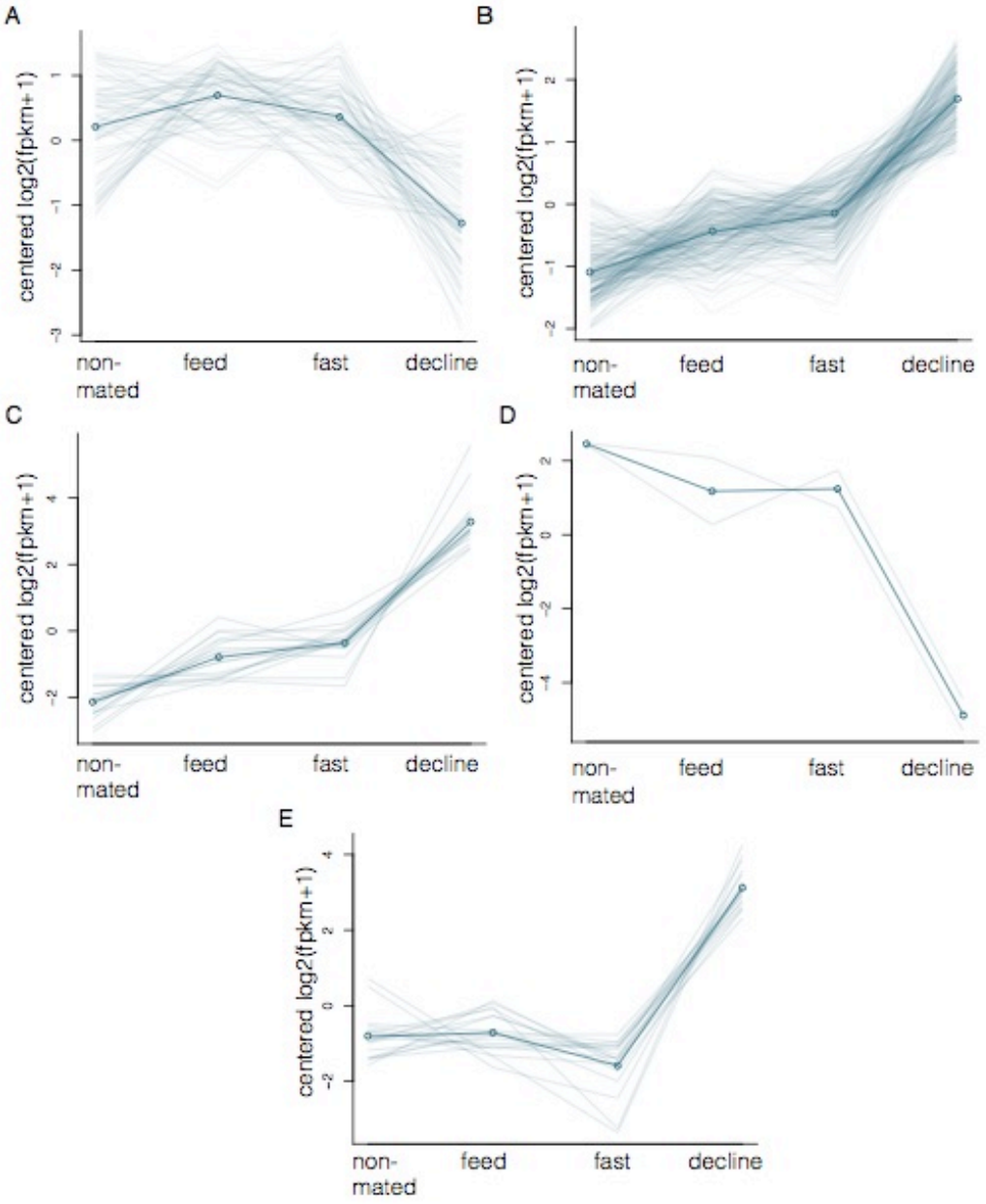

Fig 3.7 Subclusters eliminated because the changes were most marked in the decline stage.

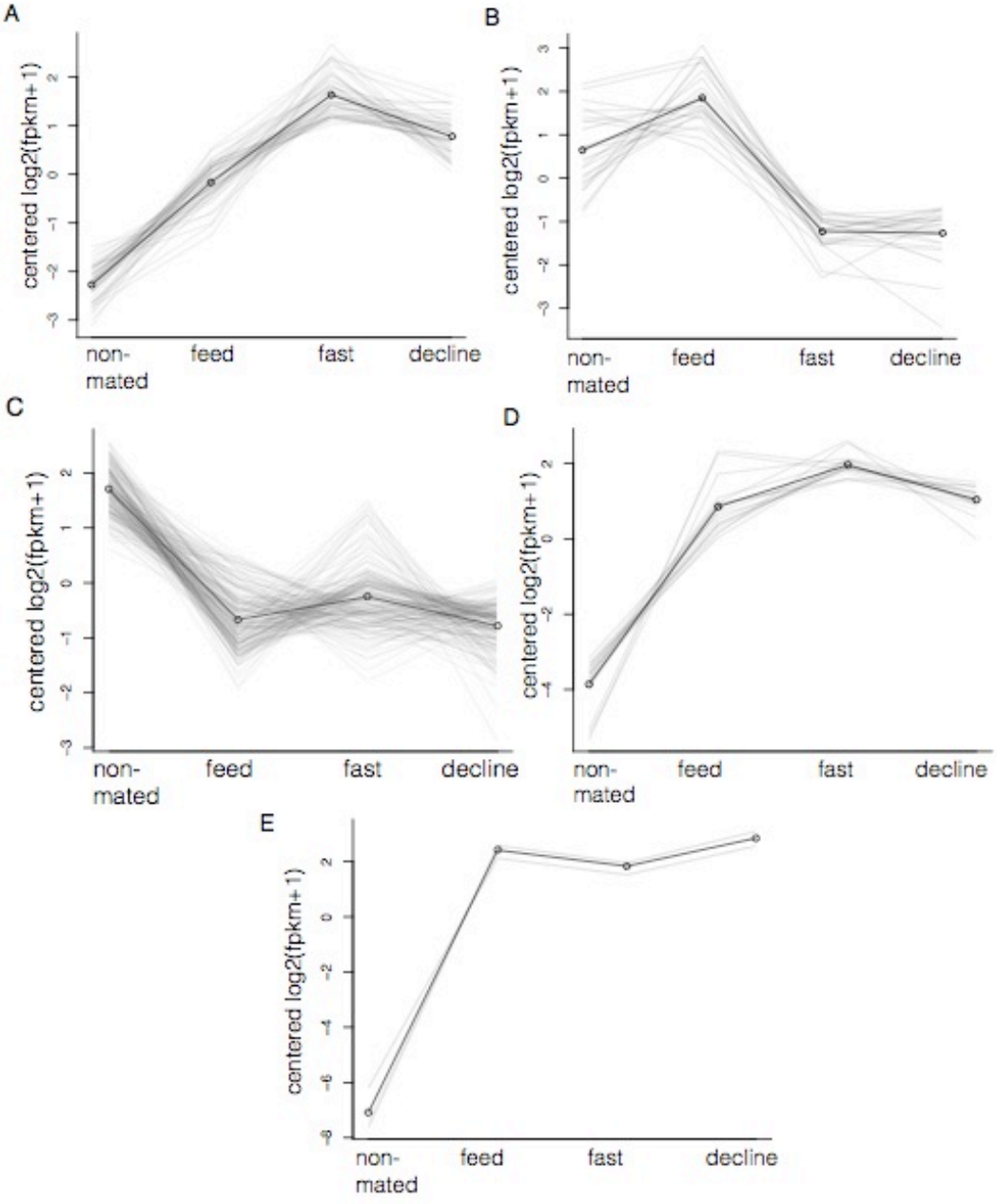

Fig 3.8 Subclusters subsequently eliminated from further consideration, as described in the text.

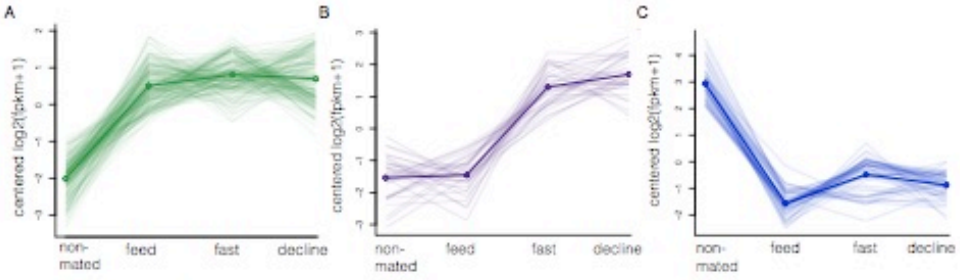

Fig 3.9 Cohorts of genes are differentially expressed across behavioral stages. Green and purple subclusters identify genes that increased in abundance as the maternal stages progressed (A and B, respectively), while the blue subcluster illustrates genes that decreased over time (C).

Genes that increase in abundance after mating and remain elevated through the maternal stages (Figure 3.10A, green cluster)

Although the optic gland is regarded as a neuroendocrine organ, its mechanisms of secretory release are unknown. We found transcripts implicated in neural signaling that increased in abundance after mating and remained elevated through all brooding stages (Figure 3.9A and Figure 3.10A): synaptotagmin 12, synaptotagmin 15b, and clathrin. Huntingtin-interacting protein (*HIP1*) and coronin showed a similar expression profile. Although not included in classical models of synaptic transmission, proteins encoded by these two transcripts have in recent years been found to be important for aspects of neuronal signaling [61,62]. We also saw increases in selected neurotransmitter receptors (Figure 3.10B), including an alpha subunit of a nicotinic acetylcholine receptor, and G-coupled protein receptors similar to octopamine and neuropeptide S receptors in other species. Finally, enzymes implicated in steroid biogenesis were present in this subcluster (Figure 3.10C). These results suggest that the optic gland is a site of active signaling during the maternal period, and that the nature of this signaling is different from that of unmated female optic glands.

Genes that increase with the transition from feeding to fasting (Figure 3.10B, purple cluster)

In this subcluster, we found that *ImpL2*, which encodes an insulin-like growth factor binding protein (IGFBP), is enriched in the optic glands of fasting and decline animals (Figure 3.10B and 3.11D). This transcript is joined in expression dynamics by two others, tribbles homolog 1 (*TRB1*) and an additional isoform of synaptotagmin.

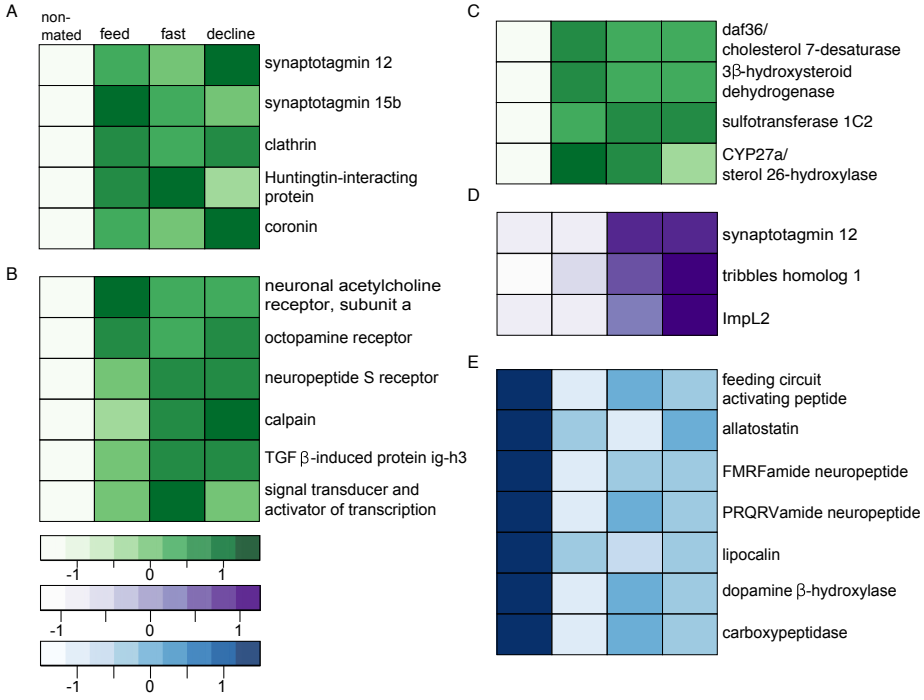

Fig 3.10 Expression profiles of differentially expressed genes important to optic gland signaling. Heatmap colors correspond to cluster colors depicted in Fig 4. Columns are organized as designated at the top of in panel A. Color key values refer to row z-scores.

Genes that decrease with the transition from unmated to mated (Figure 3.10C, blue cluster)

As in the other subclusters, we found genes encoding proteins involved in cell signaling (Figure 3.10E), such as lipocalin and dopamine beta-hydroxylase. Particularly notable in this subcluster are the feeding circuit-related neuropeptides and a carboxypeptidase (Figure 3.10E).

Are molecular changes of the optic glands a reflection of global changes in gene expression?

The abundance of genes encoding neuropeptides in the non-mated optic gland and their subsequent depletion in mated females motivated us to investigate whether molecular changes in the optic gland were mirrored in other tissues of the body. Many of these tissues were sampled in the arm transcriptomes, including axial nerve cords, suckers, muscles, chromatophores, and skin. Using BLASTP and TBLASTN, we baited the arm transcriptomes from all behavioral stages with the genes that were significantly enriched in non-mated optic glands (blue cluster, Figure 3.10C and 3.11E). We were unable to recover any of these optic gland neuropeptides in the arm transcriptomes.

Discussion

With their large central nervous systems and wide range of behaviors, coleoid cephalopods have long fascinated neuroscientists. Pioneering work from Wodinsky and Wells and Wells established that the octopus reproductive axis is similar to that of the vertebrate hypothalamic-pituitary-gonadal axis [33,35]. The optic gland, analogous to the pituitary gland, is the fulcrum of the octopus reproductive axis; it is responsible for innate reproductive behaviors and post-reproductive death. In this study, we confirmed that maternal behaviors can be observed

in the lab, including, most importantly, a period of feeding while brooding that precedes the fasting that typically defines the maternal period in octopuses [3,15].

Our transcriptomic analyses reveal a molecular portrait of the optic glands at the distinct behavioral stages of adult female octopus life. In particular, we found that reproduction and the onset of fasting trigger major transcriptional activation in the optic glands. Most importantly, multiple signaling systems of the optic glands, including catecholaminergic, peptidergic, and steroidogenic pathways, are implicated in these behaviors.

Optic Gland Signaling Systems

Feeding peptides

Circulating neuropeptides have been extensively studied in molluscan feeding and reproductive systems [63,64]. Neuropeptides can influence feeding behaviors through control of motor circuits or modulation of arousal or satiation [65]. Strikingly, we found octopus homologs of these neuropeptides enriched in the optic glands of non-mated female as compared with those of brooding females: feeding circuit activating peptide (*FCAP*), allatostatin, FMRFamide, and PRQFVamide. The latter 3 peptides have been shown to inhibit feeding behaviors in a diverse range of animals. In Aplysia, FMRFamide and its related neuropeptides inhibits closure of the radula muscle during feeding [66] and in mice, FMRFamide reduces feeding in food-deprived individuals [67]. PRQFVamide decreases the excitability of specific neurons in the buccal ganglion feeding central pattern generator and has an overall inhibitory effect on feeding [68]. Allatostatin inhibits feeding in Drosophila by mediating the balance between adipokinetic hormone and insulin-like peptides [69]. FCAP, on the other hand, initiates rhythmic feeding motor programs and may be responsible for food-induced arousal [70].

These data suggest that signaling from an ensemble of neuropeptides tightly controls the feeding behaviors of non-mated animals. In many animals, mechanisms controlling feeding and reproduction are tightly linked and enable metabolic shifts as the individual transitions from growing and maturing to reproduction and tending to young [13]. Drosophila females, for example, modify their feeding preferences to consume more protein when they are about to lay eggs [71]. The reduction in feeding circuit-related neuropeptides at the non-mated to mated transition strongly suggests that, in the octopus, feeding and reproductive states also interact.

Although neuropeptide expression precipitously drops after reproduction, mated animals continue to feed in the initial stage of brooding. However, feeding behavior between mated and non-mated animals manifested in different ways: mated feeding octopuses captured crabs that were within arm's distance of their dens and did not pursue prey outside their dens, as non-mated females regularly did. This behavioral switch suggests that different feeding strategies are optimal for non-mated and mated females: the feeding-related peptides identified may regulate energy expenditure or the drive to hunt for food. Our data also raise the possibility that redundant peptidergic pathways, or additional non-peptidergic systems, control feeding behaviors. These systems may be independent of the optic gland.

These neuropeptides may also broadly participate in neurotransmission well beyond feeding. If this is the case in the octopus, peripheral tissues might also express these neuropeptides. We checked if these neuropeptides were present in the arm transcriptomes, which included nervous tissue (axial nerve cord), muscle, skin, chromatophores, and suckers. Expression changes of these genes in the arms would suggest that global changes in neuropeptide signaling accompany the maternal and senescence process in general. However, all feeding-related neuropeptides in the blue subcluster (Figure 3.10C and 3.11E) were missing from the arm

transcriptomes, suggesting that their expression is a specific feature of the optic gland. These data are surprising since the optic glands previously have not been implicated in feeding *per se*. Future experiments will reveal if these neuropeptides are functionally conserved in octopuses.

Steroid biosynthesis

Steroids are one of the most evolutionary ancient classes of signaling molecules [72,73]. Derived from cholesterol, steroids include the sex hormones and corticosteroids. We found that a collection of cholesterol-metabolizing enzymes increased in expression in the first stage of brooding and remained elevated through the maternal period. These included enzymes known to synthesize steroid hormones in diverse animals, from ecdysozoa to deuterostomes [74]. Dafachronic acid in *C. elegans*, for example, regulates longevity and dauer formation, and its biosynthesis relies on the sequestration of cholesterol by daf36/cholesterol 7-desaturase [75]. 3-beta-hydroxysteroid dehydrogenase is an oxidoreductase that catalyzes the formation of progesterone in the adrenal gland and gonads of vertebrates [76,77]. Sterol 27-hydroxylase (CYP27a) breaks down cholesterol for both bile acid synthesis and hormone production [78]. Sulfotransferase 1C2 catalyzes the conjugation of a sulfate group to steroid hormones [79].

Our study is the first to implicate the optic glands in the production of progesterone and other steroid hormones. Cellular and molecular mechanisms of steroid hormone signaling in octopuses may be different from those that have been described previously in the vertebrate neuroendocrine systems. Substrate specificity of these enzymes may differ between species [74]. Functional characterization of these enzymes or identification of steroid metabolites will be essential going forward. Moreover, steroid signaling in molluscs may not be mediated through the nuclear receptors orthologous to those identified in vertebrates [80]. The *Octopus vulgaris*

ortholog of the vertebrate estrogen nuclear hormone receptor, for example, does not bind estrogen [81]. Our identification of the coordinate enrichment of cholesterol-metabolizing enzymes in mated female octopuses raises the exciting possibility that the optic glands produce a suite of steroid-derived hormones that are specific to the reproductive adult and may have novel cellular targets.

Insulin signaling

Our data reveal that expression of *ImpL2* increased at the transition from feeding to fasting (Figure 3.10B and 3.11D). ImpL2 is a homolog of insulin-like growth factor binding protein (IGFBP), which reduces activity of the insulin/IGF signaling pathway in *Drosophila* [82,83]. This pathway, which is present in many invertebrates, controls biological processes such as glycogen metabolism and organismal growth [84,85]. However, functional characterization of these molecules in molluscs has been limited [86,87], and the possible actions of the insulin/IGF signaling pathway in octopus are unknown.

Under starvation conditions, elevated levels of ImpL2 and other insulin growth factor binding proteins have been reported to promote cell survival [82,88]. Upregulation of *ImpL2* in fasting octopuses may be a

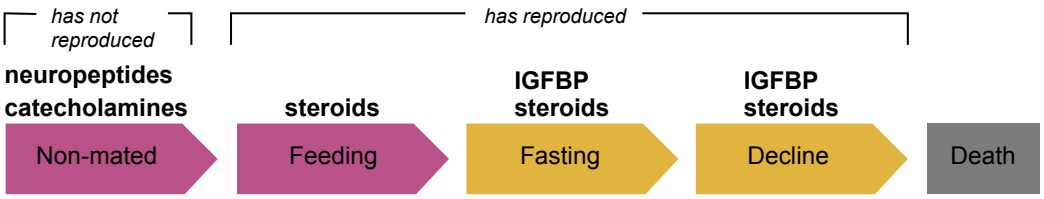

Fig 3.11 Updated model of optic gland function in maternal behaviors and death. Arrows indicate behavioral groups (pink: feeds; yellow: abstains from feeding). Signaling systems above arrows highlight enriched genes.

transcriptional response to nutrient deficiency. The highest expression of *ImpL2*, however, is found in decline females (Figure 3.10D): in this terminal stage of brooding, females exhibit behavioral and physiological changes that extend well beyond those accompanying experimental starvation [4,35]. In *Drosophila*, ImpL2 can induce tissue wasting independent of food-intake: tumor-implanted flies show high levels of ImpL2 and degradation of gonadal, muscle, and adipose tissues [83,89]. These similarities with physiological traits of females in decline lead us to predict that this role of ImpL2 is functionally conserved between octopuses and *Drosophila*.

The correlates of high ImpL2 in both *Drosophila* and octopus are remarkably consistent with symptoms of cancer cachexia in humans. Cachexia patients experience an involuntary loss of body mass, undergo substantial degradation of muscle and fat, and report a loss of appetite [90]. Medical interventions focusing on increasing caloric intake fail to counteract wasting [91,92]. Importantly, clinical work in humans has shown that cachexia and other disease conditions are associated with elevated levels of IGFBPs [93-95].

Our results suggest that ImpL2 is intimately tied to feeding behaviors in octopus and implicate the optic glands as a regulator of insulin signaling. These data raise the possibility of a conservation of function in insulin-signaling pathways with animals as distantly related as humans and octopuses. More importantly, our study is the first to implicate IGFBP enrichment in natural end-of-life physiology.

Neurotransmitter biosynthesis and neurotransmission

The optic gland regulates sexual maturation and behavior by hormone release, but cellular mechanisms of secretion are unknown. We identified a number of genes implicated in neurotransmission and regulated secretion that are enriched after reproduction (Figure 3.10A and

3.11A). Clathrin, for example, facilitates the formation of coated secretory vesicles, and synaptotagmins contribute to the cellular complex that enables vesicle fusion for regulated exocytosis [96,97]. Specific isoforms of both are enriched in the optic glands at all mated stages. Our finding mirrors existing data on the organization of the vertebrate reproductive axis: synaptotagmins and other proteins involved in classical neurotransmission are differentially expressed in the anterior pituitary gland where they are involved in the release of a variety of signals [98].

The enrichment of neurotransmitter receptors (Figure 3.10B), including an octopamine receptor, neuropeptide S receptor, and a subunit of a nicotinic acetylcholine receptor, suggests that the optic gland also undergoes shifts in the signals it receives from the central brain, from itself, or from other secretory organs after reproduction.

Optic glands of non-mated animals showed elevated expression of dopamine β-hydroxylase (DBH, Figure 3.10E), an enzyme involved in the synthesis of catecholamine neurotransmitters. DBH catalyzes the β-hydroxylation of dopamine to norepinephrine in vertebrates and tyramine to octopamine in invertebrates [99,100]. These small molecules are used for signaling throughout nervous systems. Candidate aminergic secretory vesicles have been found in the optic glands of *Octopus bimaculatus*, the sister species of *O. bimaculoides* [101]. Our results suggest that the optic gland engages in endocrine catecholamine signaling and that reproduction leads to the specific shutting down of catecholamine pathways, as opposed to an overall decrease in optic gland neurotransmission or cell signaling.

Octopus semelparity

Mechanisms of death differ among animal systems exhibiting semelparity. In several vertebrate species, it is believed that the metabolic cost of gamete production and finding a mate are so high that death is inevitable [102,103]. Semelparity in octopuses cannot be explained by the large metabolic output required to produce and deposit eggs: glandectomized animals can reproduce again [33]. Instead, it is likely that other evolutionary mechanisms drive post-reproductive death. Coleoid cephalopods are cannibalistic: hatchlings from the same clutch often eat each other, and females sometimes kill males after reproduction [3]. Post-reproductive death is an undeniably effective method in ensuring that the reproductive female does not consume her young. Moreover, longitudinal studies of octopuses, and other molluscs, demonstrate that individuals continue to undergo logarithmic growth as adults: even adult octopuses can double their weight in a month [4,8,14,86,104]. Endless growth without death could so skew octopus populations towards large, old adults that hatchlings would be unlikely to compete successfully. Programmed organismal death in coleoids may exist as a mechanism to safeguard the survival of the next generation of these voracious predators.

In Pacific salmon *Oncorhynchus kisutch*, steroid hormone signaling has been implicated as the cause of death after spawning. Elevated cortisol levels mediate programmed death through tissue degeneration and impaired homeostatic ability [105]. Our data show that steroid signaling is one of several pathways implicated in octopus post-reproductive death. Although we do not see molecular evidence of cortisol signaling *per se* in our data, the enrichment of cholesterol-metabolizing enzymes in mated females suggests that steroid metabolites are crucial to semelparity in octopuses. It will be important to identify the steroids in the optic gland and assess the contributions of steroid and ImpL2 signaling, along with the reduction in feeding peptides and catecholamine signaling, in cephalopod post-reproductive death.

Conclusions

Our transcriptome findings suggest that, far from secreting a single hormone, the optic gland likely enlists multiple signaling systems to regulate reproductive behaviors, including organismal senescence (Figure 3.11). Among these are neuropeptidergic systems and cholesterol-derived hormone signaling. Our data raise the possibility that prior to mating, optic gland signaling is dominated by neuropeptides and catecholamines, whereas after mating, steroid hormone signaling increases in importance.

Wells and Wells originally drew a connection between the direct brain regulation of the octopus optic glands and the vertebrate hypothalamic-pituitary-gonadal axis [36]. Here, we identify a difference between octopus and vertebrate systems: the endocrine signaling of the anterior pituitary gland depend on peptide hormones alone [106], whereas our data implicate steroid and catecholamine pathways, in addition to peptide signaling, in the functions of the optic gland. While steroid hormones do affect the actions and feedback of the vertebrate pituitary gland, steroidogenesis occurs in targets of the pituitary gland only, such as the adrenal cortex, and not in the pituitary gland itself [25,42]. Similarly, biosynthesis of catecholamines, such as norepinephrine and dopamine, occurs in the adrenal medulla in response to autonomic stimulation [107].

If the optic gland encompasses functions of the anterior pituitary gland and the adrenal glands, it prompts the question of what glandular targets of the optic gland, if any, might exist. The oviducal glands, which produce substances that cover the eggs, are candidates. These glands, along with the gonads and oviducts, were found to increase in size as the optic gland enlarges [23,35]. *In vitro* experiments demonstrated that oviducal secretion is modulated by

dopamine and neuropeptides, including FMRFamide [19]. However, the putative source of direct oviducal control is the fusiform ganglion, not the optic glands. The fusiform ganglion is thought to innervate the oviducal gland, the oviducts, and the systemic heart [2]. Notably, the fusiform ganglion has been found to contain FMRFamide-like immunoreactive nerve endings [108]. The optic gland may exert indirect control over glandular targets by signaling to peripheral ganglia, or act in parallel with peripheral ganglia to regulate reproductive tissues directly.

Our study extends the optic gland-pituitary analogy and also uncovers similarities between the optic glands and the vertebrate adrenal glands, demonstrating that the organization and function of the optic glands may be even more pivotal for octopus organismal physiology than previously appreciated.

CHAPTER 4

Neurochemical compartments of the optic gland

Abstract

The reproductive axis comprises neural control centers and endocrine glands that act in a coordinated fashion to orchestrate the proper timing of important life history events, such as sexual maturation and ovulation. In vertebrates, hypothalamic nuclei regulate populations of pituitary cells that produce different hormones that act on the gonads and other target organs. Much less is known about the biology of the reproductive axis in invertebrate animals, including octopuses, which have a large central nervous system and peripheral secretory glands. Here we demonstrate that the octopus analogs of the pituitary gland, the optic glands, contain distinct molecular territories. We demonstrate through dye and *in situ* hybridization histochemistry that the organization of the optic glands is wholly unlike their classical characterization as a uniform mass of secretory and support cells. They have regional organization along the aboral/oral axis with territories specialized for steroid, catecholamine, and peptide signaling. These findings expand the optic gland-pituitary gland analogy and provide the first insight into the molecular and anatomical organization of the optic gland's secretory functions.

Introduction

In vertebrates, the pituitary gland serves as the intermediary between the central brain and peripheral organs. The pituitary gland is characterized by an intricate portal vascular system enmeshed in two major tissues: the adenohypophysis, sometimes called the anterior pituitary, and the neurohypophysis, or posterior pituitary [37]. The neurohypophysis releases two

hormones, oxytocin and vasopressin, made by cells of the hypothalamus. The adenohypophysis, by contrast, synthesizes at least 7 different peptide hormones: adrenocorticotropic hormone, thyroid-stimulating hormone, follicle-stimulating hormone, luteinizing hormone, growth hormone, prolactin, and intermedin [37]. These factors are made by two different territories of the adenohypophysis: the pars intermedia, which is specialized for intermedin secretion, and the pars distalis, which contains dedicated cell populations for the production of each of the other 6 hormones. The glandular cells of the pars distalis are not uniformly distributed, but instead arranged as cords or clumps associated with blood vessels. In this way, the pituitary gland has a highly modular cellular arrangement that allows for the regulated synthesis and release of a broad array of peptide hormones.

Similar to the pituitary glands, the octopus optic glands also employ multiple hormone signals that influence the maturation of reproductive organs and maternal behaviors [38,108,109]. The secretions of the optic gland also control longevity. Removal of the optic glands in sexually mature males leads to a decrease in testis mass and, eventually, the complete abolition of spermatogenesis [110]. In brooding females, optic gland removal is even more dramatic. Typically, female octopuses stay close to their clutch of eggs, abstain from feeding during much of the brood period, and die before the clutch hatches [111-113]. Glandectomy completely abolishes maternal brooding behavior and, subsequently, precipitate death [33].

As early as 1969, the optic gland's important role in sexual maturation and reproduction was likened to that of the vertebrate pituitary gland. Wells and Wells described a negative feedback system from the subpedunculate lobe of the central nervous system to the optic glands that, when removed through surgical intervention, promotes maturation of the gonads [34]. Lesions of the subpedunculate lobe led to premature enlargement of the gland and, subsequently,

the ovary [23]. When the optic gland is removed, artificial methods of increasing gonad size were ineffective, suggesting that the optic gland is the main modulator of gonad growth and a crucial bridge between the central brain and rest of the body [23]. In these roles, the optic gland serves as the octopus analog of the vertebrate pituitary gland in invertebrate neuroendocrinology.

Until recently, the nature of optic gland ligands was unknown. Transcriptome sequencing revealed that optic gland signaling mechanisms are far more diverse than those of the vertebrate pituitary gland: in addition to peptides, the optic glands utilize steroid, insulin, and catecholamine signaling [109]. The optic gland's reported simple anatomy belies this diversity of signals: apart from cells associated with the vascular system, the optic glands contain two cell types: larger gland cells and smaller support cells [39]. These two populations were reported to be homogenously distributed throughout the gland. How these diverse signals might be deployed in the optic glands remains a major unanswered question.

To uncover the molecular anatomy of the optic glands, we investigated known representatives from peptide, steroid, and catecholamine signaling families by performing *in situ* hybridization (ISH) experiments. We also screened the optic gland transcriptome for novel neuropeptide precursors. Dye histochemistry demonstrated that the optic gland is a heterogeneous structure. *In situ* hybridization experiments on key genes revealed distinct neurochemical compartments in the optic glands of unmated adult female California two-spot octopuses, *Octopus bimaculoides*.

Results

Revisiting homogeneity: differences in optic gland structure are visible in unstained tissue

The optic glands are paired organs that sit on the dorsal, aboral end of the optic stalk between the optic lobes and the central brain mass (Figure 4.1). In mature animals, a yellow-orange color distinguishes the gland from the surrounding neural tissues (Figure 4.1) [39]. The optic glands have traditionally been characterized as having a simple internal anatomy. Unlike the vertebrate pituitary gland, which has many distinct cell types, the optic glands were described as a "uniform mass" containing only large stellate cells and smaller supporting cells [39].

Under light-field and dark-field illumination, we saw that the cell bodies and processes of nervous tissue can be readily distinguished (Figure 4.2). In the optic lobes (Figure 4.2a) and vertical lobes (Figure 4.2b), areas rich in cell bodies appear darker, whereas areas rich in processes are lighter (Figure 4.2c and d). The optic gland possesses similar differences. At the most aboral end, the optic gland is uniformly dark, but both darker and lighter areas can be distinguished at the intermediate and oral levels. If tissues of the optic gland under dark-field light illumination are similar to those of the central brain, these results suggest a cell-dense region at the aboral end and more typical ganglionic structure at the oral end, with cells on the outside of the gland and processes in the center. These observations indicate that the original descriptions [39] offered an incomplete view of optic gland anatomy.

We also performed hematoxylin and eosin (H&E) staining on the central brain and optic glands of unmated adult females. The aboral end of the gland was hematoxylin-positive, indicating that it is a territory rich in cell nuclei (Figure 4.2). In sections at intermediate and oral

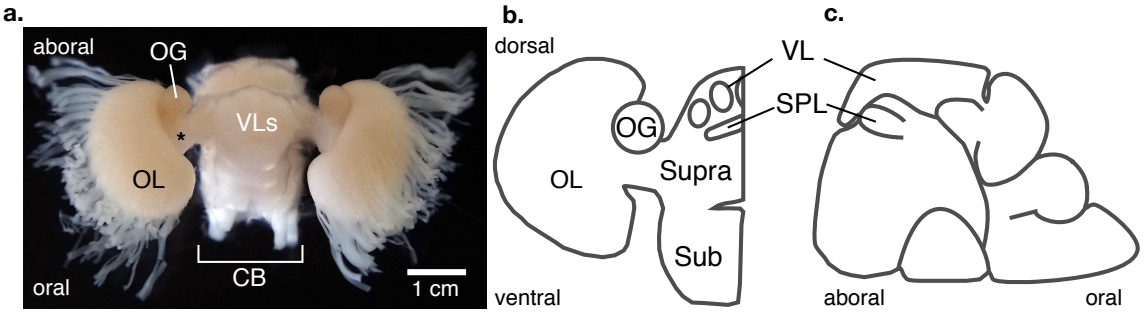

Fig 4.1. Octopus brain anatomy. a. Dorsal view. The optic glands (OG) are paired neuroendocrine organs that sit on the aboral end of the optic stalk (asterisk) between the optic lobes (OL) and the central brain mass (CB). In sexually mature adults, the yellow-orange of the optic glands make it distinct from the rest of the neural tissue. The vertical lobes (VL) are visible at the top of the supraesophageal mass (Supra in panels b and c). The oral direction is towards the arms and the aboral direction is towards the mantle. b. Coronal view, hemisected. The subpedunculate lobe (SPL) innervates the OG. Dorsal refers to the direction of the supraesophageal mass and ventral refers to the direction of the subesophageal mass (Sub). c. Midsagittal view of the supraesophageal brain. Subesophageal brain not shown.

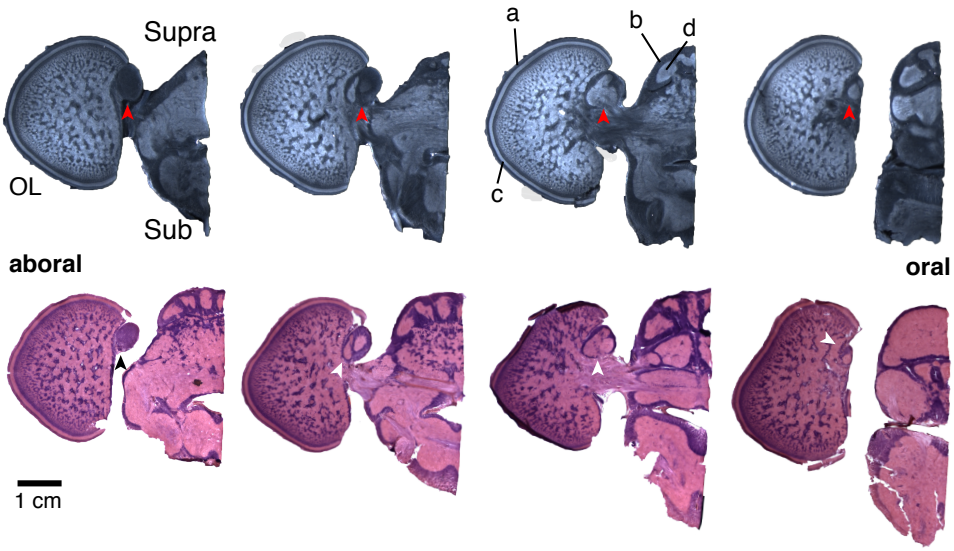

Fig 4.2. Cellular heterogeneity in the optic glands. Under dark-field illumination (top row), neural regions dense in cell bodies, such as the two granule cell layers of the optic lobes (a) or the outer shell of vertical lobes (b), appear dark. Areas rich in cell processes, such as the plexiform layer of the optic lobes (c) and the central neuropil of the vertical lobes (d), appear bright. Similar variations are also observed in the optic gland (red arrowheads) along the aboral-oral axis. Hematoxylin and eosin staining (bottom row) confirms that the aboral optic gland is entirely comprised of cells (black arrowhead) and the intermediate and oral levels of the optic gland have a ganglion-like structure (white arrowheads), similar to what is observed in the optic lobes and central brain. Different animals were used for microscopy and H&E.

levels, the optic gland was stained with both hematoxylin and eosin, again showing a ganglion-like arrangement. The results of H&E staining correspond well to our initial observations under dark field light microscopy, and motivated us to uncover the molecular nature of the optic gland heterogeneities.

Directed search for new peptide sequences

Several independent lines of evidence suggested that some optic gland secretions are neuropeptides [38,39]. We used BLAST to query the optic gland transcriptomes of sexually mature, unmated females [109], using the amino acid sequence of all known invertebrate neuropeptides deposited in Neuropred (June 2018) as bait. We identified octopus homologs of FMRFamide, FxRIamide, insulin-like growth factor binding protein 7, myomodulin, LWamide, PRQFVamide, and APGWamide. We queried these homologs for common neuropeptide cleavage motifs using Neuropred and a protein motif searching program developed by Felipe Aguilera [53]. In many of these putative homologs, we found a predicted signal sequence and cleavage sites yielding repeated short peptides (Figure 4.3).

FMRFamide: FMRFamide was one of the first peptides localized to the optic glands [108]. Recently, FMRFamide was identified as a transcript that is significantly enriched in non-mated female optic glands [109]. SignalP prediction software predicted a signal peptide 22 amino acids in length (Figure 4.3a). The octopus FMRFamide sequence shows a single copy of the decapeptide ALSGDAFLRFamide, a single copy of FLRFamide, and 6 copies of FMRFamide. The octopus FMRFamide-related peptides bear sequence similarity to other FaRPs that have recently been identified in cuttlefish and other molluscs [85,114-116].

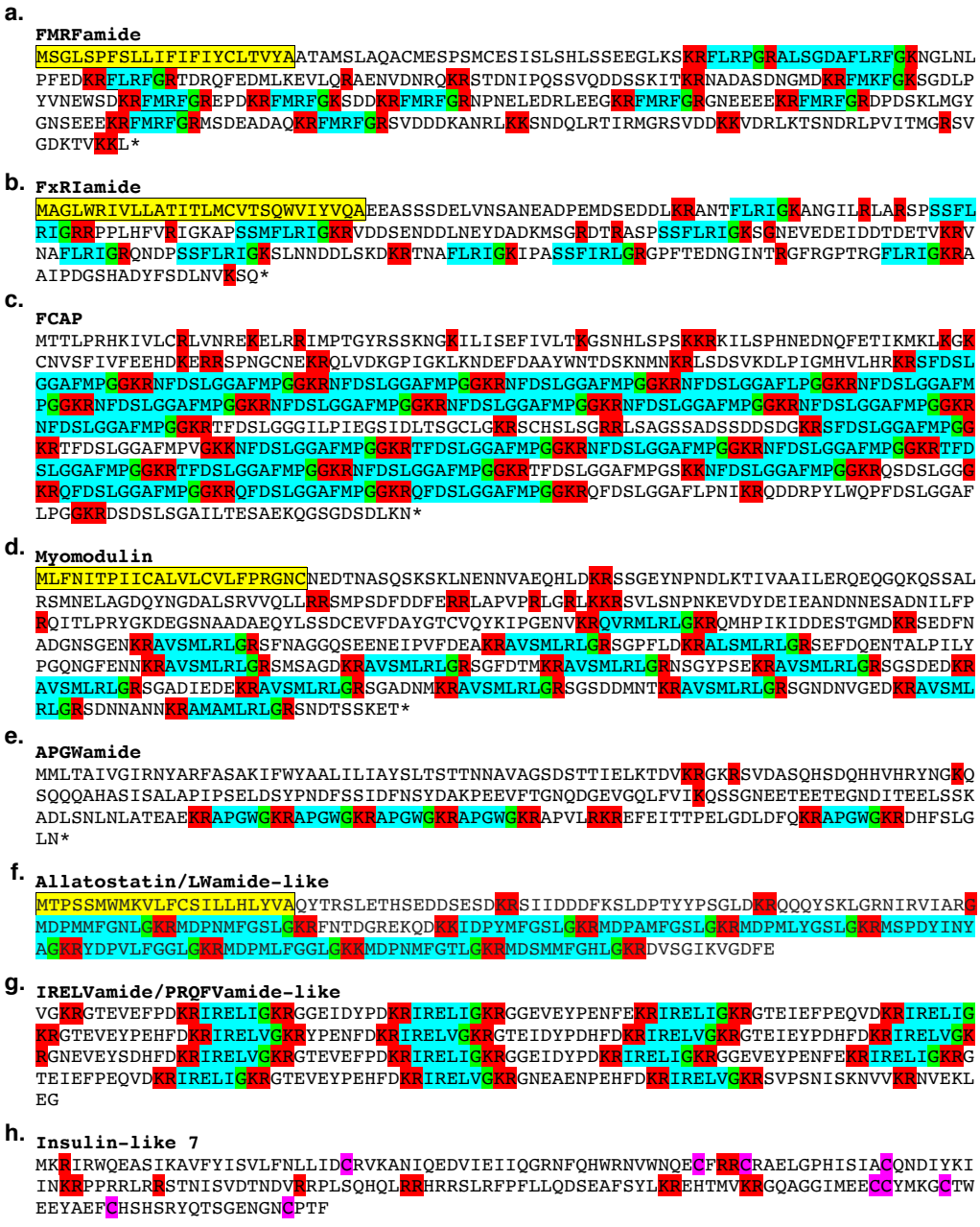

Fig 4.3. Prepropeptide sequences predicted from the optic gland transcriptomes. The putative signal peptides are boxed and highlighted in yellow, predicted cleavage sites are in red, and known diagnostic peptide sequences are in blue. In amidated peptides, glycine residues to be converted into C-terminus amides are in green. Cysteines predicted to form disulfide bridges are in magenta.

FxRIamide: FxRIamide is similar to the FaRPs that have been reported in several lophotrochozoans [85]. Previously, FxRIamide was identified by a bioinformatics screen of the whole-body transcriptome of the gray garden slug, *Deroceras reticulatum* [85]. FxRI is similar in sequence to FMRFamide, suggesting it may play related roles in modulating synaptic activity. FxRIamide has a 28 amino acid predicted signal peptide sequence and 4 copies of the heptapeptide xSSFxRI, along with several closely related peptide sequences (Figure 4.3b).

Feeding circuit activating peptide (FCAP): Originally identified in the buccal neurons of *Aplysia*, FCAP is an amidated neuropeptide thought to initiate rhythmic feeding motor programs and modulate food-related arousal [70]. *FCAP* was previously found in the optic glands of unmated female octopuses [109]. *FCAP* encodes multiple copies of closely related undecapeptides, with the major form NFDSLGGAFMPamide appearing 15 times (Figure 4.3c).

Myomodulin: We identified an octopus homolog of myomodulin, which was previously unannotated in the genome (Figure 4.3d). Myomodulin was identified in buccal motor neurons of *Aplysia*, where it was found to potentiate contraction of the accessory radula closer buccal muscles [117]. We found a predicted signal sequence of 23 amino acids and 12 copies of AVSMLRLamide and two nearly matching variants. This peptide sequence is similar to *Aplysia* myomodulin, which has a sequence of PMSMLRLamide [117].

APGWamide: APGWamide was one of the most highly-expressed transcripts in the optic gland transcriptome of unmated female octopuses. APGWamide activity has been implicated in the control of male copulatory behavior in gastropod molluscs [118]. In *Octopus vulgaris*, APGWamide-immunoreactive fibers have been found in lobes of the central brain and the glandular cells of the oviducal gland, suggesting a shared reproductive function in cephalopod

molluscs [119,120]. The octopus homolog contains several copies of APGW at the 3' terminus (Figure 4.3e).

Other neuropeptides: We also found partial sequences for two amidated peptides (Figure 4.3f and g) and an insulin-like protein (Figure 4.3h). Allatostatin/LWamide was previously reported in octopuses [109] and is known to modulate feeding in other animals [63,69,121]. However, octopus allatostatin lacks the critical LW motif diagnostic of this family of peptides (Figure 4.3f), and this function may not be conserved. Our bioinformatics screen predicted an IRELVamide peptide (Figure 4.3g). This sequence is reminiscent of PRQFVamide and may represent an octopus variant. We also recovered partial sequence for a homolog of insulin-like growth factor binding protein 7 (Figure 4.3h), which contains the conserved cysteines that form disulfide bridges. These findings corroborate new evidence that the optic gland may serve as a signaling center that coordinates reproductive processes with metabolic activities [111].

ISH experiments on candidate neuropeptides

ISH experiments on unmated females confirmed that many bioinformatic candidate neuropeptides are expressed in the optic glands (Figure 4.4, primers listed in Table 4.1). Instead of a homogenous distribution as suggested by classical characterizations of the optic gland, however, we found that neuropeptides picked out specific territories in the optic gland and that their patterns of gene expression were broadly similar to each other (Figure 4.4).

The frontline of the neuropeptide territory emerges ventrolaterally in the intermediate optic gland, eventually spreading over the entire optic gland. FMRFamide, FCAP, myomodulin, and FXRIamide show strong, dappled labeling in this territory, suggesting that cells producing these

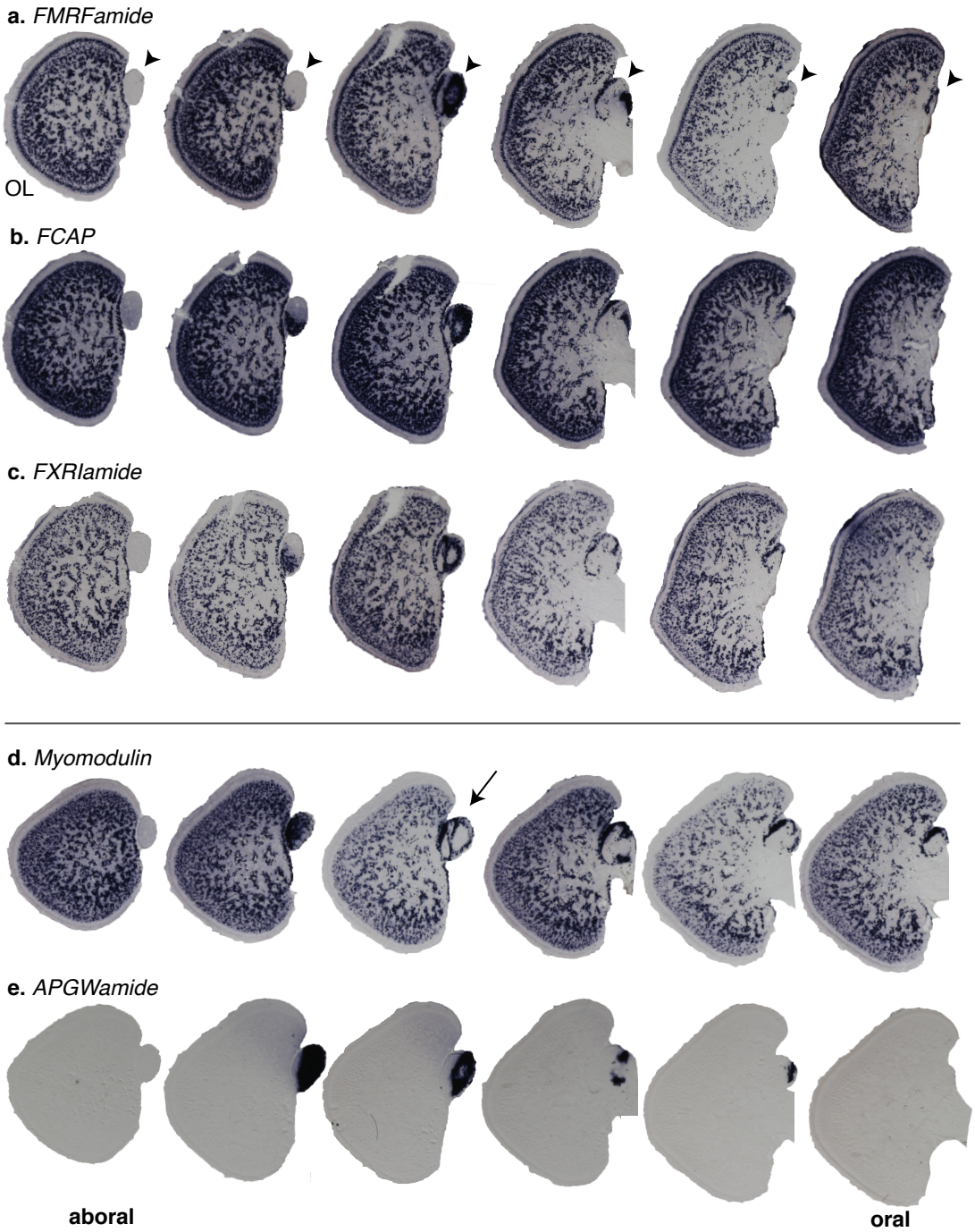

Fig 4.4. Neuropeptides define distinct compartments in the intermediate and oral optic gland. Optic glands are marked by black arrow in panel a; identical orientations are shown across all panels. All neuropeptide markers are not detected in the aboral optic gland and first appear in the intermediate optic gland. This labeling demarcates 3 oblong compartments and with a connected central neuropil (arrow). Panels a/b and b/c represent serially adjoining sections from one animal. Panels d/e are serially adjoining sections from another animal. Central brain has been cropped out.

Octopus cDNAs	PCR Primers
APGWamide	F: TGTTGACGGCTATCGTAGG R: CTTTTACCCCATCCTGGTG
Daf36	F: GCCAGACAGATTGGACCAG R: TAGGAAGTGGAGCAGGGTG
DBH	F: GAGAGAAAGTGTAAGAGAAGACTG R: TGACGACCTGTGACCTTG
Ef1α	from Express Genetics for Ragsdale Lab, 2010-2011
FCAP	F: AAAGAGACAAGATGACAGGC R: TCAAGACACTAACTACGATGC
FMRFamide	F: CAACTTCAGTGCCTGGAAC R: GTGCGTTTGTCCTTAGAGAG
FxRIamide	F: GCCAAGACAACAACTGCG R: CGTCCAAACCTCATAAACCG
HSD	F: GCTTGTATGCTGGTCTACTG R: CGAGATGAGAGGATGGTTCC
Myomodulin	F: CTTCACACCTAAGCGGAC R: GCATCAAAGACTTCACAATCC

Table 4.1. Molecular markers for analysis of octopus optic gland. F: forward PCR primer; R: reverse PCR primer.

neuropeptides are arranged in a mosaic fashion. At progressively more oral levels, neuropeptides become restricted to the outer rind of the optic gland (Figure 4.4). This outer rind forms a tripartite, clover-leaf-like shape, with sparse labeling for neuropeptide markers in its center. This rind extends to the most oral edge of the optic gland. None of the neuropeptides we examined reached into the aboral region of the optic gland.

APGWamide, one of the most highly expressed transcripts in the female optic gland, has a restricted expression territory within the larger neuropeptide territory. It appears as a thin, ventrolateral sliver at the most aboral end of the neuropeptide territory (Figure 4.4e). This sliver forms a single tubular compartment in the intermediate region of the optic gland; the lateral edge of the intermediate optic gland territory labels for other neuropeptides but not for APGWamide message. At the oral optic gland, APGWamide is restricted to the gland's medial edge, a zone conspicuously unlabeled by myomodulin gene expression. This, it is possible that this region is specific to APGWamide.

ISH of other known signaling families

In addition to neuropeptides, the optic glands express catecholamine, insulin, and steroid signaling molecules [109]. To explore the possibility that non-peptide markers may label other territories in the optic gland, we performed *in situ* hybridization for dopamine beta-hydroxylase (*DBH*), a catecholamine biosynthetic enzyme, and for two steroidogenic enzymes, cholesterol 7-desaturase/Daf36 (*Daf36*) and 3-beta-hydroxysteroid dehydrogenase (*3BHSD*). At the most aboral end, optic gland tissue labels strongly and homogenously for these steroid biosynthetic enzymes (Figure 4.5). These two genes were recently identified in the octopus optic gland, and

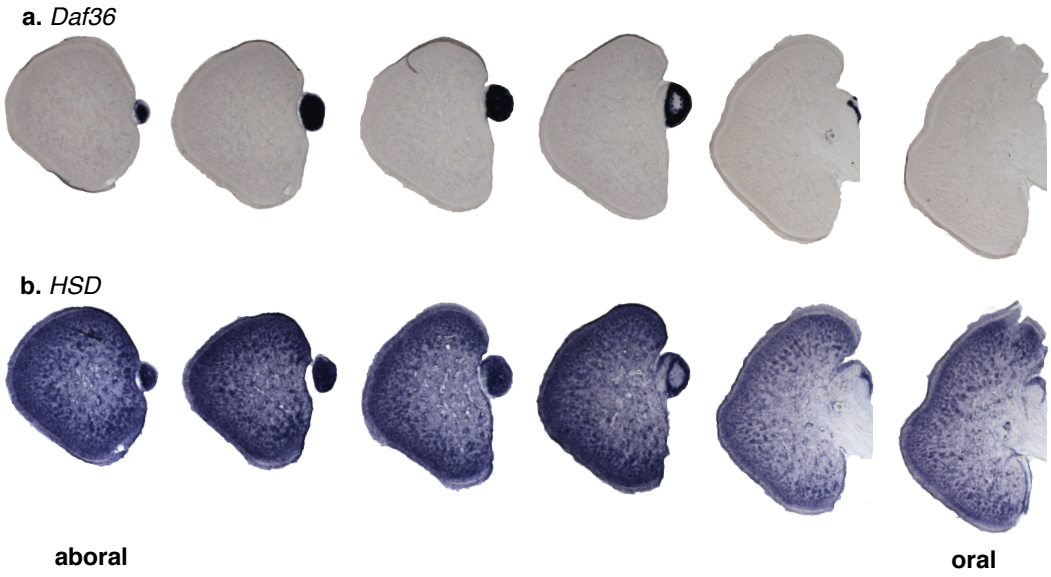

Fig 4.5. Steroidogenic enzyme labeling is concentrated at the aboral optic gland. Daf36 and HSD, enzymes that are involved in metabolizing cholesterol into steroid hormones, show largely overlapping territories that extend from the most aboral edge of the optic gland to the intermediate optic gland. Sections in a/b are immediately adjacent.

shown to be significantly upregulated in mated females, suggesting that steroid hormones may be important in maternal behaviors [109]. The *in situ* results reported here demonstrate that the optic gland has a steroidogenic-specific territory enriched in both of these enzymes.

The expression pattern of dopamine beta-hydroxylase is broadly captured within the neuropeptide domain (Figure 4.6a and d) and presents limited overlap with that of the cholesterol metabolizing enzymes (Figure 4.6c and d). The most intense *DBH* labeling exists on the dorsal lateral and dorsal medial corners of the optic gland rind and is not detected along the ventral edges of the gland.

Defining optic gland regions

We directly tested whether the steroid and neuropeptide territories are separate or overlap with each other. We performed ISH experiments with alternating sections probed for *DAF36*, *APGWamide*, and the other peptides. We found that the two signaling classes marked partially separate territories in the optic gland: at the aboral end, a territory that labels uniformly for cholesterol-metabolizing enzymes defines the steroidogenic zone, which gives way to a neuropeptidergic-rich area in the intermediate and oral optic gland (Figure 4.7).

Optic gland ligand gene expression

These results motivated us to determine whether the molecular markers we identified here accounted for the all cellular territories of the optic gland, or if other uncharacterized cell signaling zones likely exist. We performed an ISH experiment with alternating tissue sections probed for all ligands identified here (steroids: DAF36, 3BHSD; neuropeptides: APGWamide,

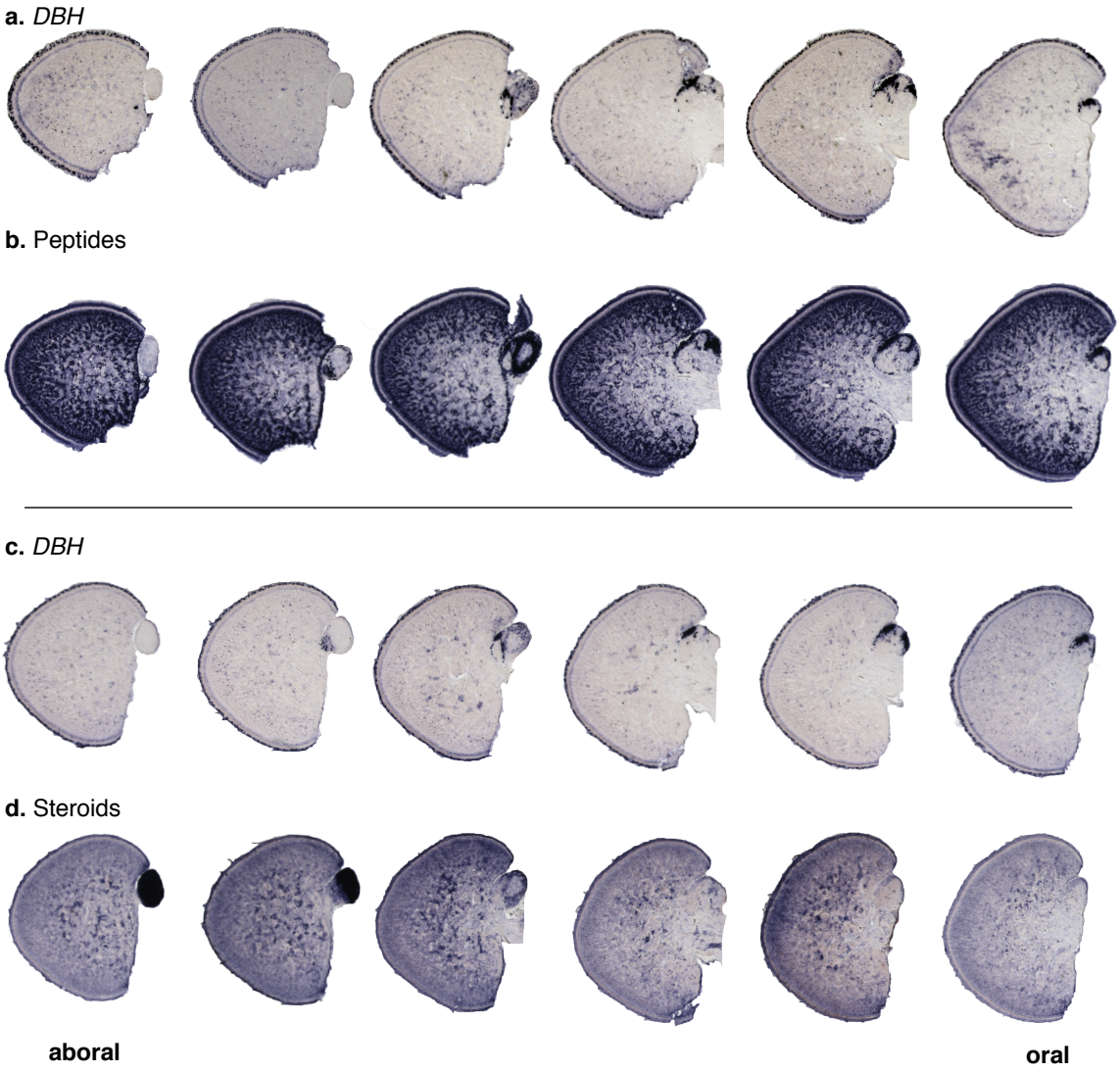

Fig 4.6. Territories for dopamine beta-hydroxylase-producing cells (*DBH*) and neuropeptidergic cells overlap. Experiments that probed adjoining section for *DBH* and peptides (a and b) or *DBH* and steroids (c and d) show that the aboral optic gland is specialized in steroidogenesis while the intermediate and oral territories express genes for multiple signaling systems. Peptides ISH (b) experiment used probes for *FMRFamide*, *FxRIamide*, *FCAP* and *myomodulin*. Steroids ISH (d) experiment employed probes for *Daf36* and *HSD*. Panels a/b and panels c/d show adjacent sections.

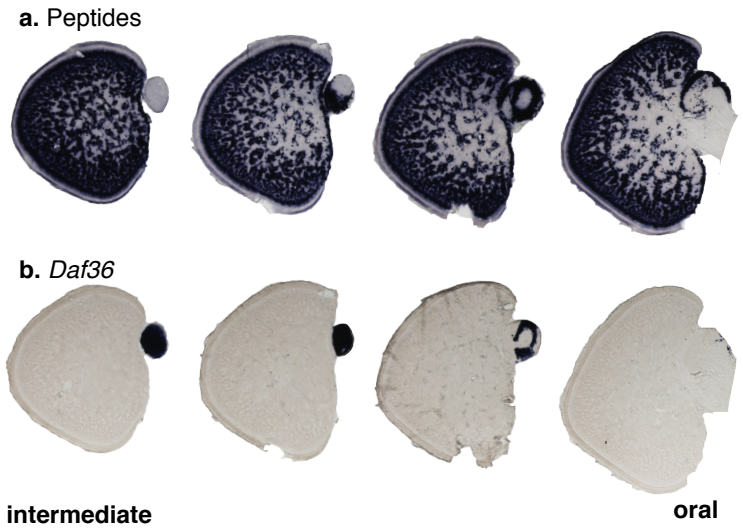

Fig 4.7. The female optic gland comprises at least 3 major neurochemical territories. The aboral optic gland is a homogenous territory labeled by steroidogenic enzymes only (see also Figs 4.5 and 4.6). The steroidogenic zone begins to retreat at intermediate optic gland levels, which features neuropeptide-producing cells around its outer shell and a sparsely-labeled core. Whether the apparent overlap of peptides and *DAF36*-expressing territories extends to co-expression in individual cells will need to be tested in 2-color fluorescent ISH experiments or with single cell transcriptomics. Panels a and b show adjoining sections. Peptides includes RNA probes for *FMRFamide, FxRIamide, FCAP,* and *myomodulin*.

FMRFamide, FxRIamide, FCAP, myomodulin; DBH) or octopus elongation factor 1-alpha (EEF1A/EF1-alpha), a general molecular marker for animal cells [122]. We found that the mixture of probes for all identified optic gland signaling systems labeled territories in the optic gland that closely corresponded to Ef1-alpha positive regions (Figure 4.8).

Discussion

Reproductive axes play a crucial role in coordinating the proper timing of life history events in both octopuses and vertebrates. Functional evidence implicates the optic gland as the neuroscretory mediator between the central nervous system and peripheral targets [23,123], but little is known about the optic gland's internal anatomy. Indeed, the few studies on optic gland neuroanatomy suggested that the optic gland is a distinct but simplistic organ: homogenously distributed chief cells secrete a single optic gland hormone that acts on reproductive organs [39]. A recent report showed that optic gland secretes a complex interplay of multiple signals [111]. Instead of a single hormone, the optic gland throughout the animal's life history employs a multiplex of secreted factors, which raised the possibility of a commensurate complexity in optic gland anatomy.

Neuropeptide signals of the optic gland

Our bioinformatics analysis yielded a panel of putative neuropeptides produced in the optic gland, including members of the evolutionarily-ancient peptide families RFamide and insulin-related peptide.

Three peptides reported here, FMRFamide, APGWamide, and FCAP, have been identified in octopuses before. FMRFamide immunoreactive fibers were detected previously in

a. *EEF1A/EF1alpha*

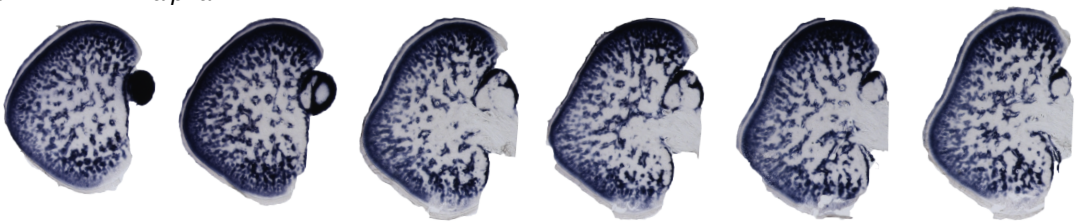

b. All Ligands

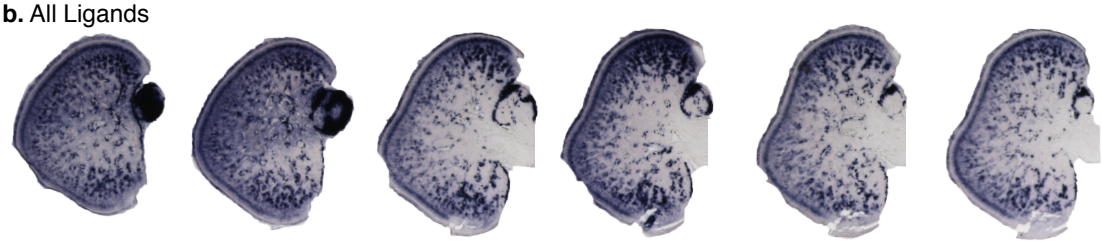

aboral **oral**

Fig 4.8. Steroidogenic, catecholaminergic, and peptidergic cells account for all cellular territories within the optic gland. *In situ* hybridization experiments in adjacent sections that probe for Ef1alpha and all identified optic gland ligands demonstrates striking similarity in labeling patterns.

the optic gland. However, the source of FMRFamide was thought to be the subpedunculate lobe (Figures 4.1 and 4.9), an upstream modulator of the gland, not the gland itself [108]. Through transcriptomics and *in situ* hybridization, we show that octopus FMRFamide message is detected in the optic lobe as well as the optic gland. The presence of a predicted signal sequence and putative cleavage sites strongly suggest FMRFamide is biologically active, though future functional proteomic studies are required. APGWamide has been implicated previously in octopus reproduction [120], though it was localized to only lobes of the central brain and the oviducal gland. Here, we report that APGWamide message is found in the optic glands themselves. Recently, *FCAP* was reported to be significantly enriched in the optic glands of unmated female octopuses as compared to that of feeding females [111]. FCAP is thought to target motor circuits involved in feeding and initiate food-induced arousal [70].

Our bioinformatics and ISH analysis adds 2 more amidated peptide signals to the extensive list of optic gland modulators: FxRIamide and myomodulin (Figure 4.3b and d). Myomodulin was previously an unannotated gene in the *O. bimaculoides* genome. Myomodulin was originally identified in *Aplysia* feeding circuit motor neurons [117], and has since been identified in several invertebrates, including other lophotrochozoans [84,124]. FxRIamide is a member of the RFamide peptide family that has close sequence similarity to FMRFamide. *O. bimaculoides* is only the second species known to contain this peptide. The success of these bioinformatic screens mirrors recent neuropeptidome research [53,84,85] that have uncovered novel prepropeptides. Our searches focused on the most enriched transcripts of the optic gland transcriptomes only: additional neuropeptides likely remain to be identified in the optic gland transcriptome of *O. bimaculoides*. Future functional proteomic studies will be vital in establishing the bioactivity of these peptides.

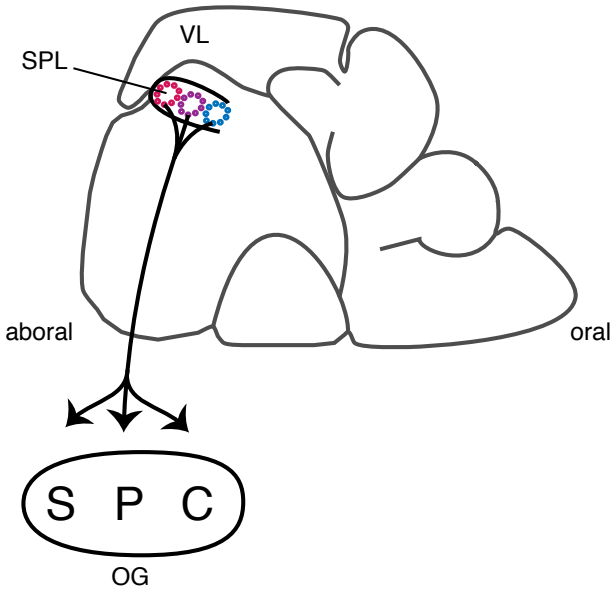

Fig 4.9. Updated view of the optic gland-pituitary gland analogy. The different neurochemical territories of the optic gland may receive input from separate populations of cells in the subpedunculate lobe (SPL) that are devoted to modulating steroid (S), peptide (P), or catecholamine (C) production in the optic glands.The intermediate optic gland may receive input from several populations of subpedunculate cells.

Cellular and Molecular Architecture of the Optic Glands

Our *in situ* experiments show that candidate genes from steroid, catecholamine, and peptidergic signaling systems demarcate at least 3 distinct cellular territories in the female optic gland. These neuroanatomical results reveal an internal organization of the optic gland for the first time.

The aboral end of the optic gland labels strongly and specifically for two steroidogenic enzymes. Both ISH and H&E data show a homogenous distribution of cells in this region, which matches previous characterizations of the optic glands [39]. Importantly, these two cholesterol-metabolizing enzymes are involved in many of the biosynthetic pathways, but nothing is known about their function in octopus. The overlap of enzymatic territories strongly suggests that intracellular cholesterol is restricted to a specific area in the optic gland preceding downstream processing, or that these two enzymes are a part the same biosynthetic pathway in *O. bimaculoides*, or both. These results extend new research that suggests the octopus optic gland produces biologically active steroid hormones [109].

The intermediate and oral regions of the optic gland are specialized for neuropeptide and catecholamine signaling. Despite the wide range of potential functions of the optic gland neuropeptides, all except APGWamide show striking similarity in labeling (Figure 4.7). Our results establish that the steroidogenic territory and the multi-ligand (neuropeptide/DBH) territory of the optic gland differ substantially in their molecular and cellular compositions. As the steroidogenic territory recedes, the multi-ligand territory advances (Figure 4.6 and 4.7), until only neuropeptide and DBH labeling is evident in the oral optic gland. Together, the steroid, catecholamine, and peptide molecular markers identified here account for the bulk, if not all, of the cell bodies in the optic gland (Figure 4.7).

Just as striking as the neurochemical regionality of the optic gland is the cellular heterogeneity demonstrated in the unstained tissue and H&E preparations. The large, unlabeled central territory is reminiscent of the neuropil found in lobes of the central brain (Figure 4.2c and d), a region rich in synaptic connections that permit neurons to communicate with each other. This result raises the exciting possibility that optic gland signaling is not a simple feed forward relay from brain, one modulated by feedback from target tissues, but includes a rich interplay of signals from within the optic gland itself.

Central innervation of the optic gland

The presence of separate neurochemical compartments in the optic gland raises the possibility that different areas of the central brain may target different areas of the optic gland, mirroring organization of the vertebrate hypothalamic-pituitary-gonadal axis. The hypothalamus is made up of a collection of nuclei with separate neuroendocrine functions [125]. Magnocellular neurosecretory cells of the paraventricular nucleus, for example, produce oxytocin, while those of the supraoptic nucleus produce vasopressin. These two neurohormones are then released to the neurohypophysis by direct neural connections [125,126]. The supraoptic nuclei are also thought to innervate the pars intermedia of the adenohypophysis through the infundibular stem [37]. While the pars distalis of the adenohypophysis is also under hypothalamic control, this modulation occurs through the portal vascular system, not through direct nervous connections. The parvocellular neurosecretory cells of the paraventricular nucleus release their hormones into the superior hypophysial artery, which supplies the adenohypophysis [37]. In this way, separate cell populations of the hypothalamus target separate regions of the pituitary gland and also distinct pars distalis secretory cells.

Very little is understood about the anatomy or mechanisms of the optic gland's upstream regulation. Efferent connections from the subpedunculate lobe leave the central brain through the optic gland nerve of the optic tract and provide inhibitory inputs to the optic gland [2], presumably into the central neuropil of the optic gland (Figure 4.2). Like the hypothalamus, the subpedunculate lobe has internal subsections: cells of the subpedunculate are segregated into distinct lobules (Figure 4.9) [2,27]. Given the remarkable similarity in anatomy and function between vertebrate and octopus reproductive axes, our results raise the exciting possibility that separate subpedunculate cell populations target different optic gland territories and are concerned specifically with steroid or peptide production.

Our study provides the first insight onto the internal structure and neurochemical complexity of the octopus optic gland. Like the pituitary gland, the optic gland has regional anatomy to support the production of a medley of signaling factors with diverse functions. We identify at least 3 distinct territories within the optic gland that are specialized for production of 3 distinct collections of secreted factors. One of these territories, an aboral region specialized for steroid production, has not previously been implicated in pituitary function.

CHAPTER 5

Cholesterol metabolites identified in the octopus optic gland

Abstract

Secreted factors from the optic gland of female octopuses coordinate critical life history events, including sexual maturation, maternal care, and post-reproductive death, in a manner analogous to that of the vertebrate pituitary gland. Both organs serve as a bridge connecting signals from the central nervous system to downstream peripheral targets. The pituitary gland secretes neuropeptides that target the gonads and other organs; the signals used in the octopus reproductive axis are largely unknown. Here, we characterize small molecule secretions of the female optic gland using an untargeted metabolomics approach. We recovered abundant cholesterol metabolites in the optic glands of mated and unmated females. In mated females, we found a significant increase in cholesterol metabolites in the steroidogenic pathway downstream of the Rieske oxygenase Daf36. These results reinforce recent bioinformatic and molecular studies that show that the female optic glands employ a multiplex of molecular signals. In particular, steroid hormones are likely crucial to the behavioral and anatomical changes that accompany reproduction in the female octopus. Our study is the first to employ mass spectrometry to identify steroid hormones in the optic glands and advances the understanding of the cholesterol metabolic pathways in the octopus.

Introduction

Octopuses have the most complex central nervous systems of all cephalopod molluscs, with almost 40 brain lobes dedicated to a wide range of functions. Their impressive array of

behaviors includes rapid adaptive coloration, behavioral mimicry, and problem-solving [3]. Usually solitary, adult octopuses come together only to reproduce. After a single reproductive event, males and females die [15].

In female octopuses, the post-reproductive period is marked by stereotyped behaviors. The female dedicates the last few months of her life to tending to her eggs. She shows an aversion to leaving her clutch and abstains from feeding [52]. Right when the eggs are about to hatch, the female undergoes a period of precipitate senescent decline marked by extreme behaviors, including self-injury, that ultimately lead to death [17,33,111].

In a pioneering study from Jerome Wodinsky in 1977, all maternal behaviors, including death, were reversed when the optic glands were removed from brooding females. The optic glands are paired neuroendocrine organs that act as the crucial intermediary between the central brain and the peripheral organs (Figure 1.1). Glandectomized animals ceased brooding and resumed normal feeding behaviors. Some females even mated a second time. Ultimately, optic gland removal led to an increase in longevity by 5.75 months in experimental animals as compared to their intact counterparts [33]. These striking behavioral and physiological changes were attributed to the actions of the optic gland and its secretions, termed the octopus "self-destruct" system.

Despite these important roles, the chemical identities of the optic gland secretions are largely uncharacterized. Recent bioinformatic, molecular, and neuroanatomical studies provided the first insight onto the nature of the optic gland secretions [111]. The regulatory molecules of the pituitary are neuropeptides, but RNA-sequencing data from octopus suggests that steroids, along with peptides, are a major signaling system of the optic glands. After mating, the optic glands of females increased expression of key cholesterol-metabolizing enzymes, including

cholesterol 7-desaturase/DAF36, and 3-beta-hydroxysteroid dehydrogenase (3BHSD), and sterol 27-hydroxylase (CYP27A1) [111]. These new data raised the exciting possibility that the optic glands may secrete steroid factors, in addition to identified neuropeptides, that are important for the behavioral changes seen in the maternal period.

We sought confirmation for this mating-induced shift in steroid signaling molecules by performing *in situ* hybridization experiments on Daf36, a steroidogenic enzyme found to increase after mating. To determine if the optic gland enzymes produce bioactive metabolites in octopuses, we developed an untargeted metabolomics approach to study whole optic gland samples from mated and unmated female octopuses.

Results

DAF36 labels corresponding regions in the optic glands of mated and unmated female octopuses.

Daf36, 3BHSD, and CYP27A were identified as significantly enriched in the optic glands of mated female octopuses in all stages of maternity by transcriptomic analyses [109]. Of these, Daf36 is of particular interest to sterol chemistry because in non-mammals, it sequesters cholesterol for steroid synthesis as opposed to production of bile acids [74].

To further explore *Daf36* expression and function, we performed *in situ* hybridization for *Daf36* in the optic glands of mated and unmated female octopuses. Coronal sections of optic gland from mated and unmated females were processed together in one mailer, incubated in the same probe mixture and same formazan solution, which provided identical reaction times. At 2.5

hrs, the color reaction was terminated. The mated optic gland showed strong and specific labeling in the aboral region (Figure 5.1a). Daf36 labeling in the unmated female was barely detectable (Figure 5.1b). These results show that Daf36 is present in corresponding regions in unmated and mated optic glands, though at strikingly different concentrations. This raised the possibility that increased Daf36 enzymatic activity accompanies reproduction and contributes to physiological and behavioral changes observed in mated females.

Methanol extraction is effective for the detection of optic gland small sterols by electrospray LCMS in positive mode

To determine if products of Daf36 and other cholesterol metabolites are present in the optic glands, we performed an untargeted metabolomics discovery experiment to capture and identify small molecule compounds. Since detection of steroids in octopus tissues by liquid chromatography-gas spectrometry (LCMS) has not been reported, we refined Cologna Lab lipidomics protocol for the detection of sterols (Figure 5.2, see Chapter 2 Methods) [127]. The protocol was first tested on steroid standards. We resolved sharp peaks for estradiol, progesterone, cortisol, 7-dehydrocholesterol (7-DHC), and cholesterol (Figure 5.2).

We tested this LCMS protocol on male neural tissue samples and the optic gland, using 4 different extraction methods. The neural tissues were the optic lobes, which are large, kidney-shaped structures located adjacent to the optic gland, and the subesophageal brain, which is thought to contain some neurosecretory cells (Figure 1.1) [2]. Three extraction methods (methanol, isopropanol, and acetonitrile; see Methods) have been employed in other animals to identify sterols [128-132].

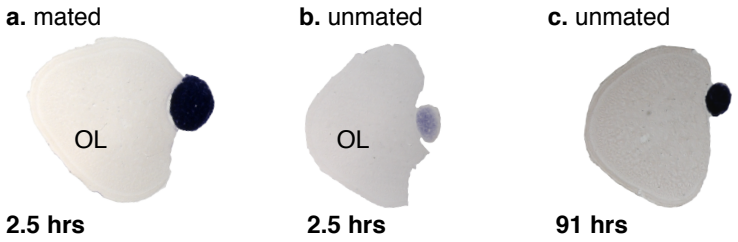

Fig 5.1. *In situ* hybridization experiment shows different levels of *DAF36* expression in optic glands of unmated and mated females. After 2.5 hours in color solution, the aboral optic glands of mated animals (a) showed intense *DAF36* labeling. The unmated optic gland (b) showed very faint, barely detectable *DAF36* labeing. A comparable level of labeling was only seen in the unmated optic gland after 91 hrs in color solution (c). Panels b and c are from separate experiments.

a. Estradiol

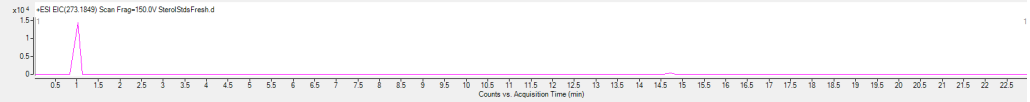

b. Progesterone

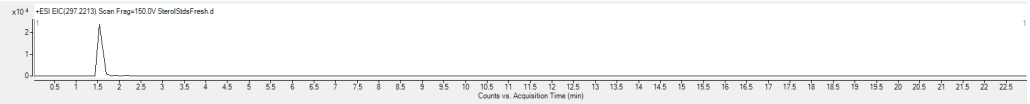

c. Cortisol

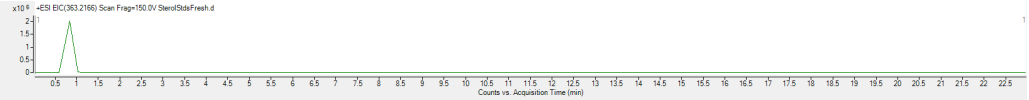

d. Cholesterol

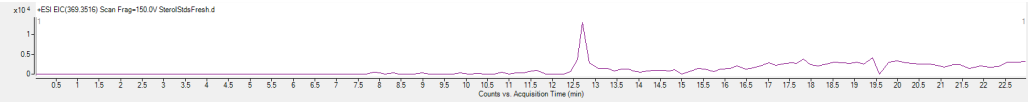

e. 7DHC

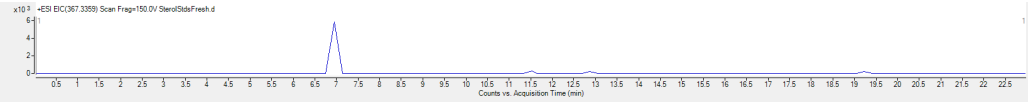

Fig 5.2. Detection of steroid standards by ESI-LCMS in positive mode. Extracted ion chromatograms (EICs) for protonated forms of estradiol (a), progesterone (b), and cortisol (c), and dehydrated species of cholesterol (d) and 7-dehydrocholesterol (7DHC, e) are shown.

Methyl tertiary-butyl ether (MTBE) extraction was recently developed to extract all lipids and is not specialized for cholesterol lipids [58,133].

We found that the four extraction methods showed different amounts of fragmented signal (Figure 5.3). Optic lobe samples extracted with MTBE yielded the most abundant signal (Figure 4d), but upon identification with a custom PCDL database, we found that this extraction was strongly biased for membrane lipids (see Methods). Methanol gave the lowest abundance of total signal (Figure 5.3c), but we found this method was the most effective at recovering steroids in octopus tissue: we recovered estradiol, cortisol, cholesterol, and 7-dehydrocholesterol (7-DHC) in methanol-extracted optic lobe samples (masses in Table 2.1). Steroid compounds in their native biological background behaved differently than in standard solution (Figure 5.4). We saw, for example, peak shape in cholesterol and 7DHC to be more complex in our biological samples (Figure 5.4d and e), and elution times were altered.

Steroid hormones are found in the female optic glands

To determine if steroid hormones are present in the optic gland, we used MassHunter Qualitative Analysis Software (Agilent) to extract individual chromatograms (EICs, masses in Table 5.1). We quantified sharp peaks for progesterone (Figure 5.5a-c) and cortisol (Figure 5.5d-f). Differences were not significant by student's t-test.

Some compounds were captured in only one sample condition. In the juvenile optic gland, we also captured pregnenolone (Figure 5.6a). Peaks for 7-ketocholesterol (Figure 5.6b) and 27-hydrocholesterol (Fig 5.6c) were identified only in the mated optic gland trials.

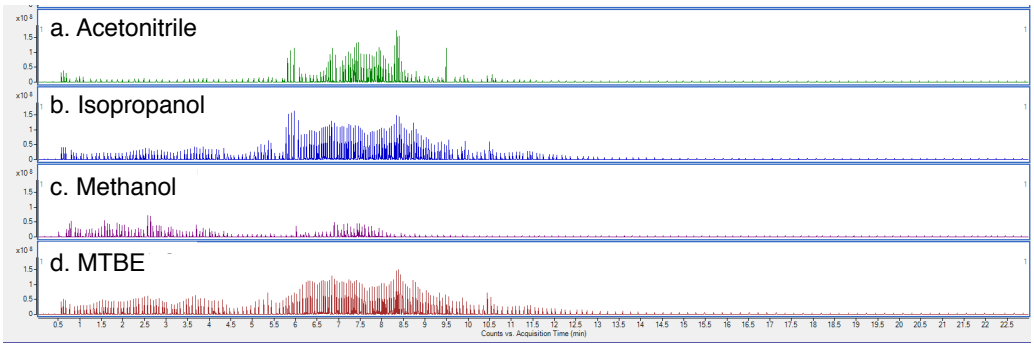

Fig 5.3. Extraction methods tested on optic lobe sample. Total ion counts (TICs) for optic lobe sample under different extraction methods are shown. MTBE (d) yielded high total abundance, but the extracted compounds were biased for membrane lipids.

Fig 5.4. Detection of steroids in optic lobe samples. EICs for protonated forms of estradiol, progesterone, and cortisol, and dehydrated species of cholesterol and 7-dehydrocholesterol (7DHC) are shown. No progesterone was detected.

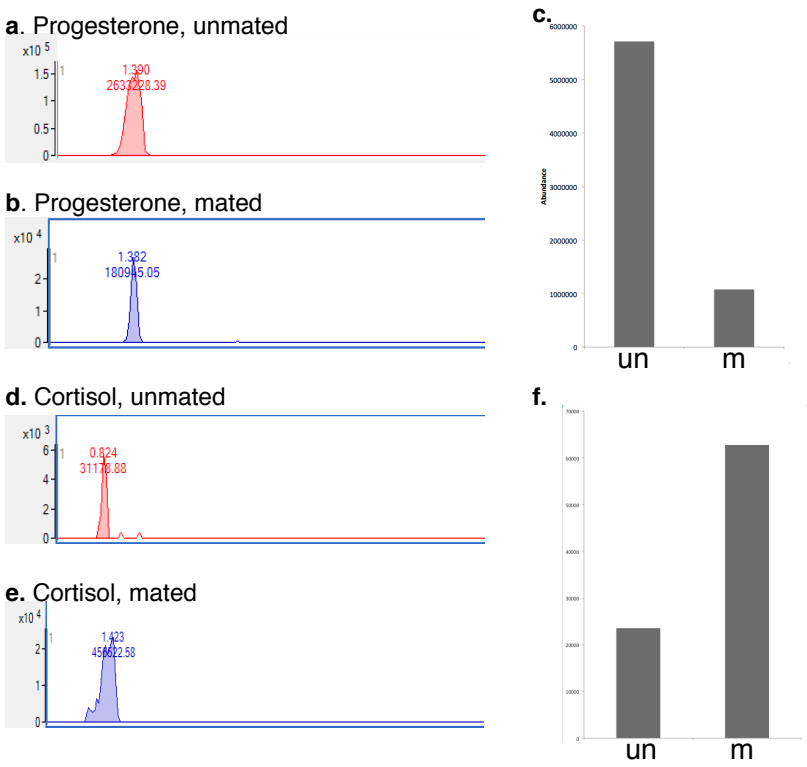

Fig 5.5. Directed EIC search identified progesterone and cortisol in the optic glands. Progesterone (a-c) eluted at 1.3 minutes and cortisol (d-f) eluted at 0.83 minutes. In a, b, d, and e, a truncated EIC for one technical replicate in each sample category is shown. Quantitative measurements of these steroids were not significantly different (c and f). un: unmated; m: mated.

a. Pregenenolone, unmated

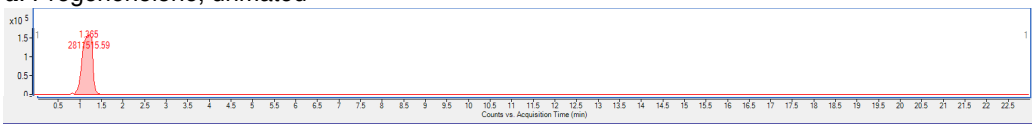

b. 7-ketocholesterol, mated

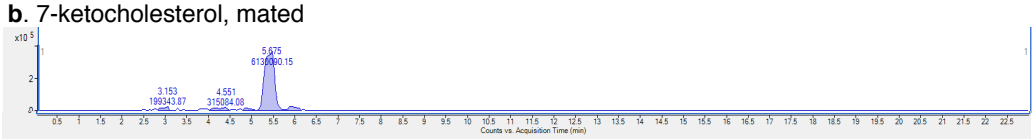

c. 27-hydrocholesterol, mated

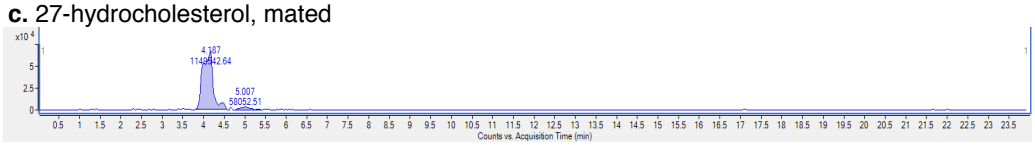

Fig 5.6. Sample-specific steroids. a. Pregnenelone, the precursor to progesterone, is found in unmated optic gland only. b. 7-ketocholesterol, an oxysteroid, is found in mated optic gland only. c. Mated optic gland also contains 27-hydrocholesterol.

In unmated and mated samples, we found cholesterol and 7-dehydrocholesterol EICs had a broad, complex shape and ancillary peaks at elution times that did not match the standard elution time (Figure 5.7). This is observed when a mixture of isomers exists in the sample. Since many reactions in cholesterol metabolism involve the simple addition or movement of a C-C double bond, many stereoisomers of cholesterol and its derivatives are possible [134,135]. In the cholesterol EIC (Figure 5.7b and c), peak complexity is likely due to the presence of cholesterol (molar mass 386.654) and delta7-lathosterol (molar mass 386.664). In the 7-DHC EIC (Figure 5.7 b and c), peak complexity could be due to the presence of 7-DHC (molar mass 384.339), 8-DHC (molar mass 384.339), and desmosterol (384.64). It is not possible to separate these compounds or deconvolute EIC peaks using liquid chromatography.

Small molecules show significant fold-change between mated and unmated optic glands

To identify secretions of the optic gland, we assayed methanol-extracted samples with our modified lipid LCMS protocol. Fold-change analysis found 96 compounds that showed at least a 4-fold increase in in the optic glands of mated females ($p < 0.05$) and 103 compounds that were significantly abundant in the optic glands of unmated females (Figure 5.8). Compound identification with MPP software yielded steroid assignments using MS1 spectra. For secondary validation, we submitted spectral profiles to Metlin. This dual-validation method positively identified the oxysterol 7-ketocholesterol in the mated optic gland (Figure 5.9a). In the unmated female optic gland, no sterols were detected. We identified lipids, including the signaling lipid, docosahexaenoic acid (Figure 5.9b).

a. Standards

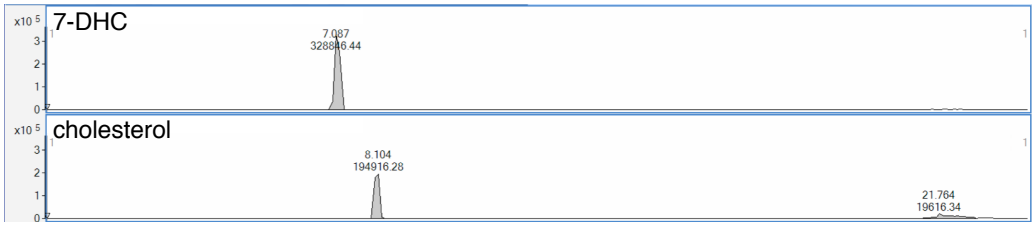

b. Unmated

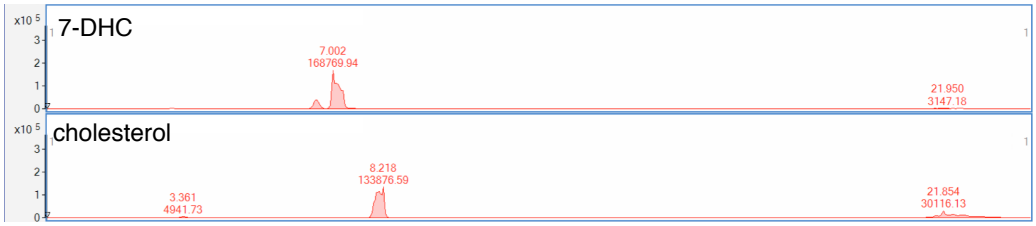

c. Mated

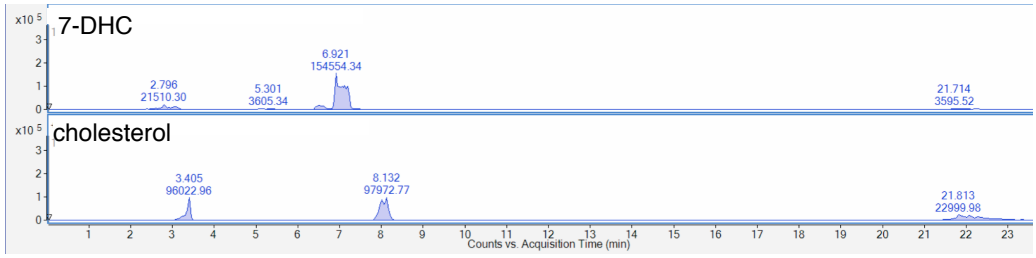

Fig 5.7. Biological 7-DHC and cholesterol have complex peak shapes. Synthetic standards of cholesterol and 7-DHC have sharp, single peaks (a). However, in unmated (b) and mated (c) optic gland samples, the peak shapes of these sterols changed. 7-DHC showed a small, secondary shoulder that eluted ahead of the major peak. Cholesterol showed a minor peak at around 3 minutes. The presence of broad, complex, and accessory peaks suggests a mix of stereoisomers are present in biological samples. Note that while the peak shape changed, the elution times for the major peaks of 7-DHC and cholesterol did not differ from that of the standard.

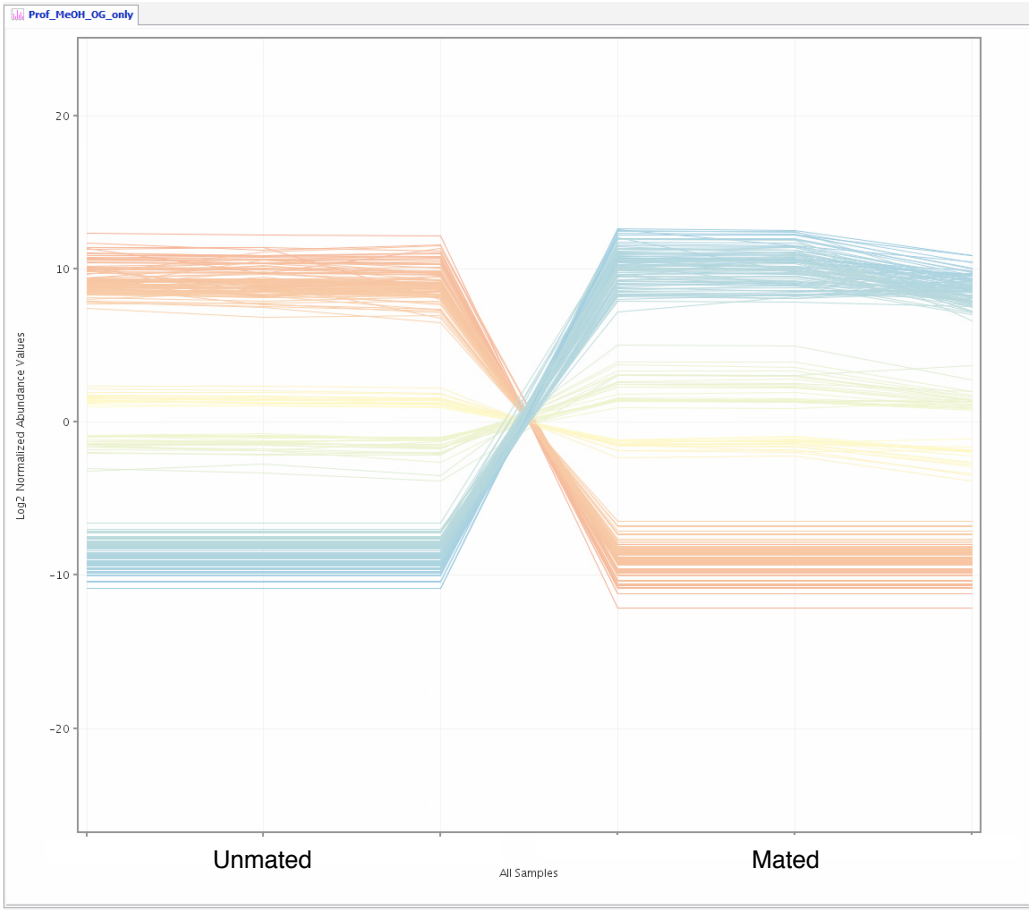

Fig 5.8. Fold-change analysis identified compounds that are significantly abundant in unmated and mated optic glands. Only compounds present in all 3 technical replicates of each category were considered for fold-change analysis (see Methods for details). 103 compounds were found to be significantly abundant in unmated optic glands (red) and 96 compounds were found to be significantly abundant in mated optic glands (blue).

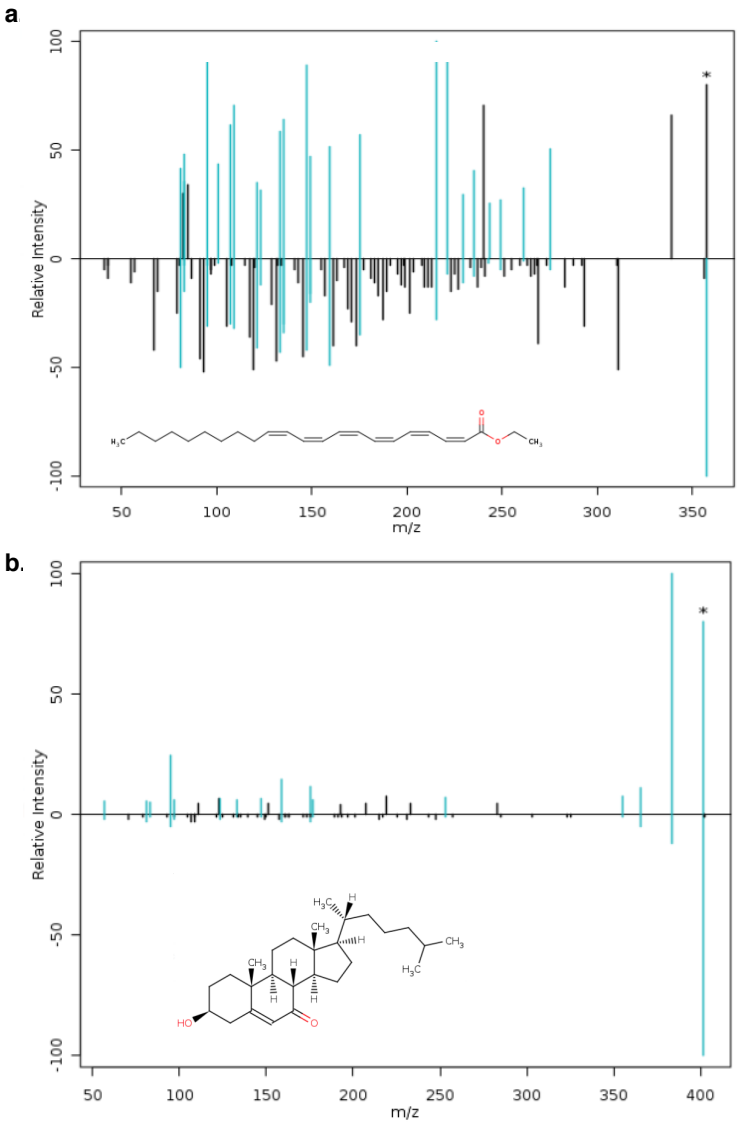

Fig 5.9. Metlin confirmation of differential compounds. MS/MS fragment searches identified docosahexaenoic acid ethyl ester in the unmated optic gland (a) and 7-ketocholesterol in the mated optic gland (b).

Sterol quantification in octopus tissues

In directed searches for steroids of interest, we made putative assignments of cholesterol and 7-DHC in the optic glands, but could not distinguish between the two, as described above. In separate GCMS analysis, levels of 7 sterols in the optic lobes, optic glands, and white bodies were quantified. The white bodies are a hematopoietic organ that surrounds the central brain and optic gland. We found cholesterol to be the most abundant sterol in the white body and optic lobes, with negligible levels of the other sterols. In both mated and unmated optic glands, however, 7DHC was the most abundant sterol (Figure 5.10). In mated optic glands, 7DHC accounted for over 50% of the total sterols. 8-DHC was not detected, ruling out its role in the complex peaks seen in 7-DHC EIC (Figure 5.7).

Discussion

We have confirmed the presence of cholesterol metabolites and identified steroid hormones in the optic glands of unmated and mated female *O. bimaculoides*. Our findings are consistent with previous prediction that the optic gland employs steroidogenic pathways in its signaling functions, and expand the mechanistic knowledge of optic gland function. We show that sterol chemistry of the optic gland changes with reproduction, biasing the sterol content of the optic glands away from cholesterol towards downstream metabolites of the Rieske oxygenase Daf36. At least one cholesterol metabolite, 7-ketocholesterol, shows increased abundance coincident with mating, strongly suggesting that these metabolites are biochemically active signaling molecules. This study is the first to employ untargeted LCMS metabolomics methods to analyze steroid compounds in the neuroendocrine center of the octopus.

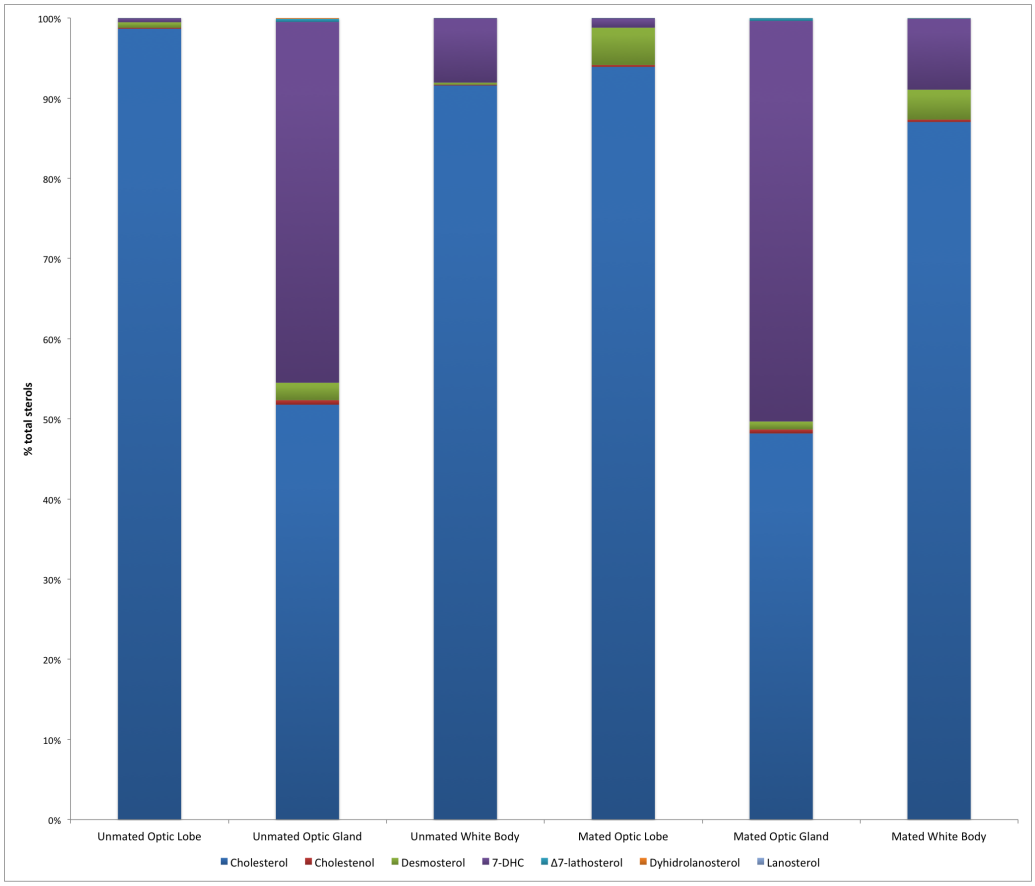

Fig 5.10. Sterol quantification by GCMS. Cholesterol stereoisomers can not be separated by LCMS, but are routinely separated and quantified by GCMS. Clinical assay for sterol levels showed that cholesterol (blue) is the dominant sterol in all tissue samples except for the optic glands. Optic gland tissue shows depleted levels of cholesterol and increased levels of 7-DHC (purple). Other sterols were detected in small quantities: desmosterol (green); delta-7-lathsterol (teal), lanosterol (light blue), dihydrolanosterol (orange), 8-DHC (not detected).

Optic gland steroids

The presence of steroid hormones in the optic glands expands original characterization of the gland as a pituitary analog: the hypothalamus and pituitary gland secrete peptide signals only [37,126]. Steroid hormones exert negative feedback in the reproductive axis, but steroids are produced exclusively by the downstream targets of the pituitary gland, not by the gland itself. The findings we report here correspond to recent descriptions of the optic gland's multiplex signaling systems. Previously, the enzymes 3BHSD, DAF36, and CYP27A1 were identified in the optic gland by transcriptomic and molecular methods [52] (see Chapter 4). 3BHSD catalyzes the biosynthesis of progesterone from pregnenolone. Here, we show preliminary identification of progesterone in the mated and unmated optic glands. In vertebrates, progesterone is produced by the corpus luteum following ovulation and inhibits the secretory functions of the hypothalamus and the pituitary gland [136]. If the inhibitory actions and upstream targets of progesterone are conserved, progesterone from the optic gland may provide negative feedback on the subpedunculate lobe of the central brain. This would, in turn, lift subpedunculate inhibition on the optic gland and promote additional glandular growth and secretion. By shutting down upstream inhibition, progesterone may act to perpetuate the production of other optic gland signals that target downstream organs.

In ecdysozoa and non-mammalian deuterostomes, DAF36 catalyzes the conversion of cholesterol to 7-DHC by introducing a double bond at the 7-C position [74,75,137]. In *C. elegans*, this first step critically separates cholesterol for the production of bile acid steroids [74]. We confirmed that DAF36 is present at high levels in the optic gland of mated females (Figure 5.1) and identified its product, 7-DHC, by LCMS and GCMS (Figure 5.7 and 5.10). These data provide compelling evidence that the enzymatic properties of DAF36 are conserved across the

deuterostomes, ecdysozoa, and spiralia lineages. Additional evidence for the importance of the bile acid pathway in octopus reproduction is provided by the presence of 27-hydrocholesterol, the product of CYP27A1. Future functional studies will be critical in testing activity of these cholesterol-metabolizing enzymes.

We were also able to make a preliminary assignment of cortisol in the optic gland. In vertebrates, cortisol is produced by the adrenal cortex [73,107]. Elevated cortisol levels in Pacific salmon, *Oncorhynchus kisutch*, mediate programmed death through tissue degeneration and impaired homeostatic function [105]. Our data do not show significantly increased cortisol in mated females, but does provide additional evidence that the optic gland takes on functions that are reserved for downstream targets of vertebrate neuroendocrine centers.

7-ketocholesterol in the mated female optic gland

Analysis of differentially abundant compounds indicated that 7-ketocholesterol is elevated in mated female optic glands (Figure 5.9). In humans, low levels of 7-ketocholesterol naturally occur as a result of autoxidation of cholesterol [138]. Elevated levels of 7-ketocholesterol are only found in human pathological conditions, such as Niemann-Pick disease type C (NPC1) [139]. Under disease states, enzymatic formation of 7-ketocholesterol from 7-DHC may occur [140,141]. In patients with Smith-Lemli-Opitz syndrome (SLOS), for example, CYP7A1 is thought to catalyze the formation of 7-ketocholesterol from 7-DHC [142]. Whether 7-ketocholesterol synthesis in the octopus occurs through enzymatic or non-enzymatic pathways remains to be determined.

It should be noted, however, that beyond the presence of identical cholesterol metabolites, striking behavioral similarities exist between mated female octopuses and patients

with SLOS and NPC1. The adult form of NPC1 presents with many behavioral symptoms, including self-mutilation [143]. Similarly, 90% of humans with SLOS report a history of self-injury [144,145]. Self-cannibalization and self-injury in octopus are prominent behavioral markers of the precipitate organismal senescence that occurs in the last phase of maternal brooding [52]. These data reveal that similar and profound effects of cholesterol synthesis deficiency or increased cholesterol utilization exist between animals as evolutionarily-distant as humans and octopuses.

Working model of cholesterol metabolism in the octopus

The molecular and metabolomic data presented here show that several mechanisms are in place to deplete levels of cholesterol in the mated female optic gland (Figure 5.11). Low levels of cholesterol may by itself suffice to cause catastrophic physiological changes like those seen in brooding female octopuses. However, given the neuroendocrine function of the gland, it is more likely that downstream cholesterol metabolites trigger a cascade of maternal behavioral effects. Intervention studies that inhibit steroidogenesis or rapidly replenish cholesterol levels will elucidate how cholesterol metabolites contribute to maternal care in the octopus and to the understanding of biological mechanisms of organismal senescence.

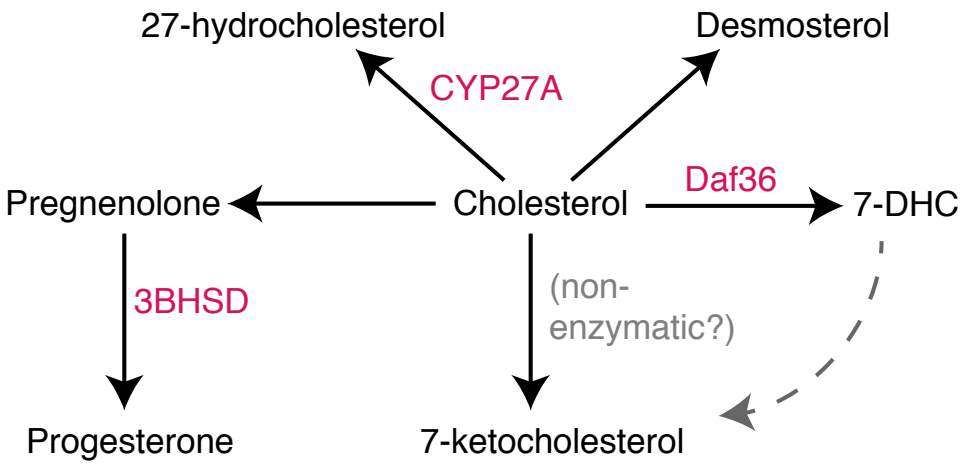

Fig 5.11. Working model of cholesterol metabolization in the optic glands of *O. bimaculoides.* Sustained utilization of cholesterol occurs in the optic gland across adult behavioral stages. Whether the increased abundance of 7-ketocholesterol in mated females is produced by enzymatic reaction, with 7-DHC as the substrate, or occurs by autoxidation, remains unresolved.

Chapter 6

Conclusions and Future Directions

Major Findings

One of the most important events in an animal's life is reproduction, a complex behavioral process tightly controlled by signaling between the nervous system and reproductive organs. The metabolic and fitness costs of reproduction are particularly high for individuals of semelparous species, including octopuses, which reproduce only once in their lives. Investigating the optic glands, the fulcrum of the octopus reproductive axis, is paramount to the understanding of life and death in this large invertebrate species. In this thesis, I characterize the optic glands using new approaches in bioinformatics, molecular neuroanatomy, and analytical chemistry, to uncover the mechanisms underlying maternal behaviors and post-reproductive death in *O. bimaculoides*.

Research on the optic gland was an early focus of cephalopod neurobiology, largely due to serendipity. Researchers studying the vertical lobes, the learning and memory centers of the octopus brain, sometimes accidentally lesioned the subpedunculate lobe as well [2,23]. Dramatic changes in reproductive physiology and behavior ensued, as reviewed in Chapter 1. The research described here is also necessarily grounded in maternal behavior. I found that adult female octopuses observed in the laboratory could be categorized into 4 stages of behavior: non-mated, feeding brooding, fasting brooding, and senescent decline. My behavioral findings demonstrate that maternal care in the octopus does not perfectly coincide with fasting, as previously described, but instead involves an initial period of feeding. I show that the behavioral stages of adult octopus life have corresponding changes in optic gland gene expression, including in the

up- and down-regulation of peptide, neurotransmitter, steroid, and insulin signaling systems [52]. The reported simple internal structure of the optic gland belies its multiplex of signals. In revisiting optic gland homogeneity, I find that the optic gland is not a "uniform mass of cells" as originally described [39]. Instead, the optic glands contain least 3 neurochemical territories specialized for the production of steroidogenic, neuropeptidergic, and catecholaminergic factors. In particular, the presence of steroidogenic signatures in the optic gland raises the possibility that optic gland function is not only analogous to pituitary function but, in fact, extends beyond it. Using new methods in analytical chemistry and discovery metabolomics developed in collaboration with Dr. Stephanie Cologna, I identify steroid hormones and cholesterol metabolites in the optic gland, including progesterone, cortisol, cholesterol, 7-dehydrocholesterol, and 7-ketocholesterol. The abundance of 7-ketocholesterol and increased utilization of cholesterol in the optic glands of mated females suggests that the biochemical pathways underlying the stark behavioral changes at the end of octopus life share similarity to those found in systems as disparate as human pathologies, including Smith-Lemli-Opitz and Niemann Pick Disease type C [139,142]. My thesis characterizes neuropeptide and steroid markers of the optic gland for the first time, and represents the first major addition to the understanding of mechanisms underlying octopus maternal behaviors in since the 1970s.

Experiments for the Future

Mechanisms of optic gland secretion

In Chapter 3, I identify several prominent signaling systems of the optic gland, which include insulin, neuropeptide, catecholamine, and steroidogenic factors. I pursue anatomical verification and characterization of the latter three systems in chapter 4. My results show that the

optic gland contains neurochemical compartments specialized for the production of these evolutionarily-ancient signals. Pursuing genes implicated in neurotransmission, which are also significantly enriched in mated optic glands, would advance the understanding of how these factors are released by cells of the optic gland.

By some anatomical accounts, the octopus optic gland does not appear to contain secretory granules [39]. However, electron microscopy demonstrates the abundant presence of secretory granules in the stellate cells of the octopus and squid optic glands [146,147]. Cells near the blood vessels of the optic gland are packed tightly with granules that resemble dense core vesicles (DSVs) found in vertebrate secretory cells, suggesting high molecular-weight cargo [96,148]. In other animals, DSVs contain neuropeptides, insulin-related peptides, dopamine, and additional neuromodulators [149]. DSVs are released by neurons and endocrine cells by synaptotagmin-mediated exocytosis [148].

My data provide preliminary evidence that octopus neuropeptide and insulin-like proteins may be secreted in a similar manner, though with additional complexity: neuropeptides are enriched in the unmated optic gland, and exocytotic genes are upregulated in the mated optic gland [52]. It is possible that neuropeptides are produced by optic gland cells in adulthood, but release of neuropeptide DSVs is triggered only after reproduction. Alternatively, the transcripts involved in vesicle release that I identified are concerned with release of insulin-like peptides only. Regardless, evidence of co-localization of exocytotic genes in the neuropeptide zones of the optic gland would be a critical first step in teasing apart the conundrum of optic gland secretion. How these functions remain intact after optic gland dissection from the optic stalk will remain an interesting enigma for cephalopod physiology.

Neurochemical characterization of the optic gland in mated females

In Chapters 3 and 5, I show that differences in expression level of *DAF36* can be measured bioinformatically and by *in situ* hybridization: at 2.5hrs, DAF36 labeling was strong in the mated optic gland and barely detectable in the unmated optic gland. This finding suggests wholesale changes in the cellular or tissue architecture of the optic gland with reproduction. Pursuing *in situ* hybridization in mated female octopuses at each stage of adult life would provide a comprehensive understanding of how, or if, the internal neurochemical territories change as the gland grows. Original accounts of optic gland growth suggest that the total number of cells does not change, but instead, the stellate cells increase in volume [23,39]. However, my data point to an alternate, more nuanced possibility of cellular remodeling in the gland. Future in situ experiments in mated optic glands may reveal that growth is not due to stellate cells at large increasing in size, but the addition of new cells in specific neurochemical compartments, or even the incorporation of entirely new, undescribed compartments. Moving forward, it will be particularly important to understand the mechanism glandular growth in mated females.

Testing the convergent evolution of steroidogenesis

Convergent steroidogenic pathways exist between species as evolutionarily-distant as humans and worms [74]. For example, delta-7 desaturation is an important first catalytic step in steroid biosynthesis in mammals and ecdysozoa [74,75,137]. Although the steroids used in insect and mammalian endocrine systems are different, their stereoisomer structures and many of their downstream effects bear remarkable similarities [74,134]. In Chapter 5, I show that conservation of function in key cholesterol-metabolizing enzymes is extended to *O. bimaculoides*. The enzymes and cholesterol products we find in the octopus optic gland correspond with

biochemical defects in human pathologies, but functional studies are needed to confirm this. In particular, it will be important to determine whether it is cholesterol depletion, signaling effects of 7-dehydrocholesterol and 7-ketocholesterol, or a combination of both that contribute to post-mating brooding, fasting, and self-injurious behaviors.

The proximal steroid instigator of maternal behaviors is unresolved in the octopus. If cholesterol depletion in the optic gland is sufficient to trigger maternal effects, we can target biochemical mechanisms of behavior by artificially lowering levels of cholesterol. Statins are a class of pharmaceutical therapies used to combat elevated circulating cholesterol levels [150]. Statins act by inhibiting HMG-CoA reductase in the cholesterol synthetic pathway [134]. Administration of statins to unmated female octopuses, either through bath application, injection, or another means, will test whether a depleted level of cholesterol itself can trigger behavioral signatures of maternity.

Delivering 7-ketocholesterol, which is significantly abundant in mated females, to unmated females will enable the understanding of cholesterol metabolite signaling in the octopus. 7-ketocholesterol inhibits cholesterol 7-alpha hydroxylase, which catalyzes the rate-limiting step in bile acid steroid synthesis [151]. Behavioral changes following 7-ketocholesterol administration may point to bile acid steroid effectors of physiological change, which was well beyond the scope of this thesis.

Discovery metabolomics is an emerging field of analytical chemistry, and all the more nascent in cephalopod biology. The dearth of molecular and biochemical techniques in cephalopod biology at large presents a major impediment to progress, and though several developmental efforts are underway, many conventional methods such as cell culture and gene manipulation are currently unavailable. Ideal experiments would target the genes and processes

of optic glands specifically, but in the absence of such techniques, I have suggested here some elementary ways of testing the limits of conservation of steroidogenic compounds before these technological barriers are broken. It is important to note that, prior to any manipulation study, the identity of optic gland steroids should be validated with ancillary methods. Cholesterol chemistry is particularly challenging because of the high number of stereoisomers. Even in human clinical studies, the biochemical determinants of SLOS and NPC1 are uncertain and remain an active area of research [139,142].

Extending investigation into iteroparous cephalopods

My findings expand the pituitary-optic gland analogy and provide critical insight onto the control of reproduction in *O. bimaculoides*. This species was particularly amenable to this research due to its semelparous nature, which I summarize in Chapters 1 and 3. However, to gain access to the evolution of reproductive strategies, exploring neuroendocrine functions in iteroparous cephalopods will be crucial.

It has long been accepted that all extent coleoid cephalopods are semelparous and die after a single spawning event [152,153]. Closer examination of cephalopod life histories demonstrates, however, that diverse reproductive patterns may be used [15]. For example, the decapod *Idiosepius pygmaeus* and the pelagic octopus *Argonauta boettgeri* appear to continuously spawn throughout adulthood [154]. *I. pygmaeus* is exceptionally short-lived, with the life cycle completed in 80 days or less; females spend most of their adult lives laying eggs [15]. The Argonauts, also known as paper nautiluses, live close to the ocean surface. Females reside in a thin, paper-like shell created from substances secreted by their arms [154]. This structure later becomes a protective case for the eggs. The life histories of these cephalopods

differ dramatically from that of benthic octopuses. Nevertheless, accounts such as these have led to a recent reframing of cephalopod reproductive strategies to include simultaneous terminal spawning (referred to in this thesis as semelparity), polycyclic spawning, multiple spawning, and intermittent terminal spawning [15]. In general, octopus species are overwhelmingly simultaneous terminal spawners, and this bias is especially true for models studied in laboratory settings [5,12,13].

One notable exception, however, is *O. chierchiae*, the Pacific striped octopus. In laboratory settings, females have been observed to have several egg-laying bouts and grow between reproductive events [155]. The consequences of this reproductive technique on population dynamics are unknown. However, *O. chierchiae* is highly tolerant of sociality and not cannibalistic [18]. In fact, this species is a commonly-sought after species for cephalopod hobbyists because many individuals can be housed in the same tank. The unique behaviors observed in this species raise the possibility that its optic gland neuroendocrine mechanisms are highly divergent from those I have identified in *O. bimaculoides*. Sequencing *O. chierchiae* optic glands and probing specifically for the signaling systems characterized here will be particularly effective for the study of cephalopod reproductive strategies at large.

Concluding remarks

The work presented in this thesis provides a multifaceted understanding of the neuroendocrine center of *O. bimaculoides*. I confirm and expand upon the pituitary-optic gland analogy that was first established in 1969, and show striking conservation in function of peptide and steroid signaling systems between octopuses and vertebrates. The technical and analytical

methods developed in this project provide a strong foundation for future neuroethological study of the octopus.

There is great merit and reward in studying natural behaviors of unconventional and under-studied animal systems. Re-examining classical experiments or widely-accepted concepts with new techniques can lead to unexpectedly far-reaching results. The field of neuroscience is greatly informed and enhanced by studies that keep the animal's behavioral ecology and life history events in mind.

REFERENCES

1. Kröger, B., Vinther, J., and Fuchs, D. (2011). Cephalopod origin and evolution: A congruent picture emerging from fossils, development and molecules. BioEssays *33*, 602–613.

2. Young, J.Z. (1971). The anatomy of the nervous system of Octopus vulgaris (Oxford University Press).

3. Hanlon, R.T., and Messenger, J.B. (2018). Cephalopod Behaviour 2nd ed. (Cambridge University Press).

4. Wells, M.J. (1978). Octopus (Springer Science & Business Media).

5. Forsythe, J.W., and Hanlon, R.T. (1988). Behavior, body patterning and reproductive biology of Octopus bimaculoides from California. Malacologia *29*, 44–55.

6. Moltschaniwskyj, N., and Jackson, G. (2000). Growth and tissue composition as a function of feeding history in juvenile cephalopods. J. Exp. Mar. Biol. Ecol. *253*, 229–241.

7. Forsythe, J.W., and Hanlon, R.T. (1988). Effect of temperature on laboratory growth, reproduction and life span of <Emphasis Type="Italic">Octopus bimaculoides</Emphasis>. Mar Biol *98*, 369–379.

8. Van Heukelem, W.F. (1973). Growth and life-span of Octopus cyanea (Mollusca: Cephalopoda). J. Zool. *169*, 299–315.

9. Lipiński, M.R. (1998). Cephalopod life cycles: patterns and exceptions. South African Journal of Marine Science *20*, 439–447.

10. Wood, J.B., and O'Dor, R.K. (2000). Do larger cephalopods live longer? Effects of temperature and phylogeny on interspecific comparisons of age and size at maturity. Mar Biol *136*, 91–99.

11. Wodinsky, J. (2008). Reversal and transfer of spermatophores by Octopus vulgaris and O. hummelincki. Mar Biol *155*, 91–103.

12. Avila-Poveda, O.H., Colin-Flores, R.F., and Rosas, C. (2009). Gonad development during the early life of Octopus maya (Mollusca: Cephalopoda). Biol. Bull. *216*, 94–102.

13. O'Dor, R.K., and Wells, M.J. (1978). Reproduction versus somatic growth: hormonal control in Octopus vulgaris. J. Exp. Biol. *77*, 15–31.

14. Wells, M.J., and Wells, J. (1970). Observations on the feeding, growth rate and habits of newly settled Octopus cyanea. J. Zool. *161*, 65–74.

15. Rocha, F., Guerra, A., and González, A.F. (2001). A review of reproductive strategies in cephalopods. Biol. Rev. Camb. Philos. Soc. *76*, 291–304.

16. Mohanty, S., Ojanguren, A.F., and Fuiman, L.A. (2014). Aggressive male mating behavior depends on female maturity in Octopus bimaculoides. Mar Biol *161*, 1521–1530.

17. Mather, J.A., and Alupay, J.S. (2016). An ethogram for Benthic Octopods (Cephalopoda: Octopodidae). J. Comp. Psych.

18. Caldwell, R.L., Ross, R., Rodaniche, A., and Huffard, C.L. (2015). Behavior and Body Patterns of the Larger Pacific Striped Octopus. PLoS ONE *10*, e0134152–17.

19. Di Cristo, C., and Di Cosmo, A. (2007). Neuropeptidergic control of Octopus oviducal gland. Peptides *28*, 163–168.

20. Ylitalo, H.A., Watling, L., and Toonen, R.J. (2013). First description of hatchlings and eggs of Octopus oliveri(Berry, 1914) (Cephalopoda: Octopodidae). Molluscan Research *34*, 79–83.

21. Anderson, R.C., Wood, J.B., and Byrne, R.A. (2002). Octopus senescence: the beginning of the end. J. Appl. Anim. Welf. Sci. *5*, 275–283.

22. Hanlon, R.T., and Forsythe, J.W. (1985). Advances in the laboratory culture of octopuses for biomedical research. Lab. Anim. Sci. *35*, 33–40.

23. Wells, M.J., and Wells, J. (1959). Hormonal Control of Sexual Maturity in Octopus. J. Exp. Biol. *36*, 1–33.

24. Jin, J.-M., and Yang, W.-X. (2014). Molecular regulation of hypothalamus–pituitary–gonads axis in males. Gene *551*, 15–25.

25. Handa, R.J., and Weiser, M.J. (2014). Gonadal steroid hormones and the hypothalamo–pituitary–adrenal axis. Front. Neuroendocrinol. *35*, 197–220.

26. Minakata, H., and Tsutsui, K. (2016). Oct-GnRH, the first protostomian gonadotropin-releasing hormone-like peptide and a critical mini-review of the presence of vertebrate sex steroids in molluscs. Gen. Comp. Endocrinol. *227*, 109–114.

27. Shigeno, S., and Ragsdale, C.W. (2015). The gyri of the octopus vertical lobe have distinct neurochemical identities. J. Comp. Neurol. *523*, 1297–1317.

28. Di Cristo, C., De Lisa, E., Di Cristo, C., and Di Cosmo, A. (2009). GnRH in the brain and ovary of Sepia officinalis. Peptides *30*, 531–537.

29. Roch, G.J., Busby, E.R., and Sherwood, N.M. (2014). GnRH receptors and peptides: Skating backward. Gen. Comp. Endocrinol. *209*, 118–134.

30. Kanda, A., Takahashi, T., Satake, H., and Minakata, H. (2006). Molecular and functional characterization of a novel gonadotropin-releasing-hormone receptor isolated from the common octopus (Octopus vulgaris). Biochem. J. *395*, 125–135.

31. Iwakoshi-Ukena, E., Ukena, K., Takuwa-Kuroda, K., Kanda, A., Tsutsui, K., and Minakata, H. (2004). Expression and distribution of octopus gonadotropin-releasing hormone in the central nervous system and peripheral organs of the octopus (Octopus vulgaris) by in situ hybridization and immunohistochemistry. J. Comp. Neurol. *477*, 310–323.

32. Froesch, D. (1974). The subpedunculate lobe of the octopus brain: evidence for dual function. Brain Research *75*, 277–285.

33. Wodinsky, J. (1977). Hormonal inhibition of feeding and death in octopus: control by optic gland secretion. Science *198*, 948–951.

34. Wells, M.J., and Wells, J. (1969). Pituitary analogue in the octopus. Nature *222*, 293–294.

35. Wells, M.J., and Wells, J. (1975). Optic gland implants and their effects on the gonads of Octopus. J. Exp. Biol.

36. Wells, M.J., and Wells, J. (1969). Pituitary analogue in the octopus. Nature *222*, 293–294.

37. Holmes, R.L., and Ball, J.N. (1975). The Pituitary Gland: A Comparative Account. Volume 4 of Biological Structure and Function. The Quarterly Review of Biology *50*, 104–104.

38. Minakata, H., Shigeno, S., Kano, N., Haraguchi, S., Osugi, T., and Tsutsui, K. (2009). Octopus Gonadotrophin-Releasing Hormone: A Multifunctional Peptide in the Endocrine and Nervous Systems of the Cephalopod. Journal of Neuroendocrinology *21*, 322–326.

39. Budelmann, B.U., Schipp, R., and Boletzky, von, S. (1997). Cephalopoda. In Microscopic anatomy of invertebrates Mollusca II. F. W. Harrison and A. J. Kohn, eds. (Wiley-Liss), pp. 119–414.

40. Froesch, D. (1979). Antigen-induced secretion in the optic gland of Octopus vulgaris. Proc. R. Soc. Lond., B, Biol. Sci. *205*, 379–384.

41. Albertin, C.B., Simakov, O., Mitros, T., Wang, Z.Y., Pungor, J.R., Edsinger-Gonzales, E., Brenner, S., Ragsdale, C.W., and Rokhsar, D.S. (2015). The octopus genome and the evolution of cephalopod neural and morphological novelties. Nature *524*, 220–224.

42. Werbin, H., and Chaikoff, I.L. (1961). Utilization of adrenal gland cholesterol for synthesis of cortisol by the intact normal and the ACTH-treated guinea pig. Arch. Biochem. Biophys. *93*, 476–482.

43. Fiorito, G., Affuso, A., Anderson, D.B., Basil, J., Bonnaud, L., Botta, G., Cole, A., D'Angelo, L., de Girolamo, P., Dennison, N., *et al.* (2014). Cephalopods in neuroscience: regulations, research and the 3Rs. Invert Neurosci *14*, 13–36.

44. Fiorito, G., Affuso, A., Basil, J., Cole, A., de Girolamo, P., D'Angelo, L., Dickel, L., Gestal, C., Grasso, F., Kuba, M., *et al.* (2015). Guidelines for the Care and Welfare of Cephalopods in Research –A consensus based on an initiative by CephRes, FELASA and the Boyd Group. Lab Anim *49*, 1–90.

45. Lopes, V.M., Sampaio, E., Roumbedakis, K., Tanaka, N.K., Carulla, L., Gambús, G., Woo, T., Martins, C.P.P., Penicaud, V., Gibbings, C., *et al.* (2017). Cephalopod biology and care, a COST FA1301 (CephsInAction) training school: anaesthesia and scientific procedures. Invert Neurosci *17*, 1–8.

46. Naef, A. (1928). Die cephalopoden (embryologie). In Fauna und Flora des Golfes von Neapel, pp. 1–357.

47. Gleadall, I.G. (2013). The effects of prospective anaesthetic substances on cephalopods: Summary of original data and a brief review of studies over the last two decades. J. Exp. Mar. Biol. Ecol. *447*, 23–30.

48. Butler-Struben, H.M., Brophy, S.M., Johnson, N.A., and Crook, R.J. (2018). In Vivo Recording of Neural and Behavioral Correlates of Anesthesia Induction, Reversal, and Euthanasia in Cephalopod Molluscs. Front. Physiol. *9*, 97–18.

49. Haas, B.J., Papanicolaou, A., Yassour, M., Grabherr, M., Blood, P.D., Bowden, J., Couger, M.B., Eccles, D., Li, B., Lieber, M., *et al.* (2013). De novo transcript sequence reconstruction from RNA-seq using the Trinity platform for reference generation and analysis. Nat. Protoc. *8*, 1494–1512.

50. Li, B., and Dewey, C.N. (2011). RSEM: accurate transcript quantification from RNA-Seq data with or without a reference genome. BMC Bioinformatics *12*, 323.

51. Robinson, M.D., McCarthy, D.J., and Smyth, G.K. (2009). edgeR: a Bioconductor package for differential expression analysis of digital gene expression data. Bioinformatics *26*, 139–140.

52. Wang, Z.Y., and Ragsdale, C.W. (2018). Multiple optic gland signaling pathways implicated in octopus maternal behaviors and death. J. Exp. Biol., jeb.185751.

53. Thiel, D., Franz-Wachtel, M., Aguilera, F., and Hejnol, A. (2018). Changes in the neuropeptide complement correlate with nervous system architectures in xenacoelomorphs. 1–57.

54. Southey, B.R., Amare, A., Zimmerman, T.A., Rodriguez-Zas, S.L., and Sweedler, J.V. (2006). NeuroPred: a tool to predict cleavage sites in neuropeptide precursors and provide the masses of the resulting peptides. Nucleic Acids Res. *34*, W267–W272.

55. Nielsen, H. (2017). Predicting Secretory Proteins with SignalP. In Protein Function Prediction: Methods and Protocols Protein Function Prediction: Methods and Protocols. D. Kihara, ed. (New York, NY: Springer New York), pp. 59–73.

56. Altschup, S.F., Gish, W., Miller, W., Myers, E.W., and Lipman, D.J. (1990). Basic local alignment search tool. J. Mol. Biol. *215*, 403–410.

57. Maeda, N., Tanaka, E., Suzuki, T., Okumura, K., Nomura, S., Miyasho, T., Haeno, S., and Yokota, H. (2012). Accurate determination of tissue steroid hormones, precursors and conjugates in adult male rat. The Journal of Biochemistry *153*, 63–71.

58. Cajka, T., and Fiehn, O. (2016). Increasing lipidomic coverage by selecting optimal mobile-phase modifiers in LC–MS of blood plasma. Metabolomics *12*, 1–11.

59. Anderson, R.C., Wood, J.B., and Byrne, R.A. (2002). Octopus senescence: the beginning of the end. J. Appl. Anim. Welf. Sci. *5*, 275–283.

60. Finn, R.D., Coggill, P., Eberhardt, R.Y., Eddy, S.R., Mistry, J., Mitchell, A.L., Potter, S.C., Punta, M., Qureshi, M., Sangrador-Vegas, A., *et al.* (2016). The Pfam protein families database: towards a more sustainable future. Nucleic Acids Res. *44*, D279–D285.

61. Borlido, J., Zecchini, V., and Mills, I.G. (2009). Nuclear Trafficking and Functions of Endocytic Proteins Implicated in Oncogenesis. Traffic *10*, 1209–1220.

62. Suo, D., Park, J., Harrington, A.W., Zweifel, L.S., Mihalas, S., and Deppmann, C.D. (2013). Coronin-1 is a neurotrophin endosomal effector that is required for developmental competition for survival. Nat. Neurosci. *17*, 36–45.

63. Jékely, G. (2013). Global view of the evolution and diversity of metazoan neuropeptide signaling. Proc. Natl. Acad. Sci. U.S.A. *110*, 8702–8707.

64. Grimmelikhuijzen, C.J.P., and Hauser, F. (2012). Mini-review: The evolution of neuropeptide signaling. Regul. Pept. *177*, S6–S9.

65. Bechtold, D.A., and Luckman, S.M. (2007). The role of RFamide peptides in feeding. J. Endocrinol. *192*, 3–15.

66. Sossin, W.S., Kirk, M.D., and Scheller, R.H. (1987). Peptidergic modulation of neuronal circuitry controlling feeding in Aplysia. J. Neurosci. *7*, 671–681.

67. Kavaliers, M., Hirst, M., and Mathers, A. (1985). Inhibitory influences of FMRFamide on morphine- and deprivation-induced feeding. Neuroendocrinology *40*, 533–535.

68. Furukawa, Y., Nakamaru, K., Sasaki, K., Fujisawa, Y., Minakata, H., Ohta, S., Morishita, F., Matsushima, O., Li, L., Alexeeva, V., *et al.* (2003). PRQFVamide, a Novel Pentapeptide Identified From the CNS and Gut of Aplysia. Journal of Neurophysiology *89*, 3114–3127.

69. Hentze, J.L., Carlsson, M.A., Kondo, S., Nässel, D.R., and Rewitz, K.F. (2015). The Neuropeptide Allatostatin A Regulates Metabolism and Feeding Decisions in Drosophila. Sci. Rep., 1–16.

70. Sweedler, J.V., Li, L., Rubakhin, S.S., Alexeeva, V., Dembrow, N.C., Dowling, O., Jing, J., Weiss, K.R., and Vilim, F.S. (2002). Identification and characterization of the feeding circuit-activating peptides, a novel neuropeptide family of aplysia. J. Neurosci. *22*, 7797–7808.

71. Ribeiro, C., and Dickson, B.J. (2010). Sex Peptide Receptor and Neuronal TOR/S6K Signaling Modulate Nutrient Balancing in Drosophila. Curr. Biol. *20*, 1000–1005.

72. Baker, M.E. (2011). Origin and diversification of steroids: Co-evolution of enzymes and nuclear receptors. Mol. Cell. Endocrinol. *334*, 14–20.

73. Nelson, D.R., and Studer, R.A. (2015). Origin of the response to adrenal and sex steroids: Roles of promiscuity and co-evolution of enzymes and steroid receptors. J. Steroid Biochem. Mol. Biol. *151*, 12–24.

74. Antebi, A. (2015). Nuclear receptor signal transduction in C. elegans. WormBook, 1–49.

75. Yoshiyama-Yanagawa, T., Enya, S., Shimada-Niwa, Y., Yaguchi, S., Haramoto, Y., Matsuya, T., Shiomi, K., Sasakura, Y., Takahashi, S., Asashima, M., *et al.* (2011). The Conserved Rieske Oxygenase DAF-36/Neverland Is a Novel Cholesterol-metabolizing Enzyme. J. Biol. Chem. *286*, 25756–25762.

76. Conley, A.J., and Bird, I.M. (1997). The role of cytochrome P450 17 alpha-hydroxylase and 3 beta-hydroxysteroid dehydrogenase in the integration of gonadal and adrenal steroidogenesis via the delta 5 and delta 4 pathways of steroidogenesis in mammals. Biol. Reprod., 789–799.

77. Aakvaag, A. (1970). Steroid formation in porcine ovarian tissue in vitro. Acta Endocrinol., 261–272.

78. Dubrac, S., Lear, S.R., Ananthanarayanan, M., Balasubramaniyan, N., Bollineni, J., Shefer, S., Hyogo, H., Cohen, D.E., Blanche, P.J., Krauss, R.M., *et al.* (2004). Role of CYP27A in cholesterol and bile acid metabolism. J. Lipid Res. *46*, 76–85.

79. Foster, P.A., and Mueller, J.W. (2018). Insights into Steroid Sulfation and Desulfation Pathways. J Mol. Endocrinol., JME–18–0086.

80. Thornton, J.W., Need, E., and Crews, D. (2003). Resurrecting the ancestral steroid receptor: ancient origin of estrogen signaling. Science *301*, 1714–1717.

81. Keay, J., Bridgham, J.T., and Thornton, J.W. (2006). The Octopus vulgaris Estrogen Receptor Is a Constitutive Transcriptional Activator: Evolutionary and Functional Implications. Endocrinology *147*, 3861–3869.

82. Honegger, B., Galic, M., Köhler, K., Wittwer, F., Brogiolo, W., Hafen, E., and Stocker, H. (2008). Imp-L2, a putative homolog of vertebrate IGF-binding protein 7, counteracts insulin signaling in Drosophila and is essential for starvation resistance. J. Biol. *7*, 10.

83. Figueroa-Clarevega, A., and Bilder, D. (2015). Malignant Drosophila Tumors Interrupt Insulin Signaling to Induce Cachexia-like Wasting. Dev. Cell *33*, 47–55.

84. Veenstra, J.A. (2010). Neurohormones and neuropeptides encoded by the genome of Lottia gigantea, with reference to other mollusks and insects. Gen. Comp. Endocrinol. *167*, 86–103.

85. Ahn, S.-J., Martin, R., Rao, S., and Choi, M.-Y. (2017). Neuropeptides predicted from the transcriptome analysis of the gray garden slug Deroceras reticulatum. Peptides *93*, 51–65.

86. Gricourt, L., Bonnec, G., Boujard, D., Mathieu, M., and Kellner, K. (2003). Insulin-like system and growth regulation in the Pacific oyster Crassostrea gigas: hrIGF-1 effect on protein synthesis of mantle edge cells and expression of an homologous insulin receptor-related receptor. Gen. Comp. Endocrinol. *134*, 44–56.

87. Hamano, K., Awaji, M., and Usuki, H. (2005). cDNA structure of an insulin-related peptide in the Pacific oyster and seasonal changes in the gene expression. J. Endocrinol. *187*, 55–67.

88. Örd, T., Örd, D., Adler, P., Vilo, J., and Örd, T. (2015). TRIB3 enhances cell viability during glucose deprivation in HEK293-derived cells by upregulating IGFBP2, a novel nutrient deficiency survival factor. BBA - Molecular Cell Research *1853*, 2492–2505.

89. Kwon, Y., Song, W., Droujinine, I.A., Hu, Y., Asara, J.M., and Perrimon, N. (2015). Systemic Organ Wasting Induced by Localized Expression of the Secreted Insulin/IGF Antagonist ImpL2. Dev. Cell *33*, 36–46.

90. Argilés, J.M., Busquets, S., Stemmler, B., and López-Soriano, F.J. (2014). Cancer cachexia: understanding the molecular basis. Nat. Rev. Cancer *14*, 754–762.

91. Op den Kamp, C.M., Langen, R.C., Haegens, A., and Schols, A.M. (2009). Muscle atrophy in cachexia: can dietary protein tip the balance? Curr. Opin. Clin. Nutr. Metab. Care *12*, 611–616.

92. Fearon, K., Arends, J., and Baracos, V. (2012). Understanding the mechanisms and treatment options in cancer cachexia. Nat. Rev. Clin. Oncol. *10*, 80–89.

93. Shin, M., Kang, H.S., Park, J.H., Bae, J.H., Song, D.K., and Im, S.S. (2017). Recent Insights into Insulin-Like Growth Factor Binding Protein 2 Transcriptional Regulation. Endocrinol Metab (Seoul) *32*, 11–17.

94. Huang, X.-Y., Huang, Z.-L., Yang, J.-H., Xu, Y.-H., Sun, J.-S., Zheng, Q., Wei, C., Song, W., and Yuan, Z. (2016). Pancreatic cancer cell-derived IGFBP-3 contributes to muscle wasting. J. Exp. Clin. Cancer Res., 1–13.

95. Baxter, R.C. (2014). IGF binding proteins in cancer: mechanistic and clinical insights. Nat. Rev. Cancer *14*, 329–341.

96. Wu, L.-G., Hamid, E., Shin, W., and Chiang, H.-C. (2014). Exocytosis and Endocytosis: Modes, Functions, and Coupling Mechanisms. Annu. Rev. Physiol. *76*, 301–331.

97. Brunger, A.T., Choi, U.B., Lai, Y., Leitz, J., and Zhou, Q. (2018). Molecular Mechanisms of Fast Neurotransmitter Release. Annu. Rev. Biophys. *47*, 469–497.

98. Jacobsson, G., and Meister, B. (1996). Molecular components of the exocytotic machinery in the rat pituitary gland. Endocrinology *137*, 5344–5356.

99. Monastirioti, M. (1999). Biogenic amine systems in the fruit fly Drosophila melanogaster. Microsc. Res. Tech. *45*, 106–121.

100. Fernstrom, J.D., and Fernstrom, M.H. (2007). Tyrosine, phenylalanine, and catecholamine synthesis and function in the brain. J. Nutr. *137*, 1539S–1547S– discussion 1548S.

101. Nishioka, R.S., Bern, H.A., and Golding, D.W. (1970). Innervation of the cephalopod optic gland. In Aspects of Neuroendocrinology (Springer), pp. 47–54.

102. Kindsvater, H.K., Braun, D.C., Otto, S.P., and Reynolds, J.D. (2016). Costs of reproduction can explain the correlated evolution of semelparity and egg size: theory and a test with salmon. Ecol. Lett. *19*, 687–696.

103. Fisher, D.O., and Blomberg, S.P. (2011). Costs of Reproduction and Terminal Investment by Females in a Semelparous Marsupial. PLoS ONE *6*, e15226.

104. Nixon, M. (1969). The Lifespan of Octopus vulgaris Lamark. Proc. Malac. Soc. Lond., 529.

105. Robertson, O.H., and Wexler, B.C. (1960). Histological changes in the organs and tissues of migrating and spawning Pacific salmon (genus Oncorhynchus). Endocrinology *66*, 222–239.

106. Davis, S.W., Ellsworth, B.S., Millan, M.I.P., Gergics, P., Schade, V., Foyouzi, N., Brinkmeier, M.L., Mortensen, A.H., and Camper, S.A. (2013). Pituitary Gland Development and Disease: From Stem Cell to Hormone Production 1st ed. (Elsevier Inc.).

107. Fujinaga, M., Chen, J.J., and Scott, J.C. (1999). Characterization of the rat adrenal medulla cultured in vitro. In Vitro Cell. Dev. Biol. -Animal *35*, 33–42.

108. Di Cristo, C., Bovi, P.D., and Di Cosmo, A. (2003). Role of FMRFamide in the reproduction of Octopus vulgaris: molecular analysis and effect on visual input. Peptides *24*, 1525–1532.

109. Wang, Z.Y., and Ragsdale, C.W. (2018). Multiple optic gland signaling pathways implicated in octopus maternal behaviors and death. J. Exp. Biol., jeb.185751–38.

110. Wells, M.J., and Wells, J. (2009). Optic glands and the state of the testis in Octopus. Marine Behaviour and Physiology *1*, 71–83.

111. Wang, Z.Y., and Ragsdale, C.W. (2018). Multiple optic gland signaling pathways implicated in octopus maternal behaviors and death. bioRxiv, 340984.

112. Alupay, J.S., Hadjisolomou, S.P., and Crook, R.J. (2014). Arm injury produces long-term behavioral and neural hypersensitivity in octopus. Neuroscience Letters *558*, 137–142.

113. Robison, B., Seibel, B., and Drazen, J. (2014). Deep-Sea Octopus (Graneledone boreopacifica) Conducts the Longest-Known Egg-Brooding Period of Any Animal. PLoS ONE *9*, e103437–4.

114. Ying Li, Zihao Cao, Haifeng Li, Huihui Liu, Zhenming Lü, Changfeng Chi (2018). Identification, Characterization, and Expression Analysis of a FMRFamide-Like Peptide Gene in the Common Chinese Cuttlefish (Sepiella japonica). Molecules *23*, 742–12.

115. López-Vera, E., Aguilar, M.B., and Heimer de la Cotera, E.P. (2008). FMRFamide and related peptides in the phylum mollusca. Peptides *29*, 310–317.

116. Zhang, Z., Goodwin, E., Loi, P.K., and Tublitz, N.J. (2012). Molecular analysis of a novel FMRFamide-related peptide gene (SOFaRP2) and its expression pattern in the brain of the European cuttlefish Sepia officinalis. Peptides *34*, 114–119.

117. Cropper, E.C., Tenenbaum, R., Kolks, M.A., Kupfermann, I., and Weiss, K.R. (1987). Myomodulin: A bioactive neuropeptide present in an identified cholinergic

buccal motor neuron of Aplysia. Proceedings of the National Academy of Sciences *84*, 5483–5486.

118. de Lange, R.P.J.E.A. (1998). Localization of the Neuropeptide APGWamide in Gastropod Molluscs by in Situ Hybridization and Immunocytochemistry. Gen. Comp. Endocrinol., 1–9.

119. Minakata, H. (2010). Neuropeptides and peptide hormones in the octopus brain. 1–8.

120. Di Cristo, C., Minnen, J.V., and Di Cosmo, A. (2005). The presence of APGWamide in Octopus vulgaris: a possible role in the reproductive behavior. Peptides *26*, 53–62.

121. Christ, P., Reifenrath, A., Kahnt, J., Hauser, F., Hill, S.R., Schachtner, J., and Ignell, R. (2017). Feeding-induced changes in allatostatin-A and short neuropeptide F in the antennal lobes affect odor-mediated host seeking in the yellow fever mosquito, Aedes aegypti. PLoS ONE *12*, e0188243–15.

122. Chung, S., Andersson, T., Sonntag, K.C., Björklund, L., Isacson, O., and Kim, K.S. (2002). Analysis of Different Promoter Systems for Efficient Transgene Expression in Mouse Embryonic Stem Cell Lines. STEM CELLS *20*, 139–145.

123. Di Cristo, C. (2013). Nervous control of reproduction in Octopus vulgaris: a new model. Invert Neurosci *13*, 27–34.

124. Wang, Y., Price, D.A., and Sahley, C.L. (1998). Identification and Characterization of a Myomodulin-Like Peptide in the Leech. Peptides *19*, 487–493.

125. Watts, A.G., and Khan, A.M. (2013). Identifying Links in the Chain: The Dynamic Coupling of Catecholamines, Peptide Synthesis, and Peptide Release in Hypothalamic Neuroendocrine Neurons 1st ed. (Copyright © 2013 Elsevier Inc. All rights reserved.).

126. Watts, A.G., and Sanchez-Watts, G. (1995). Physiological regulation of peptide messenger RNA colocalization in rat hypothalamic paraventricular medial parvicellular neurons. J. Comp. Neurol. *352*, 501–514.

127. John, C., Werner, P., Worthmann, A., Wegner, K., Tödter, K., Scheja, L., Rohn, S., Heeren, J., and Fischer, M. (2014). A liquid chromatography-tandem mass spectrometry-based method for the simultaneous determination of hydroxy sterols and bile acids. J Chromatogr A *1371*, 184–195.

128. Mendiara, I., Domeño, C., and Nerín, C. (2012). Development of a fast sample treatment for the analysis of free and bonded sterols in human serum by LC-MS. J. Sep. Science *35*, 3308–3316.

129. Ren, J.-L., Zhang, A.-H., Kong, L., and Wang, X.-J. (2018). Advances in mass spectrometry-based metabolomics for investigation of metabolites. RSC Adv. *8*, 22335–22350.

130. Gouveia, M.J., Brindley, P.J., Santos, L.L., Correia da Costa, J.M., Gomes, P., and Vale, N. (2013). Mass spectrometry techniques in the survey of steroid metabolites as potential disease biomarkers: A review. Metabolism *62*, 1206–1217.

131. Kim, K.-J., Kim, H.-J., Park, H.-G., Hwang, C.-H., Sung, C., Jang, K.-S., Park, S.-H., Kim, B.-G., Lee, Y.-K., Yang, Y.-H., *et al.* (2016). A MALDI-MS-based quantitative analytical method for endogenous estrone in human breast cancer cells. Sci. Rep., 1–7.

132. Raith, K., Brenner, C., Farwanah, H., Müller, G., Eder, K., and Neubert, R.H.H. (2005). A new LC/APCI-MS method for the determination of cholesterol oxidation products in food. J Chromatogr A *1067*, 207–211.

133. Matyash, V., Liebisch, G., Kurzchalia, T.V., Shevchenko, A., and Schwudke, D. (2008). Lipid extraction by methyl- tert-butyl ether for high-throughput lipidomics. J. Lipid Res. *49*, 1137–1146.

134. Nes, W.D. (2011). Biosynthesis of Cholesterol and Other Sterols. Chem. Rev. *111*, 6423–6451.

135. Kristiana, I., Luu, W., Stevenson, J., Cartland, S., Jessup, W., Belani, J.D., Rychnovsky, S.D., and Brown, A.J. (2012). Cholesterol through the Looking Glass. J. Biol. Chem. *287*, 33897–33904.

136. MARRONE, B.L., and KARAVOLAS, H.J. (1982). Progesterone Metabolism by the Hypothalamus, Pituitary, and Uterus of the Aged Rat*. Endocrinology *111*, 162–167.

137. Wollam, J., Magomedova, L., Magner, D.B., Shen, Y., Rottiers, V., Motola, D.L., Mangelsdorf, D.J., Cummins, C.L., and Antebi, A. (2011). The Rieske oxygenase DAF-36 functions as a cholesterol 7-desaturase in steroidogenic pathways governing longevity. Aging Cell *10*, 879–884.

138. Zerbinati, C., and Iuliano, L. (2017). Cholesterol and related sterols autoxidation. Free Radical Biology and Medicine *111*, 151–155.

139. Lin, N., Zhang, H., Qiu, W., Ye, J., Han, L., Wang, Y., and Gu, X. (2014). Determination of 7-ketocholesterol in plasma by LC-MS for rapid diagnosis of acid SMase-deficient Niemann-Pick disease. J. Lipid Res. *55*, 338–343.

140. Shinkyo, R., Xu, L., Tallman, K.A., Cheng, Q., Porter, N.A., and Guengerich, F.P. (2011). Conversion of 7-Dehydrocholesterol to 7-Ketocholesterol Is Catalyzed by Human Cytochrome P450 7A1 and Occurs by Direct Oxidation without an Epoxide Intermediate. J. Biol. Chem. *286*, 33021–33028.

141. Björkhem, I., Diczfalusy, U., Lövgren-Sandblom, A., Starck, L., Jonsson, M., Tallman, K., Schirmer, H., Ousager, L.B., Crick, P.J., Wang, Y., *et al.* (2014). On the formation of 7-ketocholesterol from 7-dehydrocholesterol in patients with CTX and SLO. J. Lipid Res. *55*, 1165–1172.

142. Griffiths, W.J., Abdel-Khalik, J., Crick, P.J., Ogundare, M., Shackleton, C.H., Tuschl, K., Kwok, M.K., Bigger, B.W., Morris, A.A., Honda, A., *et al.* (2017). Sterols and oxysterols in plasma from Smith-Lemli-Opitz syndrome patients. J. Steroid Biochem. Mol. Biol. *169*, 77–87.

143. Sevin, M., Lesca, G., Baumann, N., Millat, G., Lyon-Caen, O., Vanier, M.T., and Sedel, F. (2006). The adult form of Niemann-Pick disease type C. Brain *130*, 120–133.

144. Tierney, E., Nwokoro, N.A., Porter, F.D., Freund, L.S., Ghuman, J.K., and Kelley, R.I. (2001). Behavior phenotype in the RSH/Smith-Lemli-Opitz syndrome. Am. J. Med. Genet. *98*, 191–200.

145. Freeman, K.A., Eagle, R., Merkens, L.S., Sikora, D., Pettit-Kekel, K., Nguyen-Driver, M., and Steiner, R.D. (2013). Challenging Behavior in Smith-Lemli-Opitz Syndrome. Cognitive And Behavioral Neurology *26*, 23–29.

146. Matsumoto, A., and Ishii, S. eds. (1992). Atlas of Endocrine Organs: Vertebrates and Invertebrates (Springer-Verlag).

147. Arrieche, D. (1999). Ultrastructure of the optic gland of the squid Sepiotheutis sepioidea (Cephalopoda: Loliginidae). Rev Biol Trop.

148. Zhang, Z., Wu, Y., Wang, Z., Dunning, F.M., Rehfuss, J., Ramanan, D., Chapman, E.R., and Jackson, M.B. (2011). Release mode of large and small dense-core vesicles specified by different synaptotagmin isoforms in PC12 cells. Mol. Biol. Cell *22*, 2324–2336.

149. Grabner, C.P., Price, S.D., Lysakowski, A., Cahill, A.L., and Fox, A.P. (2006). Regulation of large dense-core vesicle volume and neurotransmitter content mediated by adaptor protein 3. Proceedings of the National Academy of Sciences *103*, 10035–10040.

150. Collaborators, C.T.T.C. (2005). Efficacy and safety of cholesterol-lowering treatment: prospective meta-analysis of data from 90 056 participants in 14 randomised trials of statins. The Lancet *366*, 1267–1278.

151. Lyons, M.A., and Brown, A.J. (1999). 7-Ketocholesterol. The International Journal of Biochemistry & Cell Biology *31*, 369–375.

152. Boyle, P.R., and Boletzky, S.V. (1996). Cephalopod populations: definition and dynamics. Philosophical Transactions of the Royal Society B: Biological Sciences *351*, 985–1002.

153. Rodhouse, P.G. (1998). Physiological progenesis in cephalopod molluscs. Biol. Bull. *195*, 17–20.

154. Nesis, K.N. (1977). The biology of paper nautiluses, Argonauta boettgeri and Argonauta hains (Cephalopoda, Octopoda), in the western Pacific and the seas of the East Indian Archipelago.

155. Rodaniche, A.F. (1984). Iteroparity in the lesser Pacific striped octopus Octopus chierchiae (Jatta, 1889). Bulletin of Marine Science *35*, 99–104.